國立交通大學應用化學研究所
碩士論文

Institute of Applied Chemistry

National Chiao-Tung University

Master Thesis

交替式共聚高分子聚醯胺型聚氨酯內超分子識別系統之研究

The Study on the Supramolecular Recognition within a

Poly(amide urethane) System

蔡佳佑

Jia-You Tsai

指導教授:張豐志 博士

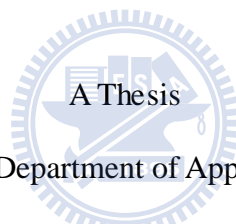Advisor: Feng-Chih Chang, Ph.D.

中華民國九十九年六月

June, 2010

交替式共聚高分子聚醯胺型聚氨酯內超分子識別系統之研究

The Study on the Supramolecular Recognition within a Poly(amide urethane) System

研 究 生：蔡佳佑   Student: Jia-You Tsai

指導教授：張豐志   Advisor: Feng-Chih Chang

國 立 交 通 大 學

應 用 化 學 系

碩 士 論 文

A Thesis

Submitted to Department of Applied Chemistry

College of Science

National Chiao Tung University

in Partial Fulfillment of the Requirements

for the Degree of

Master

in

Applied Chemistry

June 2010

Hsinchu, Taiwan, Republic of China

中華民國九十九年六月

Acknowledgement

Outline of Contents

List of Tables

List of Schemes

List of Figures

the environment.

temperature in the 1600-1800 cm^{-1} region.

The Study on the Supramolecular Recognition within a Poly(amide urethane) System

Student: Jia-You Tsai   Advisor: Dr. Feng-Chih Chang

Institute of Applied Chemistry
National Chiao Tung University
30050 Hsinchu, Taiwan

ABSTRACT

Self-assembled polymers such as block copolymers are usually formed through covalent linkages in conventional polymer chemistry, including bonds connecting monomer units and attaching functional groups to the polymer backbone. Recently, novel structural organizations of self-assembled polymers formed through highly directional and sufficiently strong non-covalent host-guest pairs have attracted great attention. These new polymers utilize non-covalent multiple-hydrogen-bonding interactions similar to those found in bio-molecules such as protein, DNA, and RNA to direct and modulate their 3-D topology. In addition, the moderately strong and highly directional multiple-hydrogen-bonding interactions within these new generation polymers also result in unique physical properties, such as high specificity, controlled affinity, and reversibility. In previous studies, the study on the complementary nature and its effect on material properties can be broadly classified into side chain and chain ends types. Until now, studying and controlling the microstructures within supramolecular polymers with different hydrogen-bonding

motifs still remain as a challenging task. In this study, the amphiphilic alkylated nucleobase, hexadecyluracil (U16) was incorporated into poly(amide urethane) which was synthesized ourselves with self-complementary group and several hydrogen bonding motifs for the study on the heterodimer recognition behavior within the alternative polymer. Biocomplementary PAU/U16 supramolecular complexes formed in dilute DMF through molecular recognition, that is, the hydrogen bonding between the diaminopyridine (DAP) groups of the PAU and the Uracil (U) of U16. Moreover, FTIR, DSC, WAXD, SAXS, and TEM analysis provided furthur detail into the nature of self-assembly of these systems. The effect of the heterodimer recognition on the microphase separation was investigated, revealing that the heterodimer recognition led the poly(amide urethane) to possessing the "plug and play" behavior even the heterodimer recognition coincided with several other hydrogen bonding motifs. The period and morphlogies of PAU/U16 complexes can be rationally tuned by the amount of U16. Upon the adding of U16, the lamellar structure within long-range lamellar changes from bilayer to bilayer with interclated and further to monolayer.

交替式共聚高分子聚醯胺型聚氨酯內超分子
識別系統之研究

學生: 蔡佳佑　　　　　　　　　　　指導教授:張豐志 教授

國立交通大學應用化學研究所 碩士班

摘　　要

　　傳統高分子化學中，自組裝型高分子(self-assembled polymers)如嵌段式共聚高分子常經由共價鍵方式將單體-單體間及單體與高分子主鏈上之對應官能基間相互以連結。近年來，藉由具高度方向性及主客配對之非共價鍵方式形成自組裝型高分子之新穎結構已逐漸獲得重視。此種作用力常見於生物體內許多蛋白質、DNA、RNA及3D立體架構，因此近年來向自然界取材之仿生材料發展相當蓬勃。此類新型高分子中適當強度及具方向性之多點式氫鍵作用力導致了許多特殊的物理性質。近期對於互補性單元導入高分子材料中的研究，可簡略分類為側鏈修飾及鏈尾修飾等兩種。如果我們可以控制多重氫鍵的鍵結能力，就可以間接改變超分子的型態。然而，藉由不同之多點式氫鍵作用力調控超分子中之微結構及研究直到現在仍相當具有挑戰性。於此篇研究中，我們將雙重極性(amphiphilic)之長碳鏈核鹼基，導入具有自身互補性基團及多種氫鍵作用力之聚醯胺型聚氨酯高分子中，用以研究在交替式高分子中異雙聚體(heterodimer)分子辯識的行為以及在導入之後微相分離的變化。研究結果顯示，即使在系統中仍有其它種類氫鍵的存在，異雙聚體的分子辯識使得聚醯胺型聚氨酯高分子呈現「熱插式」(plug and play)的行為。藉由U16混摻比例的不同，可使得整個高分子系統的型態有所改變並得以調控。隨著U16加入的量增加，鏈與鏈間之次級層狀結構由原本雙層之結構變成深入彼此之相互交錯狀態，並進而變成單層結構。

Chapter1

Introduction

1-1 An Overview on Polyurehtane

1-1.1 The Development and Utilities of Polyurethane

Polyurethanes(PUR), also known as Segmented polyurethanes(SPU or PUs), are widely used in thermal plastic elastomers, owing to their excellent mechanical and chemical characteristics. Polyurethane(PU) was earliest found by Bayer and Farbenindustric. Segmented polyurethanes (PUs), which comprise hard and soft segments, are a major consumer plastic material with an annual production capacity worldwide of nearly 12 million tons (2007). Segmented polyurethane elastomers are linear block copolymers of $-(HS)_n-$ type (H, hard segment; S, soft segment), or so called alternative copolymer, whose versatile physical properties are generally attributed to their microphase-separation structure. Soft segment means the region where polyol located and mainly consisted of polyester or polyether with 500~4000 molecular weight; hard segment indicates regimes contain no polyol but NCO end group and chain extenders, hard segments are also with 500~4000 molecular weight. Opposite to other consumer plastics they are no polymerization but condensation polymers produced in a stepwise polyaddition process without the elimination of side products. Polyurethanes are generally produced from one or more polyhydroxyl compounds and one or more polyisocyanates. Due to the numerous compounds on both sides of the reaction the type, properties, and fields of application of the resulting polyurethanes are without any limit. Otherwise, the raw materials have been produced in several steps from crude oil (or, more recently, also renewable resources), thus, they constitute high commercial value.

Time (Period)	Research Topic	References
1849	Isocyanate reaction with an alcohol	Wurtz, A. Ann 71, 326, 1849
1937	I. G. Farbenindustrie applies for first polyurethane patent	German Patent 728, 981
1938	Firest U.S. payent award to Rinke, et al.	U.S. Patent 2, 511, 544
1942	DuPont receives patents for reaction of polyisocyanates with glycols, diamine, and polyesters	
1942	Introduction of Igamid U, and Ugamid UL in Germany	
1943	Vulkollan polyester-based elastomers introduced in Europe	
1945	Allies recognize German industry and create Farbenfabriken	
1954	Patent on Lycra spandex elastomeric fiber awarded	U.S. Patent 2, 692, 893
1954	Bayer and Monsanto Co. form Mobay Chemical Co.	
1955	Patent on Estane thermoplastic elastomers awarded	U.S. Patent 2, 871, 218
1955	Union Carbide developes first one-shot foam	
1956	Teracol 30-PTMEG introduced	Bulletin HR-11 DuPont
1959	First use of chlorofluorocarbons as blowing agents	
1971	Patent on medical-grade polyurethane-silicone elastomer	U.S. Patent 3, 562, 352
1993	Patent on aliphatic biostable polyurethane elastomer	U.S. Patent 5, 254, 662

Table 1-1. Development of the significant research on polyurethane in history.[4]

Segmented polyurethanes are generally composed of polyether or polyester soft segments and urethane based hard segments along the polymer backbone giving rise to a microphase-separated morphology caused by the usual poor compatibility

between both segments. The unique properties of these polymers are directly related to their two phase microstructure, in which the hard domains act as a reinforcing filler and as a thermally reversible cross-link.[1] Such polyurethanes have been widely used industrially due to their versatile properties[2] but, due to their low degradability in nature, many research efforts have been put on biodegradable polyurethanes.[3]

Environmental concerns are also related to the use of organic solvents during the processing and even during the use of polymers in applications such as coatings, adhesives, fibers among others. Polyurethanes derived from water dispersions can overcome this type of problem by replacing more toxic solvents with water. Waterborne poly(urethane-urea)s, WPUUs, are multiblock copolymers consisting of alternating the soft and hard segments. WPUUs not only conform to environmental emission legislation, but also reduce the consumptions of both cost and energy.[4] Therefore, they are widely used as the elastomer, coating, adhesive, and nanocomposite.[5–8]

In the last years, as interest in polymers for biomedical devices is increasing, biocompatible and biodegradable polymer precursors are used to synthesise segmented thermoplastic polyurethane elastomers (STPU) which can be visualized as possible candidates for many applications as vascular prostheses, soft tissue adhesives, pericardial patches, and in tissue engineering cancellous bone substitutes.[9,10]

Shape memory polyurethanes (SMPU) with phaseseparated morphology are composed of soft and hard segments, in which the former mostly comprises the reversible phase to fix the temporary shape, while the latter forms the fixed phase to memorize the permanent shape. In the thermal sensitive shape memory function, most of the temporary deformation can be fixed well after cooling to a low temperature (T_l) under a certain temperature Ts (melting point (T_{ms}) or glass transition temperature (T_{gs}) of soft segments), subsequently, the original shape can be automatically

3

recovered from the temporary shape with the stimulus of heating to a high temperature (T_h) above Ts. In heating scan, such a sharp recovery usually happens in the vicinity of Ts. This unique feature made this type of material arouse lot of research interest from both academia and industry in recent decades. In the linear segmented SMPU system, the strong intermolecular force (physical cross-linking) among hard segments results from the hydrogen bonding and the high polarity due to the presence of urethane and urea units. The shape memory effect (SME) of SMPU therefore is significantly influenced by the hard-segment content and the moiety of its molecular structure. In addition, it is reported that the soft-segment content, its molecular weight, conformation, and morphological structure play significant roles on SME. Therefore, these parameters are paramount in controlling the shape memory properties in general.

1-1.2 Chemistry of Polyurethanes

Isocyanates can undergo a broad spectrum of chemical reactions and are of great importance for contemporary polymer chemistry. Isocyanates can, for instance, be polymerized along the nitrogen-carbon double bond producing substituted polyamides. By far the most important reaction, however, is the reaction between an isocyanate and an alcohol forming an urethane bond. Also the reaction with an amine forming an urea bond is widely used. The basic reaction of polyurethanes is the addition of an H-active compound to an isocyanate compound. The reaction is belong to nucleophilic addition and the polyol is attached to the carbon atom on the isocyanate(see eq. 1-1). The more detail mechanism(**Scheme 1-1**) discovered by H. Herlinger is a six centered ring mechanism in which a proton is shifted from the H-active compound to the nitrogen atom of the isocyanate[11]:

$$(1-1)$$
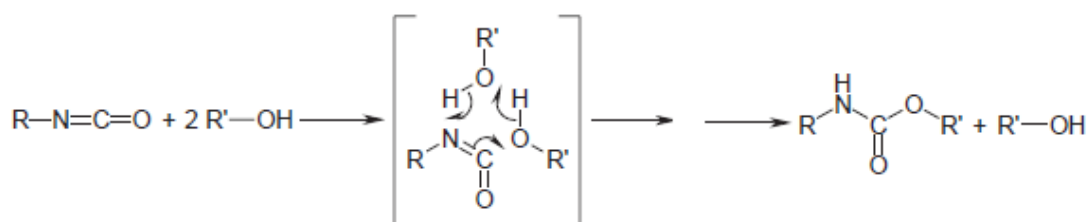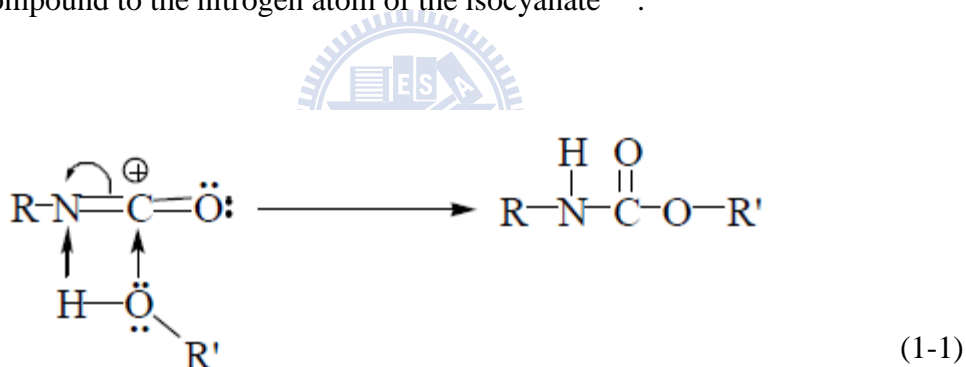
Scheme 1-1. Mechanism of Urethane Formation

There are also different reactions between H-active compound and isocyanates (RNCO) and listed as below:
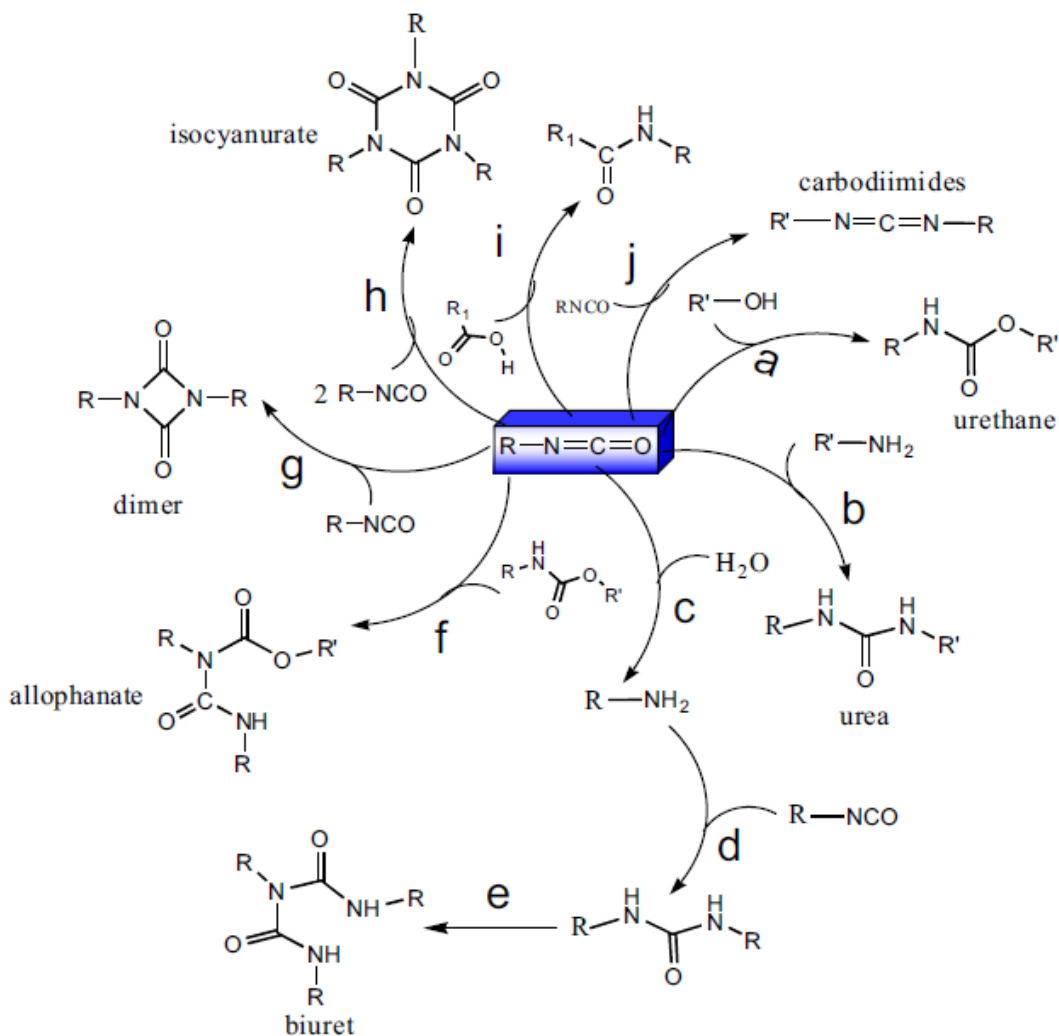
Scheme 1-2. Basic reactions of isocyanate with different reactants

At the initial stage of reaction or under the condition of excess isocyanates, urethane, urea, and amide may lead to side reactions such as route e and f in **Scheme 1-2.** These side reactions give rise to branching and crosslinking in polymers. In general, the relative reaction rate of isocyanate and H-active compound is listed as follow: aliphatic $NH2$ > aromatic $NH2$ > primary OH > $H2O$ > secondary OH > tertiary OH > phenolic OH > R-COOH > RNHCONHR > RNHCOR > RNHCOOR.

Polyurethanes belong to the class of polycondensation polymers. There are two common ways to synthesize polyurethane: the first one is let bischloroformates react

with diamine; the other one and also popular method is by the reaction between

diisocyanate and dihydroxy(diol) groups.[12]

(I) The source of bischloroformates is by the reaction between phosgene and

diol or bisphenol(1-1), and then react with diamine or bisphenol as the following:

(a) bischloroformates react with diamine to form polyurethanes(1-2):

$$2Cl\text{-}\overset{O}{\overset{\|}{C}}\text{-}Cl + HO\text{-}R\text{-}OH \longrightarrow Cl\text{-}\overset{O}{\overset{\|}{C}}\text{-}O\text{-}R\text{-}O\text{-}\overset{O}{\overset{\|}{C}}\text{-}Cl + 2HCl$$

(1-1)

$$Cl\text{-}\overset{O}{\overset{\|}{C}}\text{-}O\text{-}R\text{-}O\text{-}\overset{O}{\overset{\|}{C}}\text{-}Cl + H_2N\text{-}R\text{-}NH_2 \longrightarrow$$

$$\text{-}[\overset{O}{\overset{\|}{C}}\text{-}O\text{-}R\text{-}O\text{-}\overset{O}{\overset{\|}{C}}\text{-}Cl\text{-}NH\text{-}R\text{-}NH]\text{-} + 2HCl$$

(1-2)
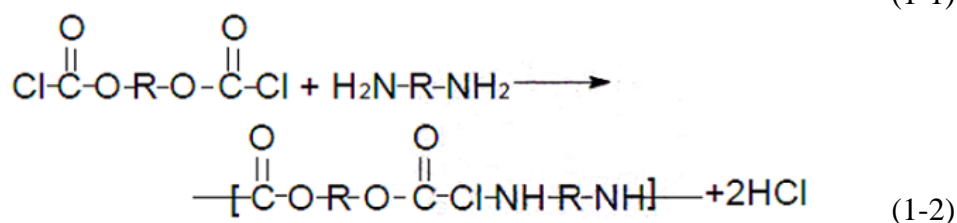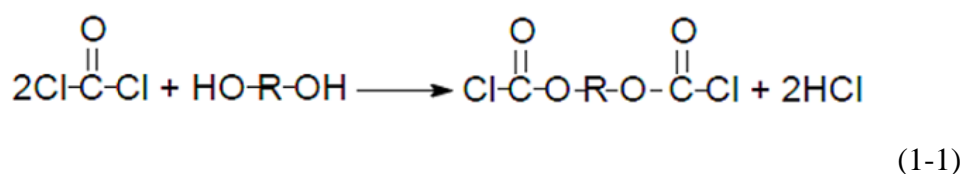
(b) or sometimes by the reaction of biscarbanyl chlorides and bisphenol A:

(1-3)
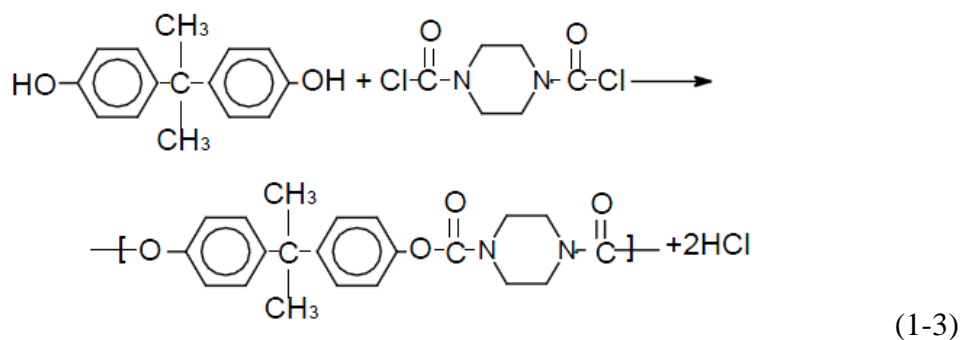
(II) In general, the synthesis of polyurethane is achieve by the polymerization

diiocyanate, diol and chain extender. There are also two types of reactions to complete

the goal: "One-shot process" and "Prepolymer process." The former one means let all

the reactants complete the reaction in only one process; and the latter is let excess

diisocyanate react with diol and forms prepolymer with NCO end group first, then add

7

chain extender to increase the molecular weight of (pre)polymers. The alternative
copolymers which contain soft and hard segments is elastic, so these elastomers also
called TPU(thermal elastomer of polyurethane).
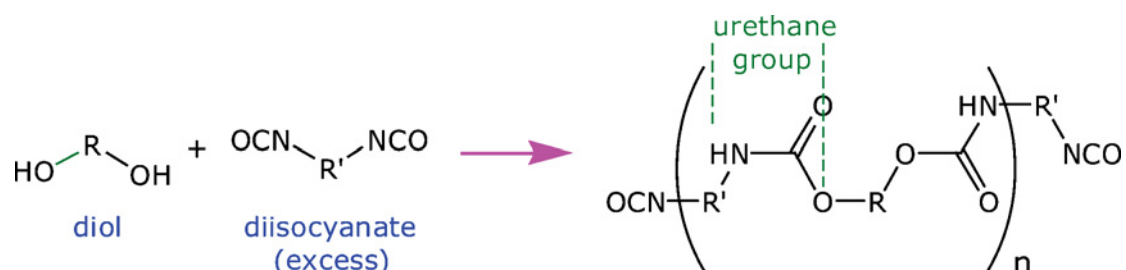
Scheme 1-3. Basic reaction scheme for urethane formation. [12]

1-1.3 The Structure and Properties of Polyurethanes

Segmented polyurethane elastomers are alternative copolymer or so-called
linear block copolymers of -(HS)$_n$- type (H, hard segment; S, soft segment) with Hard
and Soft segments on the backbone(**Scheme 1-4**).[13] The ''soft segment'' typically is
a polar polyol region, such as polyether or polyester, with 500~4000 molecular weight
and a glass transition temperature below ambient, which imparts elastomeric character
to the polymer. The ''hard segment'' indicates regimes contains the highly polar
urethane and urea linkages, typically with 500~4000 molecular weight and a glass
transition above room temperature. Hard segment may also include and chain
extenders(**Scheme 1-5**)[14] and NCO end groups. The soft segments behaves like
rubbers at room temperature, and hard segments usually is semi-crystalline or glass
state. Because of the hydrogen bonding, coulombic force and segmental polarity
difference, these two segment types tend to phase separate in the bulk. The hard
domains act as physical crosslinkers and reinforcing fillers. The variable physical
properties of PUs depend strongly on the degree of phase separation and the cohesion
of the hard domains.

Physical crosslink forms frequently within the PU structure due to

8

intramolecular and intermolecular hydrogen bonding of hard segments(**Scheme 1-6**). The content of such kind of physical crosslink structure plays an important role of several properties of polyurethane. For example, the modulus of polyurethane material mainly depends on the ratio of hard segment content to soft segment content as a result of the amount of physical crosslink. The more hard segment content, the more physical crosslinking inside the PU, thus the modulus of rigidity is larger. On the contrary, the more soft segment content, the modulus of PU material is smaller.[15-17] The structure of the physical crosslink within PAU applied in this paper was shown in **Figure1-1**.

These kinds of physical crosslink structure mentioned above are composed of varies types of intramolecular and intermolecular hydrogen bonds and exist in two kinds of forms: (1)intermolecular urethane-urethane group hydrogen bonding (2) urethane-polyol hydrogen bonding forms owing to the dispersion of hard segments in soft segments.

In general, urethane-urethane hydrogen bond is stronger in the whole PU structure because the polarity of urethane is higher than polyol segments and thus make the urethane group in hard segments attract each other. Specific interaction called inter-urethane hydrogen bonding also forms as the driving force of phase separation(segregation) due to the aggregation of hard segments led by hydrogen bonding. Therefore, the polarity of structure composition and the strength of hydrogen bonding within the PU have a big influence on the microphase separation which can be detected and known by X-ray diffraction(WAXS and SAXS).

The degree of microphase separation within PU varies due to the unevenly distributed(unhomogeneous) hard segments and soft segments then results in multiple transition temperatures. In general, there are three glass transition temperatures found in DSC or DMA scanning[17]:

(1) The first phase transition point is below 0℃ and mainly comes from the glass transition temperature of soft segment.

(2) Another phase transition temperature found generally in the range of 30℃~90℃ is higher than room temperature and mainly comes from the glass transition temperature of hard segments

(3) The rest endothermic peak locates between two glass transition temperature mentioned above and mainly bring about from the heat destruction of hydrogen bonding within hard and soft segments.

Scheme 1-4. Schematic of the PU chains studied in this work. Soft and hard segments have different lengths and length distributions. The hard segment consist of 4,4'-diphenylmethane diisocyanate (MDI) and the chain extender 1,4-butanediol (BD) whereas the soft segment consist of original diol segments.

Scheme 1-5. The hard, soft segments and urethane groups in the backbone of PU (R$_2$ may be used as chain extender)

Scheme 1-6. Physical crosslink among hard segment and soft segment in PU

□ : soft segment   □ :hard segment
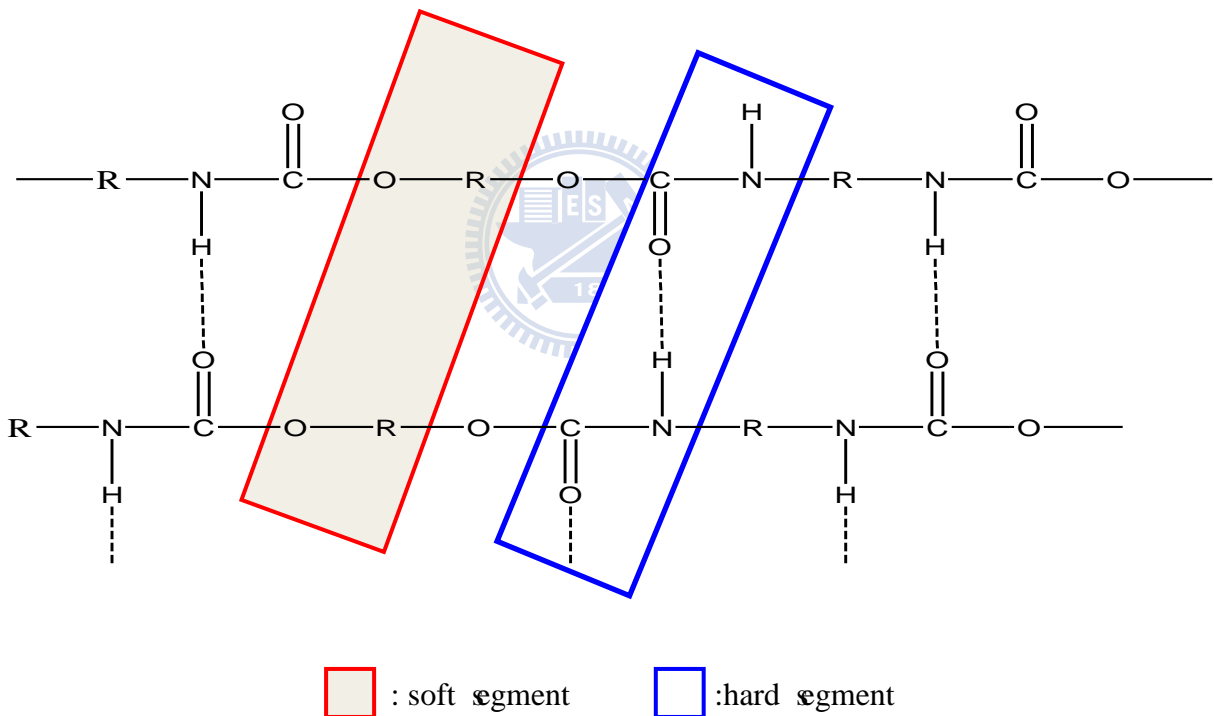
Figure 1-1. Hydrogen bonding within hard segments of PU

1-1.4 The Microstructure and Morphology of Polyurethanes

Segmented polyurethanes (PUs) have a great application potential due to their wide range of mechanical properties. Depending on the specific end use, PUs can be designed to possess either elastic or rigid mechanical characteristics, depending on the macromolecular structure.[18–20] Thus, considerable effort has been made to

understand structure–property relationships of segmented PUs. In order to tailor mechanical properties, the macromolecules of segmented PUs are built up of two types of blocks.[21–24] One block type, the so-called hard segment, is glassy (or crystalline) as it is below its T_g (or T_m) at the use temperature. The other soft block is flexible and rubbery, as it is above its corresponding T_g at the use temperature. The hard segments due to their thermodynamic incompatibility with the soft segments usually associate to form small domains that serve as physical cross-links and reinforcement sites; hence they limit flow of the other phase, which is made up by the soft segments.

The domain size of segmented PU is so small at the scale of 10nm and hardly observed by TEM. Thus, the literature on the TEM morphology of PU is seldom rarely published. Meier calculated the morphology of block copolymer of PU varies with the increasing of volume fraction by thermodynamics. Cooper et. al[41] put much effort on PB based PU and both SAXS and HVEM was utilized on the research. Hard segment distributed in soft segments with a dislike cylinder shape when PB based PUs with 31% hard-segment content (HSC)(Volume fraction: 27%) within is discovered. Also, for a 42~67% HSC PU(volume fraction: 35~61%), hard segments displays a lamella like structure. When HSC is higher than 75% (volume fraction: 68%), hard-segment domain was continuous phase and soft-segment domain shows dislike shapes. Therefore, For thermoplastic and solvent-polymerized PUs with 50% hard-segment content, a lamellar domain structure[24–26] or bicontinuous phase separation[27] is usually assumed. For PU samples with 30% HSC, a dispersed hard-segment domain structure is expected to be having spherical, disclike,[28–30] or cylindrical[31] domain shapes.

The degree of phase separation in PUs depends on the types of diisocyanate and polyol employed to produce the PU, CE(chain extender) nature, type of

polyfunctional compound used in the crosslinking process, NCO:OH ratio, sizes of HSs and SSs, method of synthesis, etc. Figure 1-2. shows the HD (hard domain) and SD(soft domain) structures of TPUs at low and high hard segment content. The domain size may range from 3 to 20 nm and depends on the reactants used as well as the polymerization conditions.
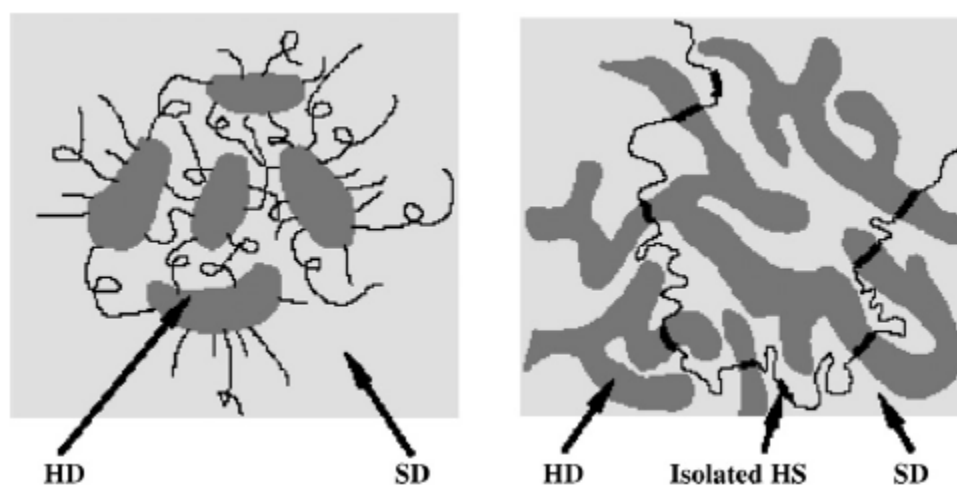
Figure 1-2. Hard domains (HD) and soft domains (SD) of TPUs with (a) a low hard segment content where HDs are isolated; and (b) a high hard segment content where HDs are interconnected.[32,33,34]

In real case, thermoset PUs are formed by using either one or a combination of the following:

• using polyols with functionalities greater than 2,

• substitution of a trifunctional hydroxyl compound in place of the normal glycol CE,

• using isocyanates with functionalities greater than 2,

• using NCO:OH ratios greater than 1, and

• introduction of a crosslinker into the HS, SS or CE.

On the other hand, the mechanical stability of PUs are low at high temperatures,[35,36] and their initial temperature of degradation is typically around 200°C, which is near their melting temperature.[36–39] Therefore, the mechanical characteristics and thermal stability are improved by altering the structure of the

segments, such as by incorporating into the hard or the soft segment an aromatic amide,[39] an aromatic imide,[37] or a silicone group.[38,39] Although the hard and soft segments of PUs influence the stability of thermal degradation, the morphology of the domains that consist of hard segments also, importantly, affects the mechanical stability in practical application.

Polyurethanes can be obtained in both amorphous and semicrystalline forms.[40–43] It was found that the morphology of semicrystalline PUs is much more complicated for polymers obtained by the so-called cast reactive method (CRM) as compared with the thermoplastic procedure.[44–48] In semicrystalline PUs obtained by CRM, multi-phase separation may occur on two levels of structural organization: of the order of tens of micrometers (micro level), corresponding to micro-phase separation (hard segment-rich spherulites, hard segment-rich globules); and of the order of tens of nanometers (nano level), associatedwith nano-phase separation (hard segment-rich fibrils and lamellae, and domain structure).[43,49–51]

There is a discussion in the literature regarding the nature of the morphological features observed by transmission electron microscopy (TEM) that exist outside hard-segment rich spherulites and globules.[51,52] The observations are not complete due to limitations of TEM and additional investigations are necessary to solve this issue. The atomic force microscopy (AFM)[53–55] has been used to study polymer morphology with great success (see, e.g., melting and crystallization of poly(ethylene oxide) in real-time,[56] the spherulitic morphology of isotactic polypropylene,[57] the lamellar organization of melt-crystallized bisotactic polypropylene,[58] the lamellar morphology of polyethylene and polyoxymethylene (POM), microfibrils of oriented POM,[59] etc.). In the work nowadays, the morphology of various semicrystalline polyetherurethanes is discussed, based on new, complementary AFM and TEM studies.

1-2 The Crystalline Behavior in Polymers (Thermal Properties of PU)

If crystalline polymers contact with specific solid when they heat to melt then cool down and crystallized, it forms a large amount of nuclei on the interface, and therefore make crystals form latter only grow toward the direction perpendicular to the interface and finally at the interior of polymers because of overcrowded in the space. This kind of columnar crystal is named as transcrystal, which is a result of heterogeneous nucleation. The grow behavior of transcrystal in polymers was earliest found in the interface between templates of hot-embossing manufacturing. After a series of research, it was found out the density and surface energy are higher in the transcrystal region than that in bulk polymers and thus enhance the mechanical properties and bonding strength in polymers.[60,61] This phenomenon has readily been utilized as an application in the reinforcement of the adhesion on polymer surfaces[62]. In recent years, the development of thermoplastic nanocomposite is prosperous, and the discussion over crystalline behavior on the surface between matrix and reinforcement material is popular. XRD analysis technique and the variation of DSC curve are both common methods to realize the detail structure and crystalline behavior in nanocompsite materials.

Seymour and Cooper[63] discovered there are three melting endothermic peaks(T_1、T_2、T_3) in the higher temperature region of DSC diagram and respectively responsible for different order of arrangements within hard segments (**Scheme 1-7**). The existence of multiple endotherms has been documented in several studies of the thermal behavior of segmented polyurethane block copolymer.[63-65] Multiple endotherms are as a result of partially amorphous and partially crystalline, or so-called semi-crytalline behavior inside the polymer microstructure because no existence of totally crystalline polymer in reality. Actually, the morphology in crystalline polymers contain amorphous, short-range order, long range order and

crystalline regions. In general, three distinct endotherms are observed in differential scanning calorimeter (DSC) experiments.[63-66] The lowest temperature endotherm (T_1) is observed at temperatures ca. 20-30℃ higher than the annealing temperature and has been attributed to a local restructuring of hard-segment units(short-range order of unknown nature) within the hard microdomains. An intermediate temperature endotherm (T_2), found generally in the range 120-200 ℃, has been associated with the destruction of long-range order of an unspecified nature or the onset of microphase mixing of the hard and soft microphases. A higher temperature endotherm (T_3) observed above 200 °C is generally ascribed to the melting of microcrystalline regions within hard microdomains (hard segments).

As for soft segments in polyurethanes, the constrain of hard segments on both side ends of soft segments has a tremendous influence on the crystalline behavior of soft segments due to the stereo structure and continuous circumstance of hard segments. In general, the ability of crystallization of soft segments decrease as the increasing of specific volume(surface area/volume, S/V). Although the specific volume(S/V) of block copolymer varies with morphology, the value of S/V decreases with the increasing of molecular chain length for all kinds of morphologies. Therefore, it is concluded that the chain length of soft segments in both styrenic block copolymers or linear copolymers should be long enough to induce crystalline behavior.
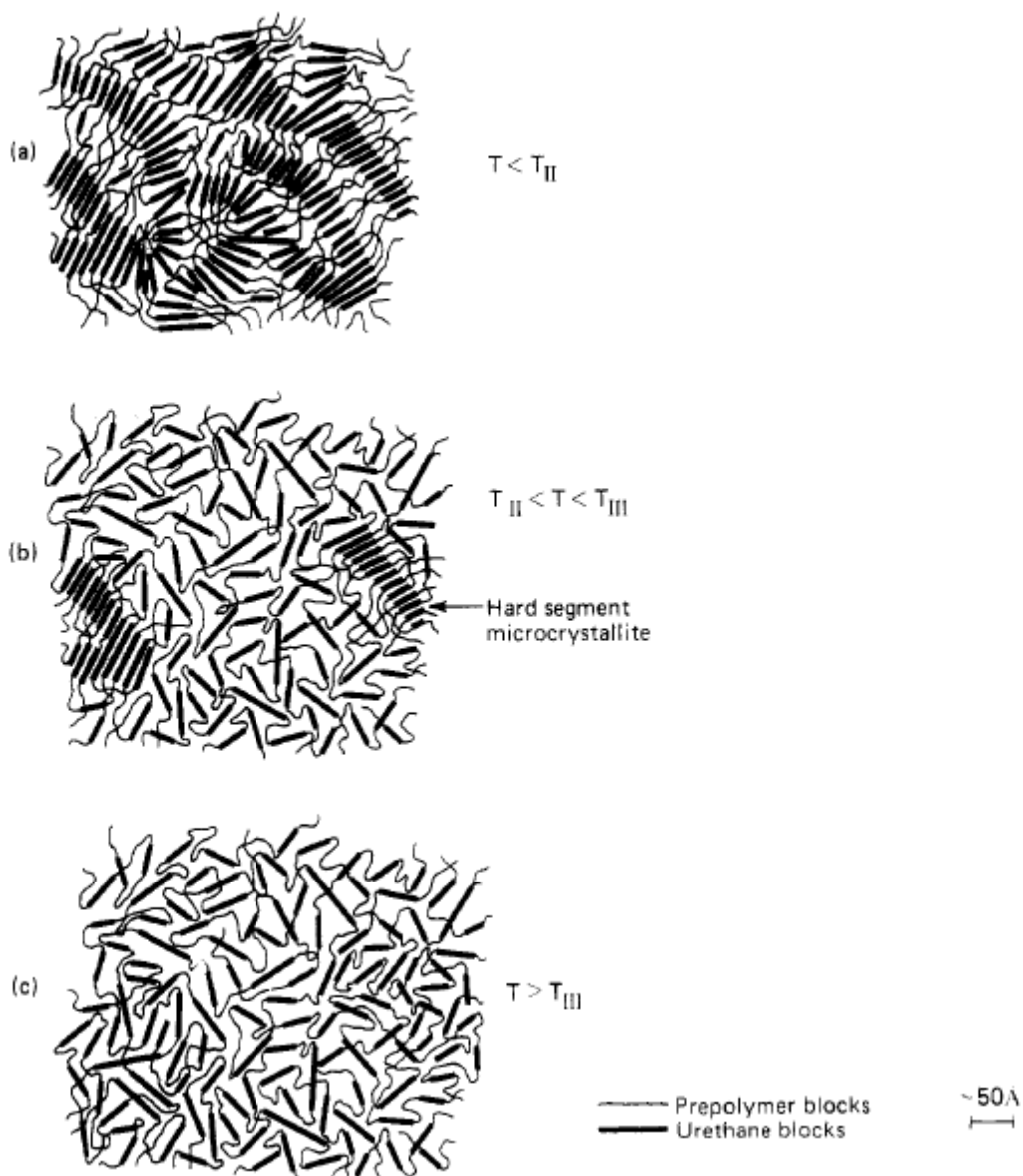
Scheme 1-7. Schematic model for the morphological changes that occur during DSC scans of polyurethane elastomers: (a) below the microphase mixing transition temperature; (b) between the microphase mixing temperature and the melting temperature; and (c) above the melting temperature. The microcrystalline hard-segment domains are indicated

1-3 Hydrogen Bonding within Polymers

A hydrogen bond is the attractive interaction of a hydrogen atom with an electronegative atom, like nitrogen, oxygen or fluorine (thus the name "hydrogen bond", which must not be confused with a covalent bond to hydrogen). The hydrogen must be covalently bonded to another electronegative atom to create the bond. A hydrogen atom attached to a relatively electronegative atom is a hydrogen bond donor.[67] This electronegative atom is usually fluorine, oxygen, or nitrogen. An electronegative atom such as fluorine, oxygen, or nitrogen is a hydrogen bond acceptor, regardless of whether it is bonded to a hydrogen atom or not (**Scheme 1-11**). An example of a hydrogen bond donor is ethanol, which has a hydrogen bonded to oxygen; an example of a hydrogen bond acceptor which *does not* have a hydrogen atom bonded to it is the oxygen atom on diethyl ether.

In general, the strength of hydrogen bonding is (ca. 1~10 kcal/mol) is weaker than covalent or ionic bonds(50 kcal/mol), but far stronger than a van der Waals interaction(0.2 kcal/mol). Hydrogen bonds break and reform continuously because of thermal motions in molecules. Polymers contains polar functional groups, such as hydroxyl group, carbonyl group, urethane group and amide groups forms physically hydrogen bonding within or between polymers. The hydrogen bonds in polymers can occur between molecules (*intermolecularly*, self-association, **Scheme 1-8**)[68], or within different parts of a single molecule (*intramolecularly*, inter-association, **Scheme 1-9**). In general, the hydrogen bonding in polymer forms dimers in dilute polymer solution but timers in concentrated solution (**Scheme 1-10**). Hydrogen bonding forms among different functional groups of molecules is called intermolecular hydrogen bond. Also, the hydrogen bonding among molecules make the charge density of electron cloud rearrange and also the total energy of electromagnetic radiation altered with the strength of interaction. The change of

interaction can be detected and measured by FT-IR spectrum at suitable frequency.

Many polymers are strengthened by hydrogen bonds in their main chains. Among the synthetic polymers, the best known example is nylon, where hydrogen bonds occur in the repeat unit and play a major role in crystallization of the material. The bonds occur between carbonyl and amine groups in the amide repeat unit. They effectively link adjacent chains to create crystals, which help reinforce the material. The effect is greatest in aramid fibre, where hydrogen bonds stabilize the linear chains laterally. The chain axes are aligned along the fibre axis, making the fibres extremely stiff and strong. Hydrogen bonds are also important in the structure of cellulose and derived polymers in its many different forms in nature, such as wood and natural fibres such as cotton and flax.

Hydrogen bonding also plays an important role in determining the three-dimensional structures adopted by proteins and nucleic bases. In these macromolecules, bonding between parts of the same macromolecule cause it to fold into a specific shape, which helps determine the molecule's physiological or biochemical role. The double helical structure of DNA, for example, is due largely to hydrogen bonding between the base pairs (**Scheme 1-12**), which link one complementary strand to the other and enable replication. **Figure 1-4** also shows the hydrogen bonding between base pairs in the compound utilized in this study.

In the secondary structure of proteins, hydrogen bonds form between the backbone oxygens and amide hydrogens. When the spacing of the amino acid residues participating in a hydrogen bond occurs regularly between positions i and $i + 4$, an alpha helix is formed. When the spacing is less, between positions i and $i + 3$, then a 3_{10} helix is formed. When two strands are joined by hydrogen bonds involving alternating residues on each participating strand, a beta sheet is formed. Hydrogen bonds also play a part in forming the tertiary structure of protein through interaction

of R-groups.
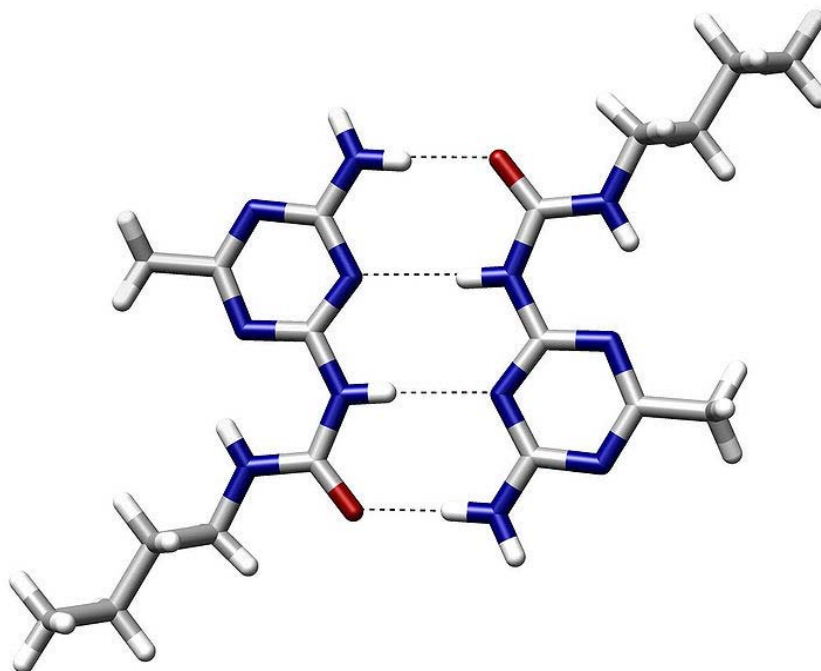
Scheme 1-8. An example of intermolecular hydrogen bonding in a self-assembled

dimer complex reported by Meijer and coworkers.[67]
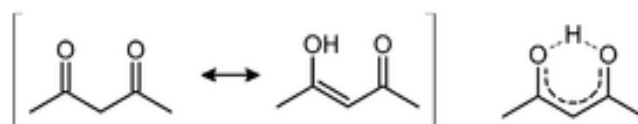
Scheme 1-9. Intramolecular hydrogen bonding in acetylacetone helps stabilize the
enol tautomer
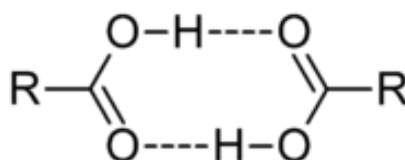
Scheme 1-10. Carboxylic acids often form dimers in vapor phase.
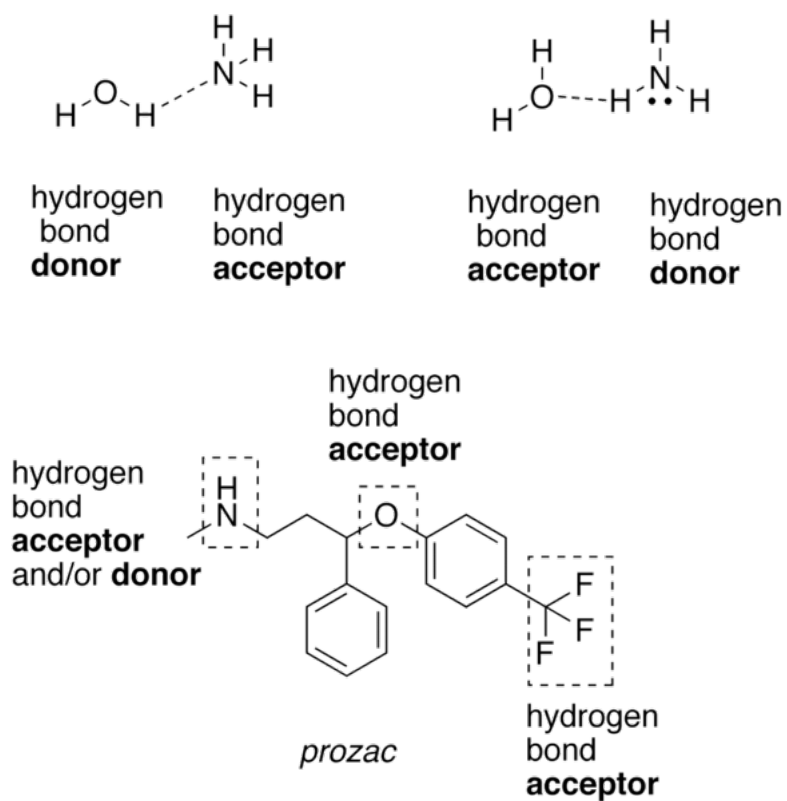
Scheme 1-11. Examples of hydrogen bond donating (donors) and hydrogen

bond accepting groups (acceptors)
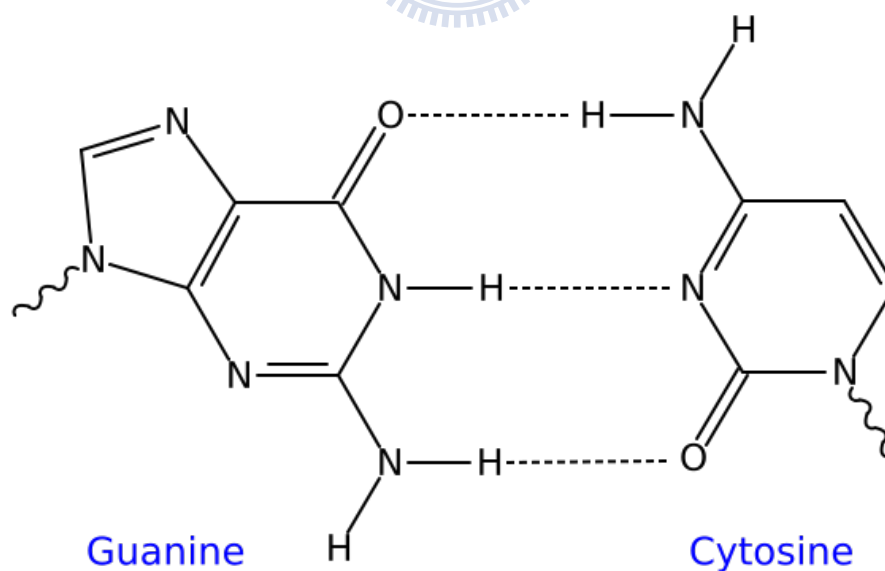
Scheme 1-12. Hydrogen bonding between guanine and cytosine, one of two types of
base pairs in DNA.
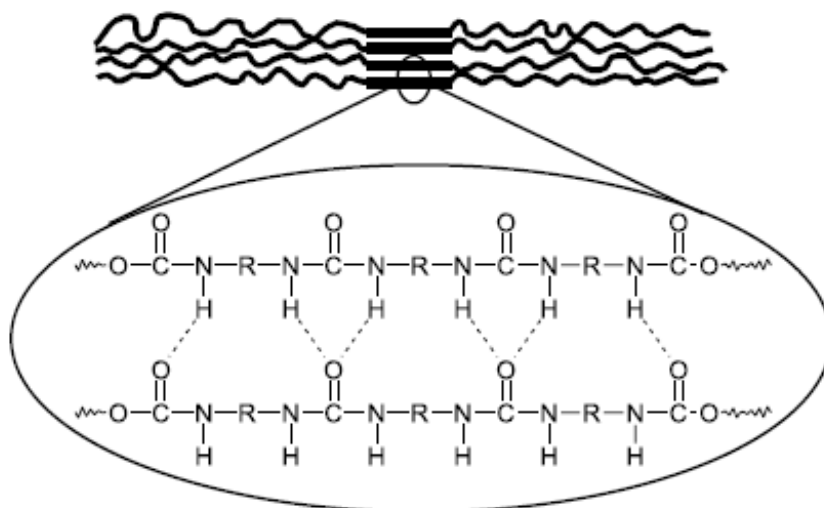
Figure 1-3. The microstructure within PU and hydrogen bonding among hard segments[69]
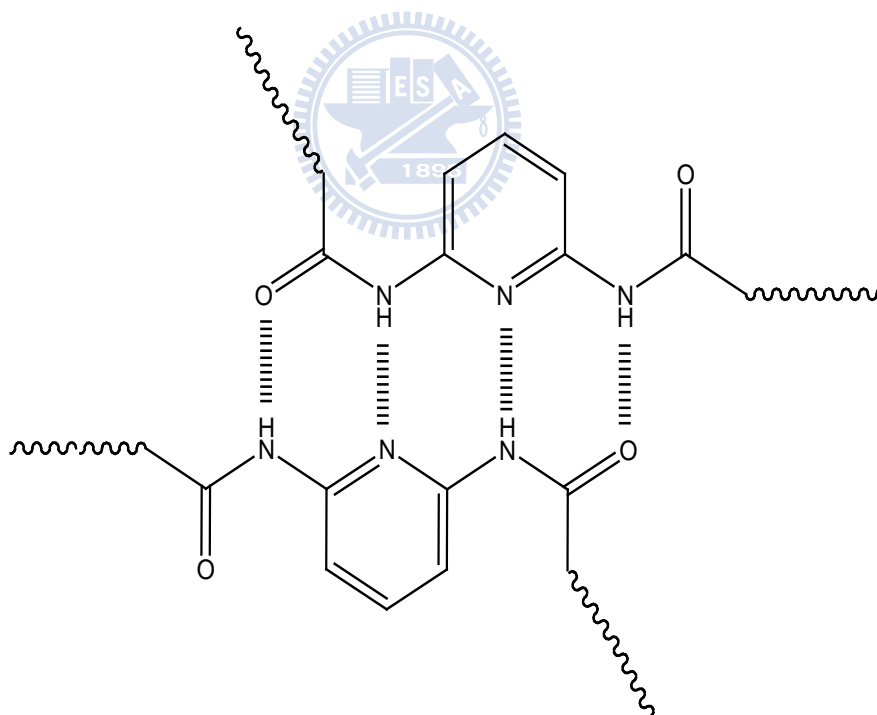
Figure 1-4. The hydrogen bonding within diamidepyridine

22
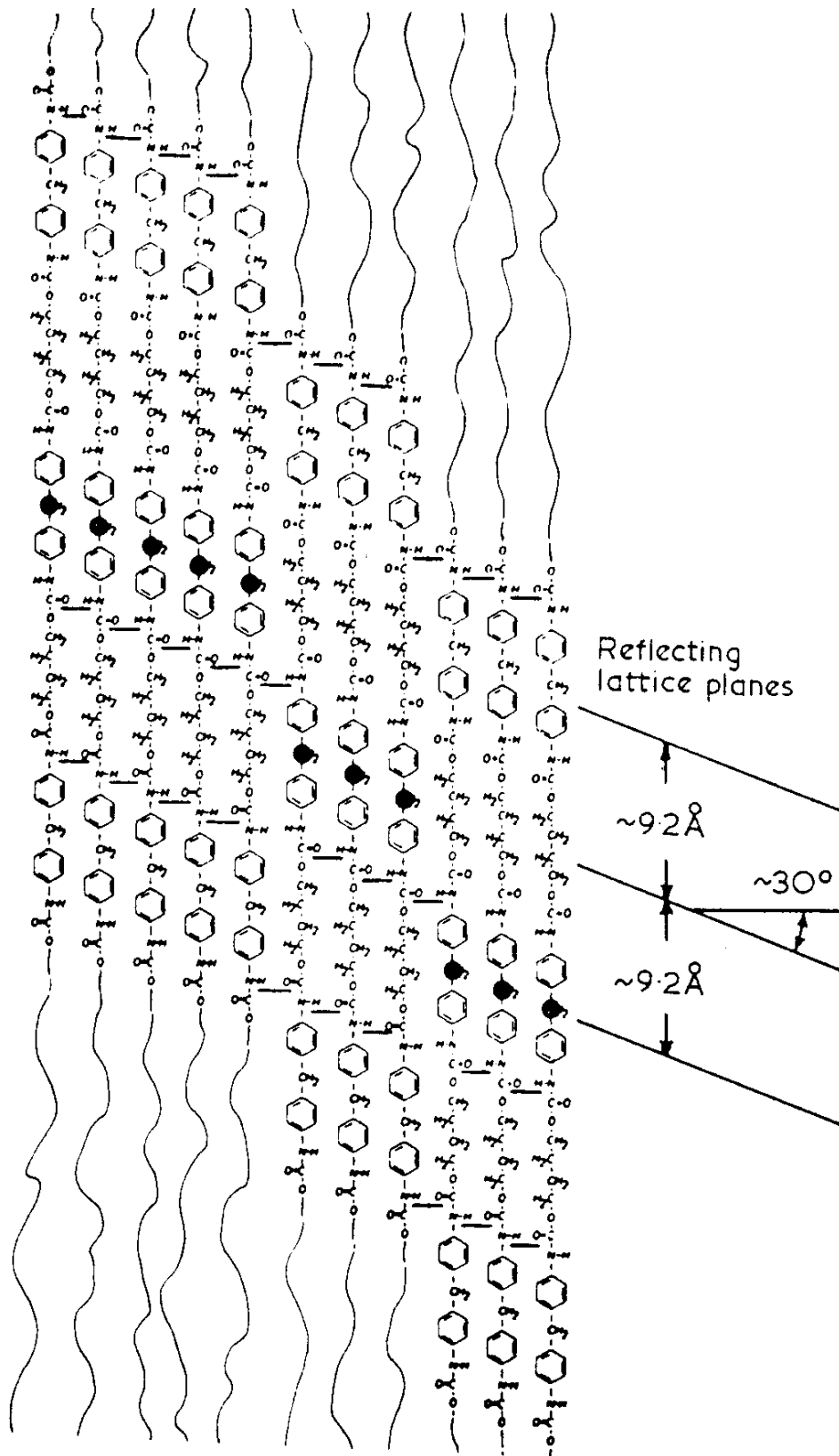
Figure 1-5. Schematic of the hydrogen-bonding in MDI-butanediol hard segment ,as proposed by Bonart et al. The staggering of the chains leads to planes in this projection at 30° to the perpendicular as indicated[70-71].

Chapter 2

Literature Review and Motivation

2-1 Introduction to Natural Nucleobases and its Applications in Supramolecular

The five main natural nucleobases adenine, cytosine, guanine, thymine and uracil are involved in the self-assembly of one of nature's most interesting and intriguing biopolymers, namely the nucleic acids DNA and RNA. As such, these nucleobases have held a fascination to researchers in a diverse range of fields. With the growth in the field of supramolecular chemistry and consequently a better understanding of how molecules interact with each other, more and more information is emerging on the complex supramolecular behaviour of these nucleobases.

Nature has excelled at utilizing supramolecular chemistry to store, transmit and replicate information in a challenging environment with a limited number of structural units. DNA and DNA-like materials offer the opportunity of preparing controlled self-assembled architectures. The interaction between two DNA strands is primarily mediated by four nucleobases adenine (A), thymine (T), guanine (G) and cytosine (C). The two anti-parallel strands of DNA are held together by A-T and C-G base-pairs to form the famous double helix. While the selectivity of these base-pair interactions is controlled mainly by hydrogen bonding, both $\pi-\pi$ stacking and hydrophobic effects also play a role in stabilizing the resulting structure. Utilization of the common nucleobases in supramolecular chemistry offers the flexibility of exploiting four different binding units A, C, G, and T (or U), all of which offer different binding characteristics. A limiting factor, however, in the utilization of single base-pairing interactions lies in the fact that in polar solvents, in which functionalized purine (A, G) and pyrimidine (C, T) derived systems are generally most soluble, the energies of the complementary base-pair interactions are small. Biological systems have overcome this problem by utilizing a combination of non-covalent interactions, in addition to

multiple base-pairs, to contribute toward the formation of desired complexes. **Figure. 2-1**, as an example, shows some of the possible non-covalent interactions of guanine and its corresponding nucleotide deoxyguanosine monophosphate which could be utilized in supramolecular systems. All nucleobases offer a similar plethora of potential non-covalent interactions, and so a multiple site binding approach, where the weak base-pairing interactions are complemented by additional binding forces, adds an extra dimension to the use of nucleobase recognition in supramolecular chemistry. Furthermore, nucleotides, which also contain a charged sugar phosphate, expand on these molecules repertoire of non-covalent bonds by including electrostatic interactions.
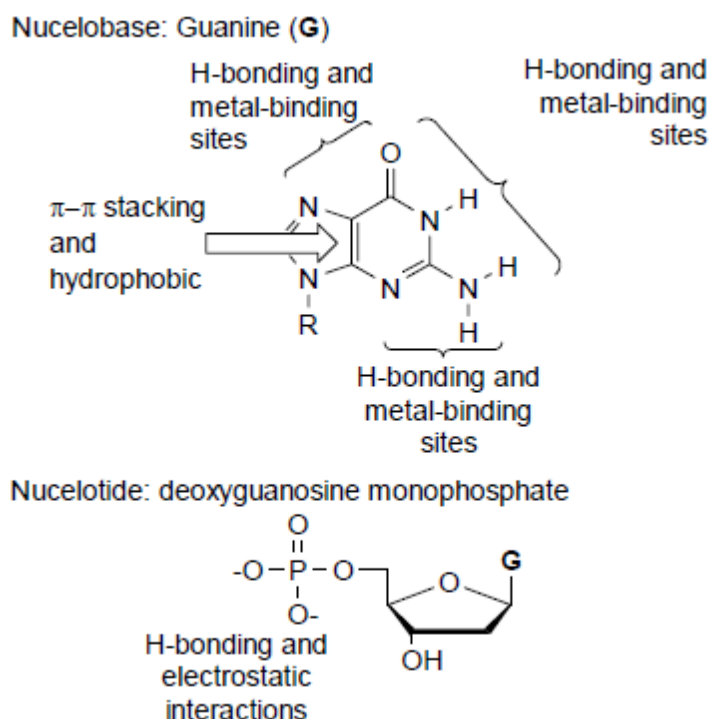
Figure 2-1. Some of the non-covalent interactions which are present in the nucleobase guanine and the nucleotide deoxyguanosine monophosphate.

Supramolecular self-assembly has attracted great attention because of the novel structural organizations formed through highly complementary molecular recognition events.[72,73] Nature has excelled at utilizing supramolecular chemistry to

store, transmit, and replicate information in a challenging environment with a limited number of structural units such as DNA and RNA offering the opportunity of preparing controlled self-assembled architectures.[74] These noncovalent interactions containing materials exhibit unique physical properties, such as high specificity, controlled affinity, and reversible, selective, self-healing, and spontaneous self-assembly behavior.[75] Recently, several supramolecular structures have been incorporated into polymers[5] to form novel materials with features of conventional polymers and reversibility in the bonding between monomer units.[77] On the other hand, chemists have not only started to learn how to mimic natural use of noncovalent chemistry in polymer science but also how we might be able to harness these interesting biomolecules to construct complex nanostructures and materials in the foundation of supramolecular polymer science. In this chapter, the discussion of the scope and limitations of supramolecular chemistry and nature of hydrogen bonds in polymeric materials with an emphasis on properties of the resulting materials will be presented. In addition, the design principles and the methodology of supramolecular materials in particular multi-functionalization indicated in the published literatures will also be discussed.
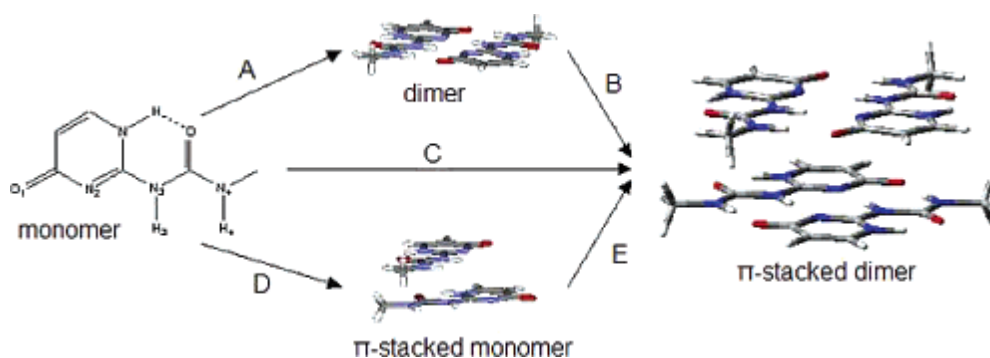
Scheme 2-1. Stepwise Construction of π-Stacked Dimers from Monomers for Homostack of **1k**

2-2 Versatile Hydrogen-Bonding Motifs Through Nucleobase-pairing

2-2.1 Nature and Stability of Hydrogen Bonds

Hydrogen bonds between neutral organic molecules play an important role in determining the three-dimensional structure of chemical and biological systems as a consequence of their specificity and directionality. The most familiar hydrogen bond motifs are the nucleobases found in DNA and RNA. Hydrogen bonds connect atoms X and Y which have electronegativities larger than that of hydrogen, such as C, N, O, F, P, S, Cl, Se, Br, and I. The XH group is generally referred to the "proton donor" (D) and the Y atom is called the "proton acceptor". The strength of a hydrogen bond increases with the increase in the dipole moment of the X-H bond and the electron lone pair on atom Y (**Table 2-1**). Thus, the strongest hydrogen bonds formed between atoms N, O, and F acting as X and Y. Recently, it have been reported that C-H also acts as a donor and hydrogen bonds involve an interaction between a partially positive hydrogen atom and the electrons of unsaturated double or triple bonds.[78]

The stability of any hydrogen-bond assembled complex will be strongly influenced by the number of hydrogen-bonds – in general, two hydrogen-bonds will be stronger than one hydrogen-bond, three hydrogen-bonds will be stronger than two, and so on. This can be seen for DNA base pairs where the Guanine-Cytosine (G-C, $K_a = 10^4$-10^5 M^{-1}) complex is two to three orders of magnitude more stable than the Adenine-Thymine (A-T, $K_a = 10^2$ M^{-1}) complex (**Figure 2-2**). In addition, this suggests that multiple hydrogen-bonding systems should posses relatively higher K_a attributed to four (or more) attractive secondary interactions (**Figure 2-3**). Indeed, the association constants based on this system were reported as values of more than 10^4-10^7 M^{-1}.[21,22] In summary, among various multiple hydrogen bonded modules, the association constant increases in the order, but the complexity does not refer to the objects directly. Compared to the DNA types, the systems, G-C and A-T, are

relatively easy to be synthesized through molecular design. For the molecular assembly, the trouble should be avoided in the synthesis of a modular component, as possible.

Table 2-1: The length of hydrogen bonds[104]

Bond length (nm)			Bond length (nm)		
OH---O	0.272	O----O	Adenine(A)-Thymine(T)	0.281	N----O
OH---N	0.279	O----N		0.295	N----N
OH---S	0.331	O----S	Guanine(G)-Cytocine(C)	0.281	O----N
OH---F	0.272	O----F		0.295	N----N
OH---Cl	0.312	O----Cl		0.301	N----O
OH---Br	0.328	O----Br			
NH---O	0.289	N----O			
NH---N	0.298	N----N			
NH---S	0.342	N----S			
NH---F	0.292	N----F			
NH---Cl	0.323	N----Cl			
NH---Br	0.337	N----Br			
FH---F	0.244	F-----F			

Figure 2-2 Hydrogen bonding in DNA base pairs.

Figure 2-3 Selected multiple hydrogen bonded complexes with high association constants.[79,80]
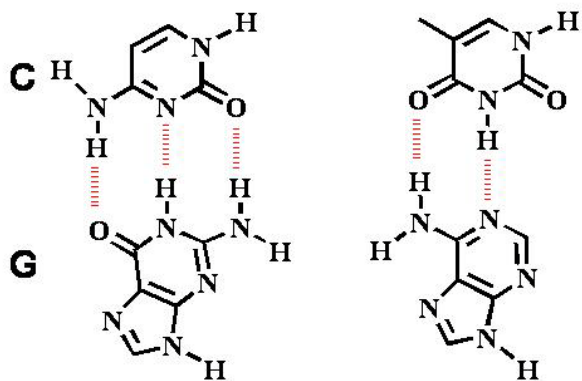
2-2.2 Hydrogen Bonding of Nucleobase-pairing Allows for Versatility

Before discussing the various structural architectures that synthetic chemists can prepare using nucleobases, a review of the base-pairing characteristics of the natural nucleobases is appropriate. This is because, in order to comprehend better the plethora of synthetic structures that can be constructed through nucleobase interactions, a summary of the various modes of hydrogen-bonding between nucleic acids is in need. Also, from a design perspective the advantages of base-pair derived systems must be recognized and exploited while the disadvantages must likewise be noted and addressed. There are two major nucleobase binding motifs present in nucleic acids, the adenine-thymine, AT (or adenine-uracil, AU in RNA) and guaninecytosine, GC. These nucleobase-pairs interact via 2 or 3 hydrogen bonds, respectively (**Figure 2-4**). The Watson–Crick motif (**Figure 2-4**), found in a range of DNA- and RNA-containing structures, is the most widely recognized hydrogen-bonding interaction in Nature. This canonical motif is defined by the pairing of guanosine with cytidine and adenosine with either thymidine or uridine. The guanosine–cytidine (GC) couple (Ka $\sim 10^4$–10^5 M^{-1} in CDCl$_3$)[81] is stabilized by a three-point hydrogen-bonding interaction, while the adenosine–thymidine (AT or AU) grouping (Ka $\approx 10^2$ M^{-1} in CDCl3)[82] contains a two-point hydrogen-bonding mode. Thus, based solely on the strength of association, the GC couple represents a stronger base-pairing motif. It is therefore more attractive for incorporation as a recognition ''subunit'' into new structures. For this reason, GC binding interactions have been popular and widely used. However, there are many examples where the AT (or AU) Watson–Crick motif has been used with good effect to stabilize a number of elegant supramolecular structures. Both types of ensembles are covered in the research of our laboratory. However, while this Watson-Crick base-pairing is dominant within nucleic acids and prevalent within DNA-duplex, it is important to note that the

nucleobases are not exclusive in their binding behaviour. Other hydrogen-bonding motifs are available and expand the possibility for the creation of different structural networks even though the Watson–Crick mode of bonding is prevalent in natural systems.[83] There are 28 possible base-pairing motifs that involve at least two hydrogen bonds which can be formed between the four common nucleobases.[85] These include reverse Watson-Crick (**Figure 2-5a**), Hoogsteen (**Figure 2-5b**) or 'wobble' (or mismatched) base-pairs (**Figure 2-5c**), and various homo dimers (self-pairing). Special attention needs to be paid to the Hoogsteen[84] mode of bonding, which is another mode that we have exploited for the development of new, synthetic self-assembled ensembles. Hoogsteen interactions occur on the opposite face, between the C6–N7, of the purine nucleosides. Along with Hoogsteen interactions, other non-traditional base-pairs (see **Figure 2-5**) are found extensively in various DNA and RNA structures. In addition, these modes are also present in protein–DNA and drug–DNA interactions. These, and other nucleobase binding modes, can play important roles in any nucleobase self-assembly process which is controlled by its hydrogen bonding, especially but not exclusively when the interaction is not constrained by the geometry of the double helix. The conformation of the sugars with respect to a base-pair (i.e., *cis* or *trans* conformation with regard to the sugar on the complementary nucleobase) can also lead to variant basepairing modes. For example, the 'reverse' base-pairing mode is defined by a *trans* or antiparallel conformation of the two sugar moieties. Such a conformation can lead to reverse Watson–Crick (see **Figure 2-5a**) and reverse Hoogsteen (**Figure 2-5b**) base-pairing modes. Other dimeric binding modes are also possible due to tautomerism and ionization of nucleobases, but these are far less prevalent. In addition to base dimerization, individual nucleobases can also form trimers and other higher order oligomers. Furthermore, the purines, A and G, also contain two major hydrogen bonding sites,

31

the Watson-Crick and the Hoogsteen sites. Thus, in addition to being able to form 1:1

complexes through either of these two sites, both of these nucleobases can form 2:1

aggregates (or base-triplets) with an appropriate partner (**Figure 2-6**). Such

complexes are involved in the formation of triple helix DNA.[86] In the case of the

C^+:G:C base-triplet, the N^3 of one of the cytosines needs to be protonated in order to

allow the donation of a hydrogen bond to the N^7 of guanine (**Figure 2-6**).

Furthermore, in addition to interacting with other nucleobases, each of the

nucleobases can also homo-dimerize(**Figure 2-5d**). In the case of purines, A and G,

larger aggregates are also possible on account of the two binding sites. Guanine in

particular is known to self aggregate[87] into tapes and macrocycles aided by its

relatively high association constant for dimerization (K_{GG} *ca.* 10^2-10^4 M-1 in CDCl$_3$,

c.f. K_{AA} *ca.* < 5 M^{-1} in CDCl$_3$).[88,89]

In fact, in addition to the complementary interactions, all of the nucleobases

can homodimerize, albeit with greatly reduced binding constants ($K_{TT} = 3.5$ M^{-1}, K_{AA}

$= 2.4$ M^{-1}, $K_{CC} = 40$, $K_{GG} = 10^2$-10^4 M^{-1}). Therefore, monomer units containing single

nucleobases for binding generally exhibit degrees of interaction too low to form

polymers through the *MSOA mechanism* in solution. However, of the natural

nucleobases, homo-oligomers of guanine derivatives are perhaps the most diverse.

The presence of two complementary hydrogen bonding arrays, a donor/donor site

comprised of the N^1H amide and N^2H amine and an acceptor/acceptor site comprised

of the O^6 and N^7 functionalities, allows it to oligomerize via hydrogen bonding. This

supramolecular arrangement combined with the strength of the interaction (K_{GG} ca.

10^2-10^4 M^{-1} in CDCl$_3$), makes it the most studied homo-nucleobase interaction.

Guanine derivatives can utilize hydrogen bonding to self-assemble into either linear

tapes[90] or macrocycles. **Figure 2-7** shows an example of a guaninebased linear tape

that self–assembles through Hoogsteen interactions. The other possibility is for the

self-assembly to result in macrocycles. In fact, guanine is well known to self-assemble into hydrogen-bonded cyclic tetramers, the so-called G-quartet, in the presence of metal ions (**Figure 2-7**).

On the other hand, non Watson–Crick binding modes, such as the Hoogsteen motif, can be exploited to assemble architectures that are not possible to access via simple Watson–Crick base pairing. Further, the aforementioned binding modes can be used in conjunction with other intermolecular forces to prepare synthetic molecular cages and supramolecular polymers. Indeed, a number of supramolecular architectures assembled through non Watson–Crick base-pairing interactions will be highlighted in some examples within this article.
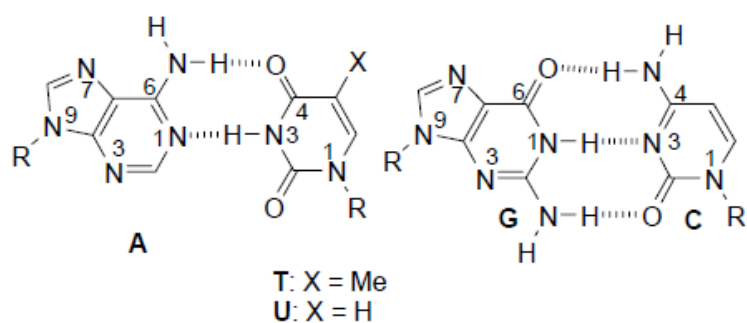
Figure 2-4. The canonical Watson-Crick hydrogen bonding motifs.

(a) Reverse Watson-Crick mode

A-T   Reverse Watson-Crick   G-C
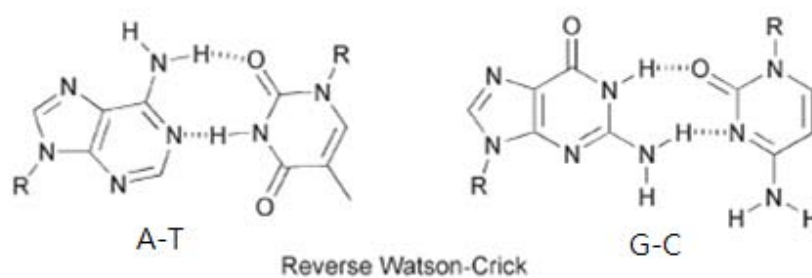
(b) Examples of Hoogsteen and Reverse Hoogsteen base-pairs

A-T Hoogsteen   A-T Reverse Hoogsteen
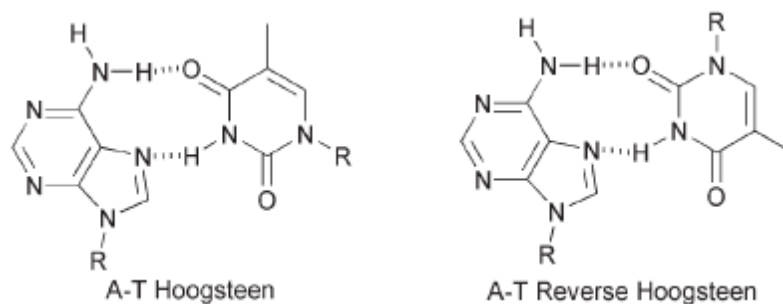
(c) Two Wobble (Mismatched) base-pairs and an Reverse Wobble base-pair

G-T Wobble   G-A Wobble   G-T Reverse Wobble
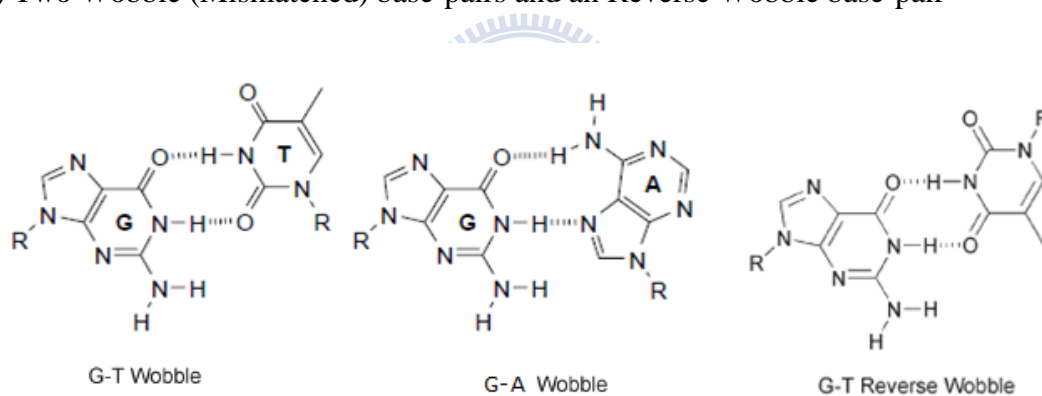
(d) Self-dimerization (homo-dimerization)

Self-dimerization (GG)
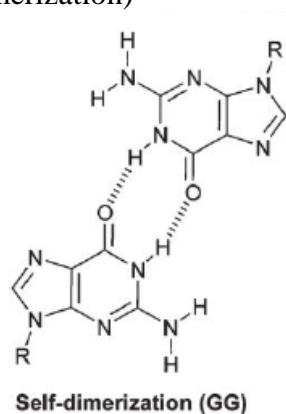
Figure 2-5 Some common non Watson–Crick (non-traditional) base-pairing modes

UAU base triplet (Watson-Crick and Hoogsteen)

Hoogsteen · Watson-Crick

G-G-C trimer
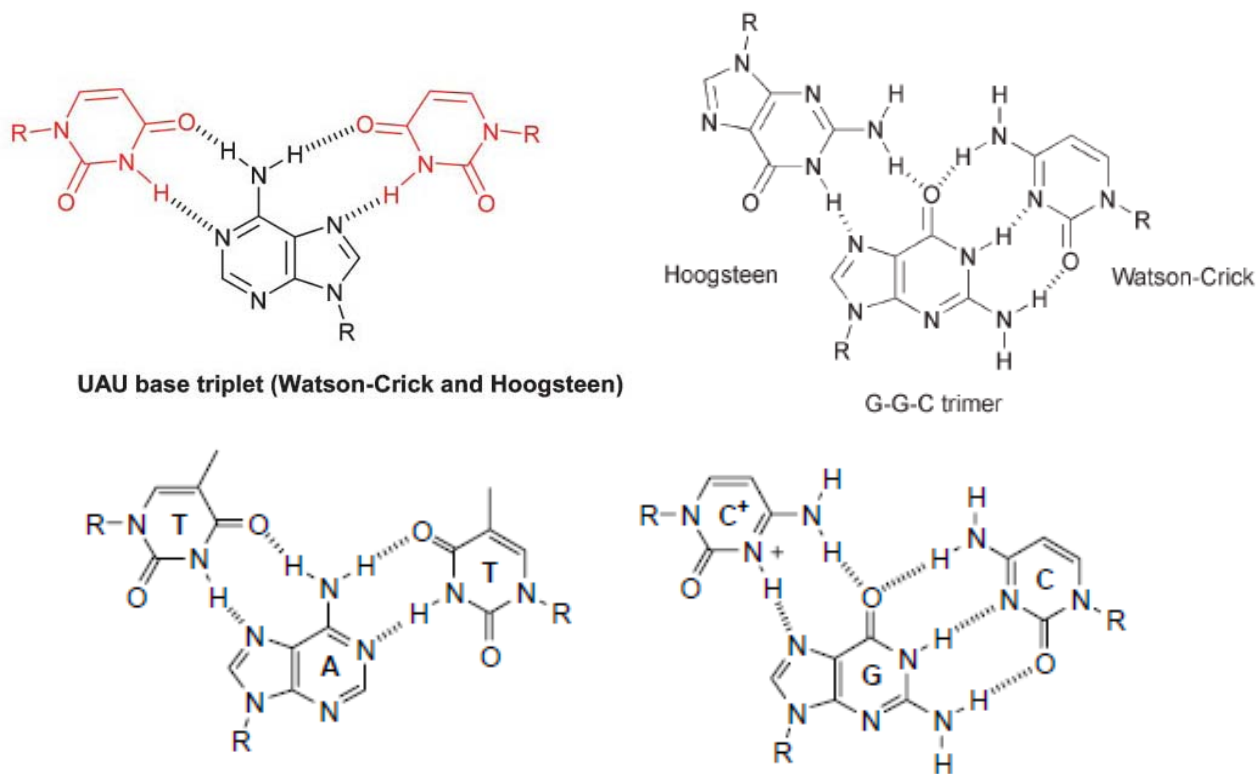
Figure 2-6 Some Examples of base-triplets as a combination of different forms of base-pair binding modes.

(a) G-Ribbon

(b) G-quartet

(c) G-quadruplex

(metal ion)
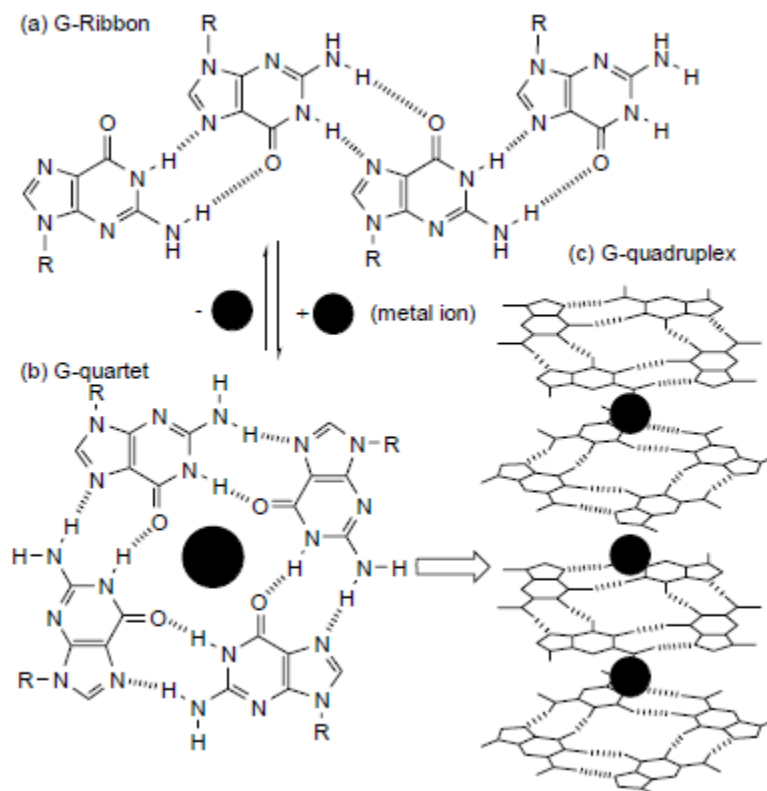
Figure 2-7 Self-assembly of guanine derivatives into (a) G-ribbon, (b) G-quartet, and (c) G-quadruplex formed by stacking of G-quartets around a column of cations.

2-3 An overview on Supramolecules

2-3.1 Basic Principle of Supramolecules

"Molecular Chemistry" and "Supramolecular Chemistry" is two famous topic in recent researches. Research related to molecular chemistry is mainly focus on the interaction between molecules; and supramolecular chemistry, earliest investigate by J.M. Lehn[91-92] and also called chemistry superior than molecular, is a research field study on non-covalent bonding among molecules. The formation of supramolecules is mainly due to the intermolecular interaction and thus make two or more chemical compounds combine with each other to form highly complex but ordered structures. (see **Figure 2-8**). These specific supramolecules not only owns the characteristics of original monomers but also with new forming structures and physical properties. Supramolecules forms mainly via self-assembly and molecular recognition. The novel sturctures and properties provide fancy ways of thinking and challenges on the molecular design and applications in real products, therefore, supramolecules fix everyone' eyes on and developed prosperously in recent decades.
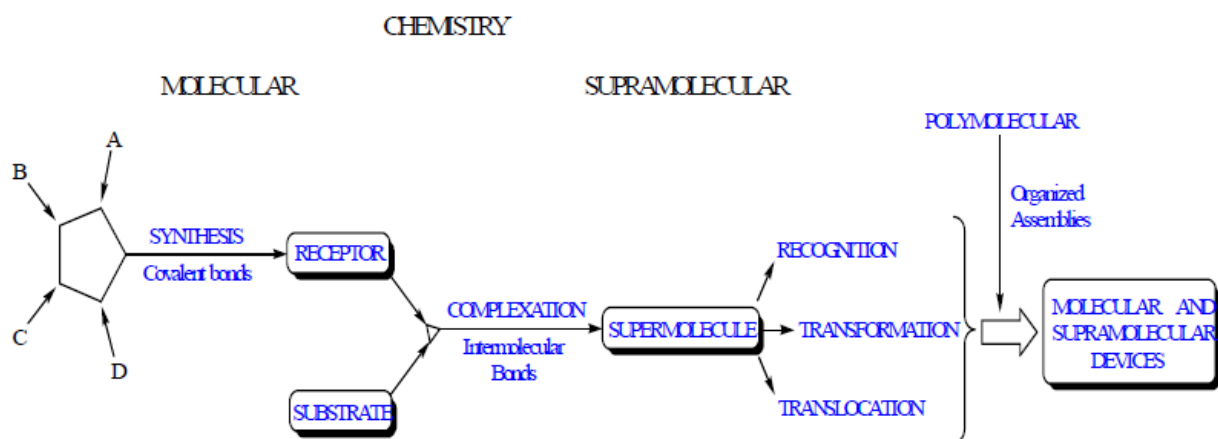
Figure 2-8. The route from "Molecular Chemistry" to "Supramolecular Chemistry."

In fact, supramolecules exist not only in artificial systems but do also exist in living organisms and human bodies. For example, highly complex and effective

molecules is everywhere in living organisms. The interactions between molecules control almost all the specificity, regulation of human body function, and mechanisms of specific reactions within biochemical processes. Such as the bonding between substrate and specific receptor, enzyme catalytic, complex combination within proteins, the recognition and combination of antigen and antibody in immune systems, storages and translations of genetic codes in DNA, and even the message transfer and feedback controls in cells. Scientists design easier and simplified supramolecular models from biology systems, which is called biomimetic or biomimic systems. Also, the principles of self-assembly and molecular recognition can be further apply in material sciences.

2-3.2 Basic Principle of Recognition in Supramolecules

The assembly and combination of supramolecules includes the recognition process which storage the molecule messages within the structures. Therefore, the recognition process has a remarkable influence on the structure and properties of supramolecules. As for supramolecules, the driving forces of the fabrication of supramolecules can be simply categories as followings:

(I) Hydrogen bond:

Hydrogen bonding is quite suitable for the construction or stabilization of non-covalent bonding molecular and the framework of supramolecules since the highly orientation and directional selectivity. The most evident example is the DNA and protein structures within living organism and human bodies. The recognition process of hydrogen bonds are not only vital interaction in biological systems but also an efficient tool for artificial design and synthesis of self-assembly systems. Many hydrogen bonding models has been reported in articles to synthesize and stabilize the molecule structure. For example, a simple system designed by A. Hamilton illustrated in **Figure 2-9** forms through the six-point complementary hydrogen bonding among

host-guest molecules and gives rise to a highly stable complexes after the mix of host and guest molecules.

The hydrogen-bonding interactions in terms of complementary recognition can be broadly classified into self-complementary and heterodimer recognition. Generally, in a self-complementary system, the hydrogen bonded units are attached covalently to the polymer backbone and exhibit a strong tendency for self-association resulting in interchain association. Hydrogen bonds has been utilized in many research fields to design the architectures of solid state materials due to its highly orientation and direction selectivity. These include non-linear optical materials, organic conductors, organic and inorganic ferromagnetic materials, and solid state reaction materials.
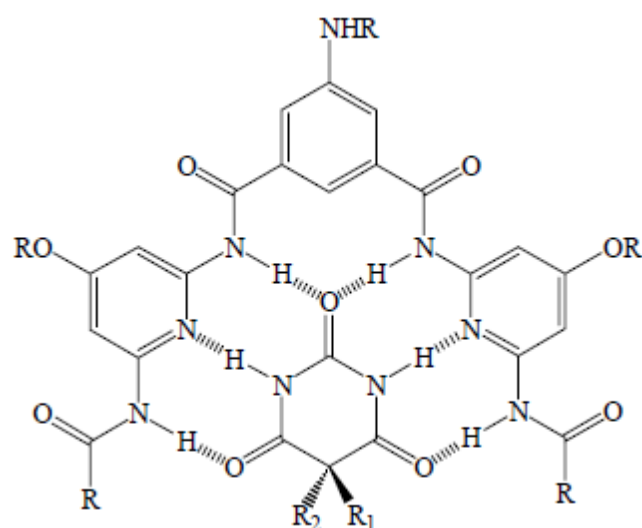
Figure 2-9 Supramolecules form through multiple hydrogen bonds.

(II) Recognition via π- π interaction

Systems form by the recognition of π- π interaction usually contain electron-rich and electron-deficient aromatic rings. Charge transfer occurs between two types of aromatic rings mention above and give rise to large ring systems by mutual chain crosslink between ring and rings. These π- π interaction stabilize molecular structures as shown in **Figure 2-10**.
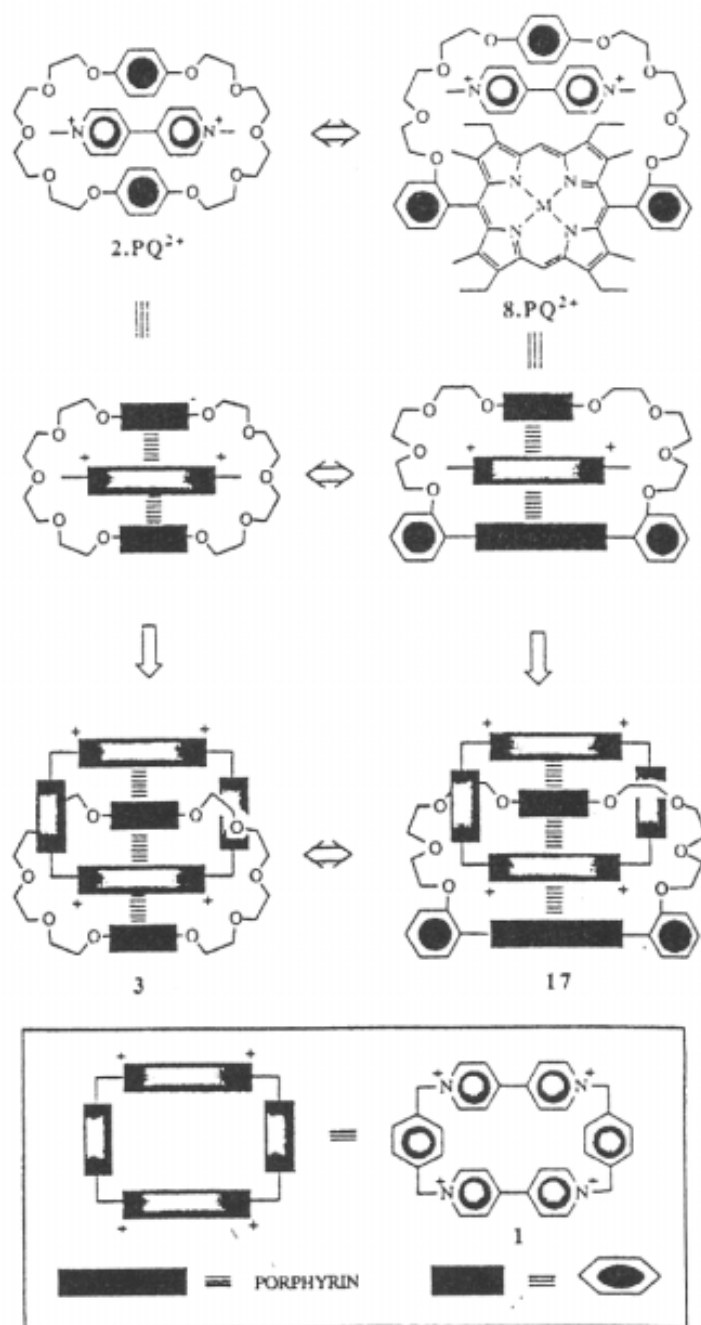
Figure 2-10 large ring system form via π- π interaction and crosslink between rings.

(III) Coordination bond

Most of these kind of molecules are inorganic complexes forms through the designed interaction between multiple ligands and transition metals. Inorganic complexes with specific conformation can be obtained via the design of appropriate multiple ligands since the specific geometric conformation and coordinate

numbers of transition metals. This kind of inorganic is called "Metallosupramolecules" and owns not only the properties of supramolecules but also physical or chemical properties different from general organics due to the natural of central metal molecules. Thus, metallosupramolecule has many additional special properties such as magnetic, catalytic, and electro-optical properties and utilities in real applications.

2-3.3 An overview of Supramolecular Materials

Supramolecular materials permit a rapid response to a change in environment whilst their strength and selectivity can be controlled easily by synthesis strategy. A perfect example is the assembly and disassembly[93] of structural motifs such as DNA–fundamental to translation and transcription in biology. The requisite structures are formed by non-covalent interactions where and when they are needed, and then disassembled when their biological objective is complete. Synthesis of polymers by linking the monomers via non-covalent interactions, or of polymer networks by using non-covalent interactions of functionalized side chains, would therefore represent an attractive approach to the construction of stimuli-responsive soft materials (**Figure 2-11**).[94,95] However, only recently has supramolecular chemistry evolved to a stage where this paradigm can be explored, with building blocks now widely available that (a) are easy to make in multi-gram quantities and (b) interact in a defined manner with sufficient strength.

Although the area of self-assembly of molecules into one-dimensional multicomponent structures has been known for decades, it is only the recent date that the supramolecular polymers attract a steadily increasing interest due to the fact that they exhibit unprecedented and highly useful properties. More recently, Meijer and co-workers established series of supramolecular polymers exhibiting mechanical

properties that were thought to be reachable only with covalently linked monomers in macromolecules.[95] The material shown in **Figure 2-12** is from a supramolecular polymer built by the reversible linking of repeating molecular units by quadruple hydrogen-bonded end groups. The relatively higher association constant (K_a) and self-complementary units are responsible for excellent mechanical properties while the reversibility takes care of the ease in processing at elevated temperatures.

Supramolecular interactions such as hydrogen bonding, ionic interactions, metal coordination, electrostatic interactions, and stacking can be used individually or in concert with one another to obtain homofunctionalized or multiply functionalized polymers. These noncovalent synthetic strategies can be advantageous over covalent analogues for several reasons:[97] (a) It can form well-defined molecules with intermediate structural complexity. (b) The multiple copies of one or several of the constituent molecules, or of polymer can be employed to simplify the synthetic task. (c) The noncovalently functionalized polymers have the ability to self-heal due to the reversibility of noncovalent bonds. (d) A generic polymer backbone can be used to obtain a library of fully functionalized polymers. (e) Different types of noncovalent interactions are orthogonal to one another, while many covalent modifications are not. (f) Such polymers are highly responsive to external stimuli. Aside from simply adding functionality to a polymer, this approach also allows for the tuning of bulk properties such as morphology or the degree of crosslinking. In this thesis, our research emphasis will follow the above by examining the influence of noncovalent functionalities on polymer properties and applications.
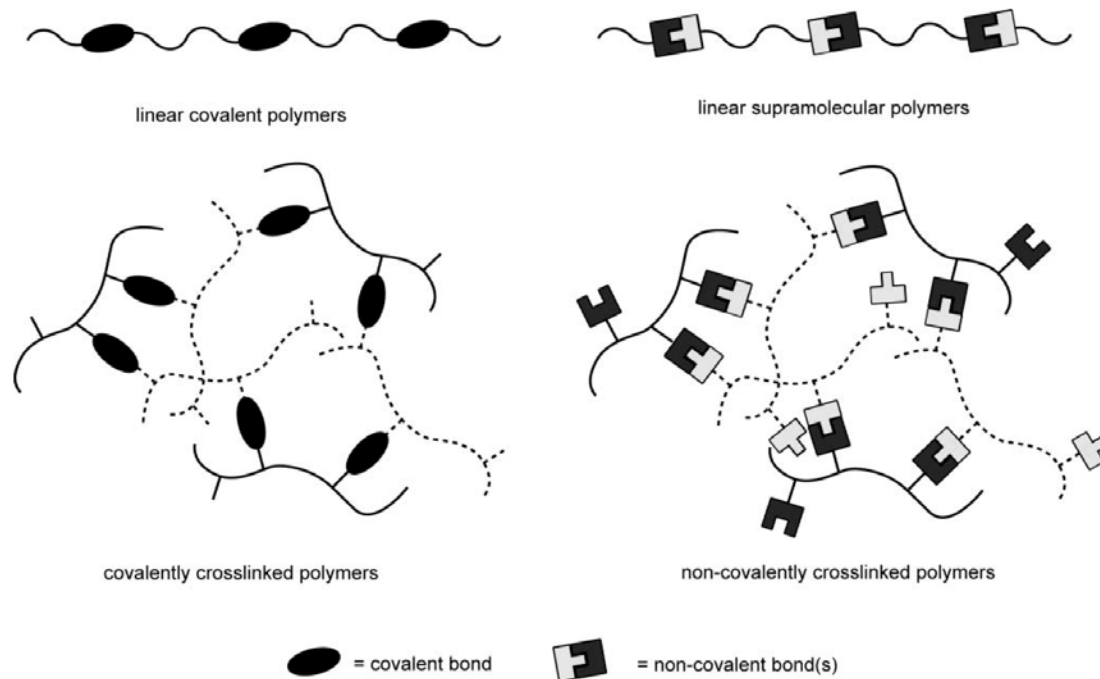
Figure 2-11: Cartoon representations of polymer architectures made using covalent and non-covalent links between building blocks.
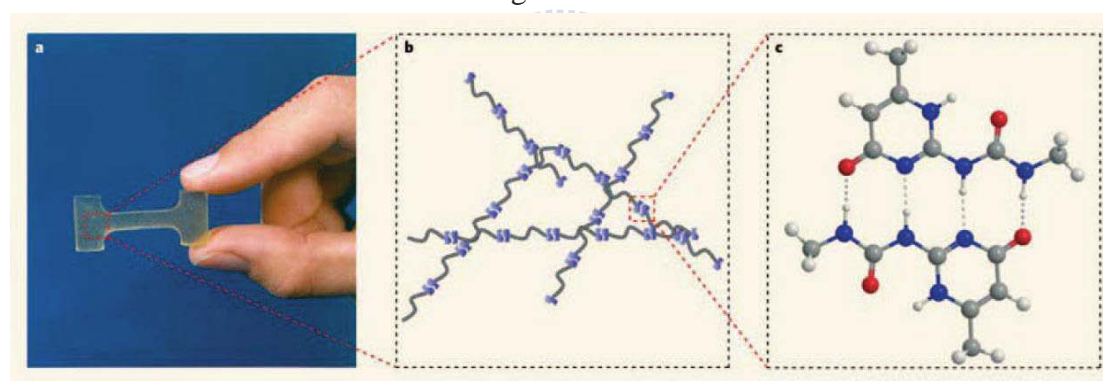
Figure 2-12: (a) Supramolecular polymeric material based on a low molecular weight compound equipped with two ureido-pyrimidinone (UPy) units. (b) Schematic picture of the underlying polymeric network. (c) Schematic picture of the self-complementary UPy dimer.

2-3.4 Supramolecular Chemistry

The directed association of synthetic molecules into defined architectures is the area of supramolecular chemistry, which is also known as chemistry beyond the molecule.[98] Much of the field of supramolecular chemistry finds its origin in the remarkable observations such the research on crown ethers, spherands, and carcerands from Pedersen,[99] Cram,[100] and Lehn,[101] respectively. Their studies allowed for the

development of numerous synthetic binding motifs for the orientation of a guest molecule into a host molecule through specific interactions. These host-guest complexes display size and shape selectivity formed through compounds such as crown ethers (host) and ammonium salts or small organics (guests).[102]

Supramolecular chemistry concerns with intermolecular interaction forces and the interplay between the energy of association (enthalpy) and the penalty for the loss of degrees of freedom (entropy) after association.[103] The intermolecular interactions involved in constructing supramolecular aggregates are of a non-covalent nature and are, as a result, weaker than conventional covalent bonds (Table 2-2).[104] Due to the reversibility of these weak interactions, however, large structures can be assembled via a self-organization process. **Table 2-2** is a wealth of different available interactions with interaction energies ranged from 4 to 400 kJ mol^{-1}. It focus was mostly focused on hydrogen bond interactions, interactions between electropositive or acidic hydrogen and other electronegative or basic atoms. Hydrogen bonds are similar to both dipole–dipole and ionic interactions in terms of interaction energies ranged from 4 to 120 kJ mol^{-1}.

The use of each non-covalent interaction has its own advantages and chosing the type of interaction should be considered carefully. For example, although metal-coordination is directional and strong, the strength of the interaction often restricts its dynamic nature and consequently reversibility. Coulombic interactions between ionmers on the other hand suffer from the fact that these interactions are non-directional in many cases, giving rise to aggregation. Solvophobic interactions have the same limitations and are generally weak in solvents other than water. Although (multiple) hydrogen bonds are not the strongest noncovalent interactions, they hold a prominent place in supramolecular chemistry due to their synthetic accessibility and directionality, and because they allow for the tuning of binding

constants between $10\text{-}10^9 \ M^{-1}$ in organic solvents.[105]

Interactions	Energy / kJ mol^{-1}
ion–ion	50–400
ion–dipole	50–200
hydrogen bond	4–120
dipole–dipole	4–40
π–π stacking	4–20
dispersion	4–20
solvent effects	4–40

Table 2-2: Some selected non-covalent interaction energies useful in supramolecular chemistry[104]

2-3.5 Supramolecular Polymerization

Supramolecular polymerization,[106-108] *i.e.,* the self-assembly of polymer-like materials through the utilization of the non-covalent bond, has been a developing area of research over the last decade. One aspect of this field entails the use of non-covalent interactions between small molecules to induce the formation of polymeric materials[109-117] and nano-particles. Such supramolecular polymerization potentially results in the materials exhibiting a number of interesting properties: 1) they form spontaneously, without the need for an initiation process (or catalyst); 2) they are 'dynamic' *i.e.,* are formed under reversible conditions, thus imparting the potential of such materials to be thermally self-repairing; and 3) termination processes during the polymerization (self-assembly) are limited given the absence of impurities. As a result, the degree of polymerization depends, to a large extent, on the strength of the supramolecular interaction between the monomers and the monomer concentration. If growth of the supramolecular polymer operates through a *Multi-Stage Open Association (MSOA)* mechanism, where the binding constant is independent of the molecular weight (each monomer has an identical binding constant

at each step of polymerization, i.e. no cooperativity) and no ring formation is occuring, the extent of growth may be related to the probability that a monomer has reacted according to the Carothers equation

$$DP = 1/(1-p) \tag{1}$$

where DP is the number-average degree of polymerization and p is the percent of bound monomer. In this case, given the binding constant is independent of molecular weight, the DP will be proportional to $2(K_a[M])^{1/2}$ where K_a is the binding constant and [M] is the total concentration of monomers. As such, large values of K_a are generally required to obtain aggregates of significant molecular weight. For example, at 1 M monomer concentration, a $K_a > 10^4 \, M^{-1}$ is required to obtain a DP of 200.

2-4 Nucleobase Hydrogen Bonding as Applications in Polymer Material Systems

2-4.1 Nucleobases in Polymeric and Material Systems

The self-assembly of two single-stranded oligonucleotides into a double stranded helix is driven by many intermolecular forces. These include aromatic p-stacking interactions, hydrophobic forces, van der Waals forces, and hydrogen bonding interactions.[118] Of these forces, the self-complementary Watson–Crick hydrogen-bonding interactions[119] that dictate specific base-pairing are arguably the most crucial for establishing the fidelity required for efficient storage, replication, and transcription of genetic information. The question then arises whether hydrogen bond driven base-pairing can be used for purposes other than those intended by nature. Indeed, base pairing within long chain DNA oligonucleotides and artificial nucleic acid base (''nucleobase'') derived polymeric systems can be used to assemble elegant macroscopic structures. Not surprisingly, these systems are attracting considerable current interest as a result of their possible applications in materials chemistry and nanotechnology.[120] Smaller synthetic systems, of a mainly non-biological nature but also inspired by the complementary hydrogen bonding concept embodied in DNA have also been intensively studied.[121] Our entry into this fascinating branch of supramolecular chemistry came from a desire to use the base-pairing paradigm of individual nucleobases as a means of preparing novel synthetic suprastructures. Other investigators have also taken a similar approach and have succeeded in preparing new synthetic structures, many of which are quite elegant.[122] In this article we will also highlight some of these contributions, but will focus primarily on retracing the work carried out in our laboratory.

Molecular organization via the formation of complementary hydrogen bonding provides a powerful tool for creating well-defined nanostructures. These materials utilize non-covalent interactions similar to those found in biological molecules such

as protein, DNA, and RNA, to direct and modulate their 3-D topology. Multiple-hydrogen-bonding interactions, which are moderately strong and highly directional, lead to the biomimetic polymer with unique physical properties, such as high specificity, controlled affinity, and reversibility. However, controlling the supra molecular polymer with secondary (and higher) bonding through specific interactions from different hydrogen-bonding motifs remains a challenge task. Thus, the combination of non-covalent interactions and their higher structures at the molecular level is a key to appending further function in the design aspect of bio-inspired macromolecules.

In order to utilize the complementary nature of nucleobase pairs, numerous reports regarding the effect of the placement of chain ends on polymers or small molecules using supramolecular motifs on material properties have been reported.[124] One of the most elegant and successfully employed motifs for supramolecular polymerization is the quadraple hydrogen-bonding ureidopyrimidone developed by Sijbesma, Meijer and co-workers which strong self-dimerize through four hydrogen bonds arranged in doner-doner-acceptor-acceptor sites.[125] However, in the last section of this literature review we will focus on some recent developments where single nucleobase interactions are used to control the self-assembly of new materials.
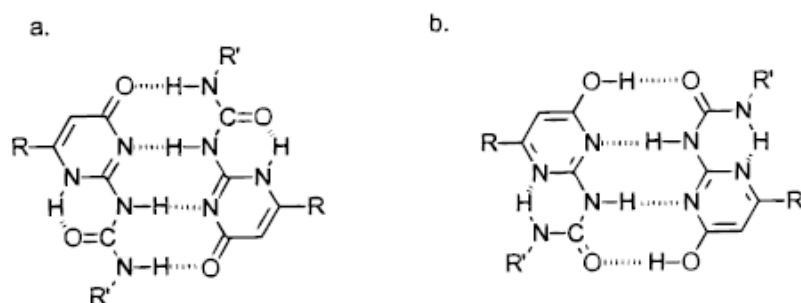
Figure 2-13. Modes of dimerization of the UPy functional group via quadruple hydrogen bonding: keto tautomer (a) and enol tautomer (b).

2-4.2 Chain-End Nucleobase Modified Monomers and Polymers

Over the last decade the area of supramolecular polymerization, i.e. the self-assembly of small monomeric units into polymer-like materials through the use of the non-covalent bond, has received a growing amount of attention.[126] In an effort to utilize the complementary nature of the nucleobase hydrogen bond interactions there has been a number of investigations aimed at examining the effect that placement of such supramolecular motifs on the ends of small molecules or polymer chains has on the organization of the systems and subsequently its material properties. Conceptually, a very simple way to achieve supramolecular polymers is by the attachment of appropriate supramolecular motifs on to the ends of a core unit. The backbones of the resulting polymeric systems will therefore contain non-covalent bonds, in addition to covalent bonds, which imparts upon the system reversibility and temperature sensitivity. This behavior, in turn, offers the potential of developing "easy to process" polymeric materials. One interesting opportunity offered by such systems is the ability to self-assemble functional units into processable polymeric materials, which, for example, exhibit desirable electronic and/or optical properties.[127] The properties of such non-covalently bound aggregates have a strong dependence not only on their functional core components but also on the nature (stability and dynamics) of the supramolecular interactions which control the self-assembly process. In addition, if the supramolecular motif used in the assembly of the polymer is asymmetric (i.e. consists of two different complementary units) then the supramolecular polymer will only be formed when both of these complementary units are present. A heteroditopic monomer, in which both complementary units are placed on the same molecule, will result in a self-assembling $(A-B)_n$ polymer (**Figure 2-14a**). However, homoditopic monomers, which only have one of the complementary units placed on each monomer (e.g. A-A or B-B) and results in $(AA-BB)_n$ type model

(**Figure 2-14b**), will only exhibit polymerlike properties upon mixing of the two complementary monomers. In such case, there exists the potential that the formation of the supramolecular polymer will result in the expression of new functional properties not exhibited by the individual monomers, such as the viscosity of new formed supramolecular polymer usually increases after hydrogen bonding complexes. Another significant example of such a supramolecularaided function is the growing area of supramolecular liquid crystalline materials.[128-130] Molecular anisotropy is important for the formation of a liquid crystalline phase. For example, rigid and semi-rigid molecules which have a high axial ratio often exhibit liquid crystalline behavior. Therefore, the self-assembly of small (semi)rigid units into a larger linear array, with a high aspect ratio, can result in the formation of liquid crystalline materials.[131-134] The induction of a LC phase in such a case is a 'macroscopic expression of the molecular recognition' designed into the molecules. Furthermore, the formation of an LC phase with long range order will aid the formation of higher molecular weight aggregates.[135,136] If a specific designed system contains two different cores that have different, yet complementary nucleobase sequences at their termini, the resulting system should assemble into a very precise $(AB)_n$ copolymer (**Figure 2-15**). Such supramolecular mentioned above systems have potential applications as the next generation of materials in a wide range of fields such as information storage[137], mass or charge transportation[138], and molecular sensing[139].

Shumizu and coworkers has reported the preparation of nucleobase-appended bolaamphiphiles (without the phosphate sugar component) with thymine or adenine residues separated by oligomethylene spacers (**Figure 2-.16a**). In this case, the molecules self-assemble in water to produce supramolecular nanofibers in a crystalline state without forming a hydrogel.[140] The thymine bolaamphiphile (**T-10-T**) produced interesting doublehelical ropes in 10% ethanolic/aqueous solutions. These

ropes are thought to be initiated by a small amount of macrocyclic dimers [cyclo(**T-10-T**)$_2$] which are formed via thymine photodimerization. The adenine-appended **A-10-A** did not form fibers by itself however nano-fibers were formed from an equilmolar mixture of the homoditopic **T-10-T: A-10-A** as well as from the heteroditopic **A-12-T**. X-ray studies of these materials containing the complementary nucleobases is consistent with the formation of a multilamellar arrangement in the solid-state with nucleobase interactions extending the chain length and a combination of hydrogen bonding through the amide linkers and nucleobase $\pi-\pi$ stacking between the chains (**Figure 2-16b**).
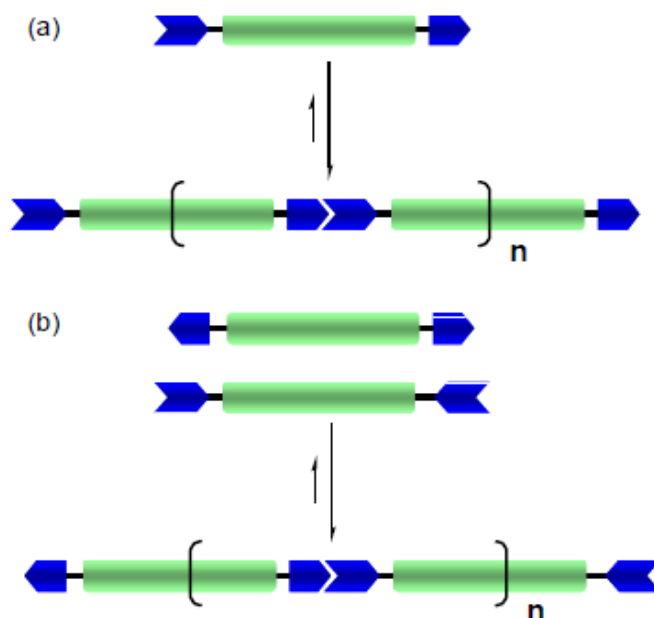
Figure 2-14: Schematic representation of two different types of supramolecular polymers which are formed by the association of monomers with complementary end groups. (a) Self assembly of a heteroditopic monomer to yield a (AB)$_n$ supramolecular polymer and (b) self assembly of two complementary homoditopic monomers to yield a (AA-BB)$_n$ supramolecular polymer. The dynamic nature of these polymers allows them to break and recombine in response to changes in the environment.
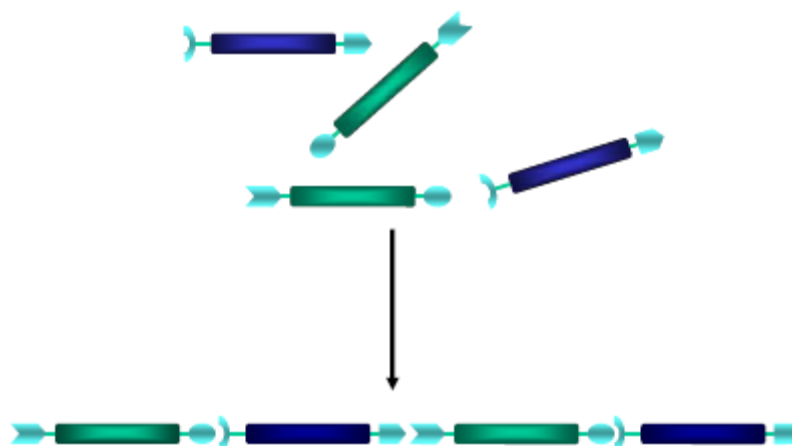
Figure 2-15. Self-assembly of monomers with different but complementary endgroups resulting in an (AB)$_n$ copolymer.
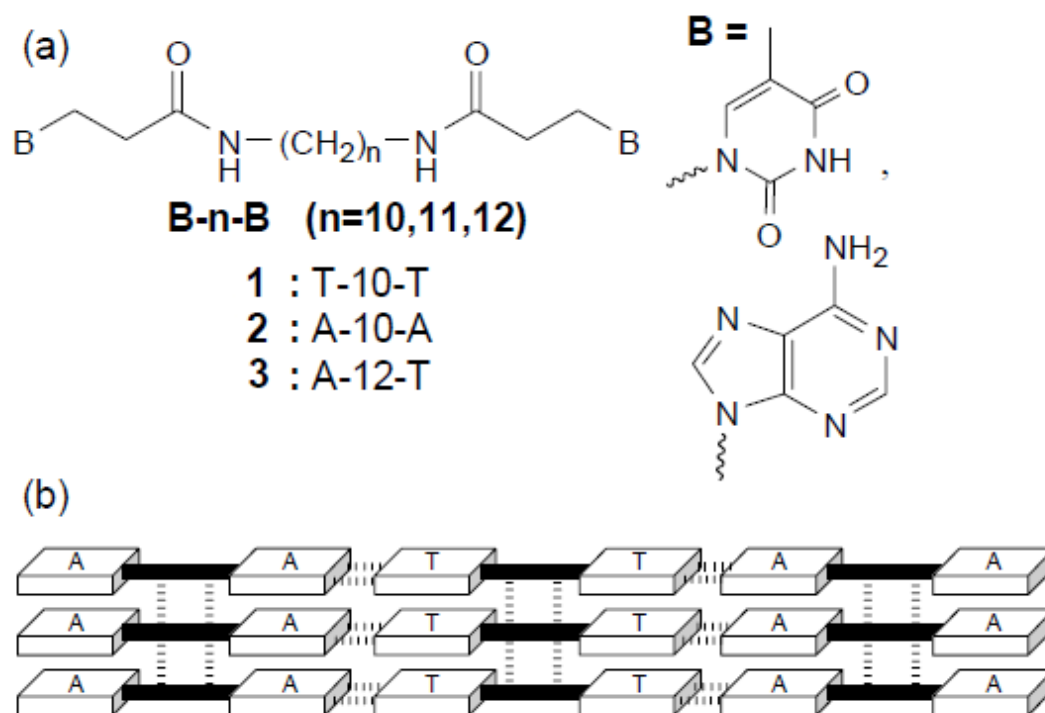
Figure 2-16 (a) Nucleobase terminated bolaamphiphiles and (b) a possible hydrogen bond scheme for the heteroassembly formed from an equimolar mixture of **1** and **2**.

The utilization of the nucleobase interactions in supramolecular chemistry offers the opportunity to prepare precise self-assembled architectures,[142] and allows

51

for the exploitation of different units, all of which offer various binding motifs.[143]

Sivakova and others, have shown that the placement of a single nucleobase at either

end of a chain results in dramatic changes in material properties.[141,144–146] To this end,

homoditopic monomers (**Scheme 2-2**) in which the nucleobase thymine (**T**) and the

nucleobase derivative N^6-(4-methoxybenzoyl) adenine ($\mathbf{A^{An}}$) are substituted on both

ends of an alkoxy-substituted bis(phenylethynyl)benzene core ($\mathbf{B^P1aB^P}$ and $\mathbf{B^P1bB^P}$,

$\mathbf{B^P}$=nucleobase derivative) have been designed. Thus, this system should exhibit

polymer-like properties only upon mixing of the complementary monomers. Not

surprisingly, derivatization of the ends of the alkoxy-substituted bis(phenylethynyl)

benzene cores with thymine units results in a significant reduction of the temperature

range in which these materials exhibit liquid-crystalline behavior, primarily through a

dramatic increase in the primary melting temperature. $\mathbf{T1aT}$, $\mathbf{T1bT}$, and $\mathbf{T^{Me}1aT^{Me}}$

displays a liquid-crystalline phase over a narrow temperature range, but at much

lower temperatures, clearly revealing the importance of thymine hydrogen-bonding in

determining the primary melting point.

(a) Br(CH₂)ₙBr [n=6,9], K₂CO₃, THF; (b) **B^P**H, NaH, DMF; (c) Pd(PPH₃)₄, CuI, DIA, Toluene.

Scheme 2-2. Synthesis and structures of the homoditopic (A-A, B-B) nucleobase terminated bis(phenylethynyl)-benzene monomers. ($\mathbf{B^P1aB^P}$ and $\mathbf{B^P1bB^P}$). $\mathbf{B^P}$=nucleobase derivative.

Scheme 2-3. Synthesis of the supramolecular telechelic macromonomers $\mathbf{C^{Pbz}43C^{Pbz}}$, $\mathbf{G^{Cbz}43G^{Cbz}}$, $\mathbf{A^{An}43A^{An}}$, **T43T**, **BIP43BIP** and **H43H**.

In addition, previously in the S. J. Rowan group at Case Western Reserve University, we have designed and synthesized a series of low molecular weight poly(tetrahydrofuran) functionalized with nucleobase derivatives (thymine and *N*-protected adenine, cytosine and guanine) which are homoditopically connected via an amide linkage to both ends of a bis(3-aminopropyl) terminated

poly(tetrahydrofuran) chain. The desired supramolecular macromonomers were achieved by reacting the appropriate acetic acid nucleobase derivative (either thymine (**41T**), N^6-(4-methoxybenzoyl)-9-(carboxymethyl)adenine (**41A^{An}**), 1-(carboxymethyl)-N^4-(4-tertbutylbenzoyl) cytosine (**41C^{Pbz}**), or 2-(N-[benzyloxycarbonyl])-N^2-(carboxymethyl)guanine) (**41G^{Cbz}**) with the bis(3-aminopropyl)terminated poly(tetrahydrofuran) (**42**) chain using mixed anhydride peptide coupling conditions (**Scheme 2-3**).

The attachment of the nucleobase derivatives on to the ends of the low molecular weight *bis*(3-aminopropyl) terminated poly(tetrahydrofuran) resulted ina marked change in the properties of the resulting materials. Most of the melting temperature (T_m) changes from ca.20℃ to ca.180℃.
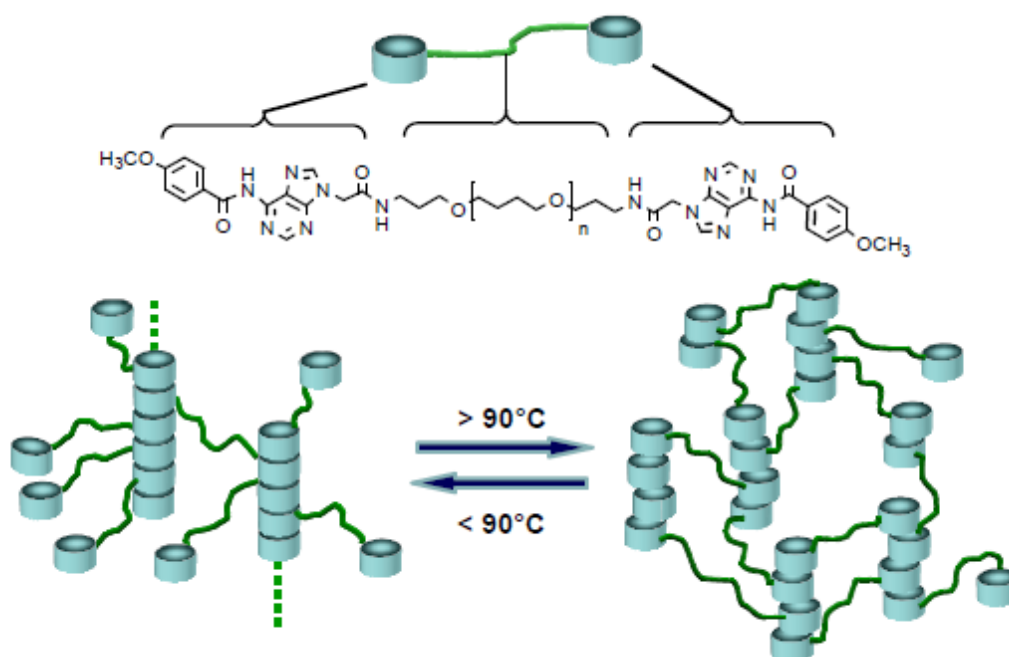
Figure 2-17. Schematic model of the **A^{An}43A^{An}** assembly as it transitions at 90 ºC from a linear system to a gel-like material. The schematic shows the segregation of the nucleobase hard segments [blue disks] connected by chains of poly(tetrahydrofuran)s [green lines].

While the mechanical properties of the **C^{Pbz}43C^{Pbz}** and the **A^{An}43A^{An}**

macromonomers allowed the melt processing of self-supporting films, these materials did behave very differently from each other. The films of $C^{Pbz}43C^{Pbz}$ were flexible while the films of $A^{An}43A^{An}$ were of a more brittle nature and easily developed cracks under stress. We believed that the distinct properties of these two films were a consequence of the different nature of the self-assembly induced by the two chain-end nucleobase derivatives.

2-4.3 Side-Chain Nucleobase Modified Polymers

As well as functionalizing chain ends of a polymer, it is also possible to place nucleobases on polymer side-chains. For side-chain architectures, these proton donors and acceptors are appended to polymers that have main chains in forms of homo- or block copolymers , and which the self-assembly occurs via hydrogen bonding interaction, usually in multiple fashion(**Figure 2-18**). Binding of polymers, nanoparticles, or other nanosized objects, has become a new area of research in nanotechnology. Rotello and co-workers have investigated this area utilizing side chain functionalized low molecular weight polystyrene copolymers containing randomly dispersed chloromethylstyrenes along the polymer backbone which served as functional handles and were reacted with recognition copolymers. These copolymers could then be functionalized non-covalently using hydrogen bonding. To speak more in detail, side chain functionalized low molecular weight polystyrene was utilized through the three hydrogen bonded thymine/diamidopyridine supramolecular motif. For example, the low molecular weight polystyrene which is derivatized with diamidopyridine units (**2a**) can be non-covalently crosslinked with bis-thymine units (**2b**).[147] Upon combination in noncompetitive solvents, discrete and stable micron-scale spherical aggregates were formed arising from specific three-point polymer-crosslinker hydrogen bonding interactions. (**Figure 2-19a**). The diameter of

these gel microspheres could be controlled by varying the length of the spacer in the crosslinker. The cross-linking process was fully thermally reversible, with complete dissolution observed at 50°C and reformation of the aggregates upon return to ambient temperature. This process could be repeated, with lower particle dispersity observed as a result of annealing. If thymine is itself attached to the side chain of the low molecular weight polystyrene polymer (**2c**), then addition to **2a** results in slightly different behaviour with the formation of spontaneously self-assembling giant vesicles (**Figure 2-19b**).[148] These recognition-induced polymersomes (RIPs) form through very specific interactions between the complementary random copolymer chains and thus are sensitive to the presence of units which contain the complementary supramolecular motif. For example, addition of monovalent imide guest **2d**, results in an initial swelling of the RIPs before the vesicles dissociated due to competitive binding of the small molecule guest resulting in decrosslinking of the polymers. Incorporation of multivalent guests was also investigated by adding gold nanoparticles which have about *ca.* 10 thymine units on their surface per nanoparticle. Here a contraction is observed in the size of the vesicle as the nanoparticle is incorporated. This behavior was shown to require the supramolecular interaction as nanoparticles containing a methyl group on the N^3 of the thymine units show no incorporation into the vesicles. The most importantly, such side-chain strategies have become a critical component of polymer science and are expected to expand further in the future.

When contemplating nucleobase interactions, it is common to consider only the Watson-Crick base pair, but over the years research from a variety of different disciplines has shown that nucleobases are much more versatile with their non-covalent interactions. The ability to further understand how nucleobases interact

with not only each other but also with other molecules will not only allow the construction of systems which can bind more specifically to targeted DNA sequences but also how we might be able to harness these interesting biological molecules to construct complex nanostructures and materials.
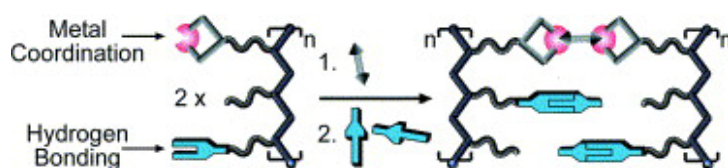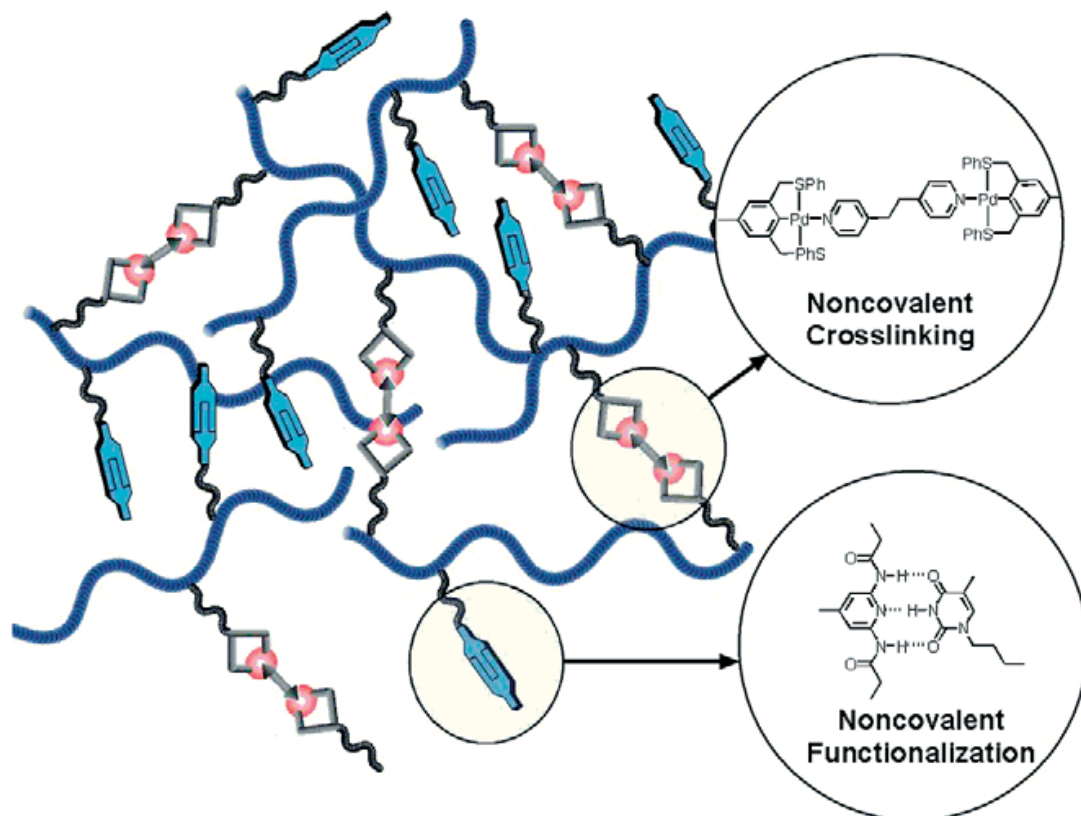
Figure 2-18. A cartoon depicting multi-step self-assembly via metalcoordination based cross-linking and polymer functionalization via hydrogen-bonding.
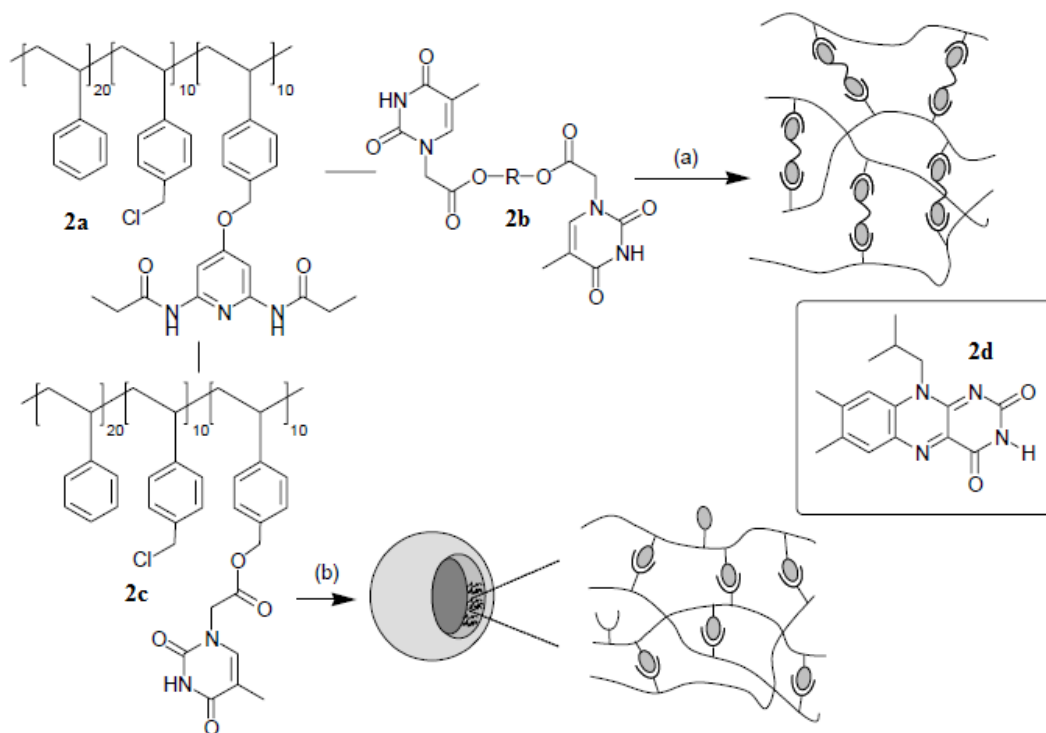
Figure 2-19. (a) Schematic illustration of noncovalent polymer cross-linking of copolymer **2a** using a complementary bifunctional cross-linker **2b**. (b) Schematic representation of the diacyldiaminopyridine – and thymine-based random copolymers, **2a** and **2c,** as assembled in three dimensional vesicles.

2-4.4 Supramolecular Block copolymers

Self-assembled polymers such as block copolymers are usually formed through covalent linkages in traditional polymer chemistry, including bonds connecting monomer units and attaching functional groups to the polymer backbone. Block copolymers constitute a special class of material capable of self-assembling into a series of long-range ordered nanostructures owing to their mutual incompatability.[149] Polymers with comb-shaped architecture also display the propensity to self-organize due to repulsion between the backbone and the short side chains.[150] A variety of order nanostructure can be constructed if the comb architecture is introduced into the block copolymer by selectivity complexing one of the blocks in a coil-coil diblock copolymer with surfactant(**Figure 2-20**, **Figure 2-21**).[151] Recently, novel structural

organizations of self-assembled polymers formed through highly directional and sufficiently strong noncovalent host-guest pairs have attracted great attention. During the past few years, several reports regarding the incorporation of nucleobase functionality into main- and side-chain polymers mediated by complementary hydrogen bonds (arrays of hydrogen bonds) have been explored. This concept stemmed from the direct observation of complementary materials where the complexity and molecular functionality can form noncovalent bonds to construct materials exhibiting specific structures such as proteins. The "supramolecular comb-coil diblock copolymer" systems construct polymeric structure with two length scale of solf-organization: one gives rise to the length of scale of several nanometers forms due to the microphase separation between comb and coil blocks, and the other yields a smaller length scale lamellar structure (with interlamellar distance of several nanometer) due to the segregation between the polymer backbone and amphiphile tail in the comb block. The supramolecular comb-coil concept was pioneered and widely investigated by Ikkala and coworkers(**Fig. 2-22**).[152] In addition to the rich variety of hierarchical nanostructures, the mesomorphic order of the comb block also exerts interesting influence on the self-organization behavior of the coil block. For instance, the smaller-scale lamellar mesophase was found to induce large-scale lamellae domains organized by the coil block in a supramolecular comb-coil diblock formed by complexation of polystyrene-*block*-poly(4-vinylpyridine) (PS-*b*-P4VP) with zinc dodecylbenzenesulfonate, $Zn(DBS)_2$.[153]

Another Elegant Example is that the three hydrogen bonded thymine/2,6 diaminotriazine supramolecular motif has been utilized to make self-assembled pseudo-block copolymers and thus molecules of potential use for immiscible component compatibilization.[154] Poly(isobutylene) (PIB) and poly(etherketone) (PEK) are two such

immiscible polymers that macrophase separate upon blending. The addition of complementary binding units to the ends of these polymers should provide an enthalpic driving force to aid miscibility. Blending the telechelic PEK with 2,4-diamino-1,3,5-triazines moieties, and PIB with thymine units attached resulted in a dramatic increase in their miscibility and electron microscopy shows that a nanophase separated structure with a periodicity of 70nm is formed. Interestingly, if PIB modified with cytosine, instead of thymine, is blended with the functionalized PEK then the result a disordered structure with phase separation on the micrometer scale. This can be by the nature of the non-covalent interaction within these two blended materials. The thymine and 2,6-diaminotriazine binding constant (890 M^{-1} in $CDCl_3$) is much larger than the homodimerization of the supramolecular components, thus encouraging the formation of an altering self assembled system. However this is not the case for the cytosine and 2,6-diaminetriazine where the heterodimer formation is much less than the homodimerization of the cytosine (8 M^{-1} vs 40 M^{-1} in $CDCl_3$), which would therefore encourage a more phase separated structure.

In light of this information, we seek in this dissertation to design, synthesize, and characterize novel, nucleobase functionalized monomers that are aimed at the development of a new class of thermally responsive polymers. The materials targeted utilize nucleobase interactions to control the self-assembly of the monomeric units into polymeric architectures in the solidstate. Such a *supramolecular polymerization* process yields materials, which contain non-covalent bonds as an integral component of the polymeric architecture. The main goal of the utilization is to investigate how the individual nucleobases along with the functionality of the monomer core play a part in tuning the resulting material properties.
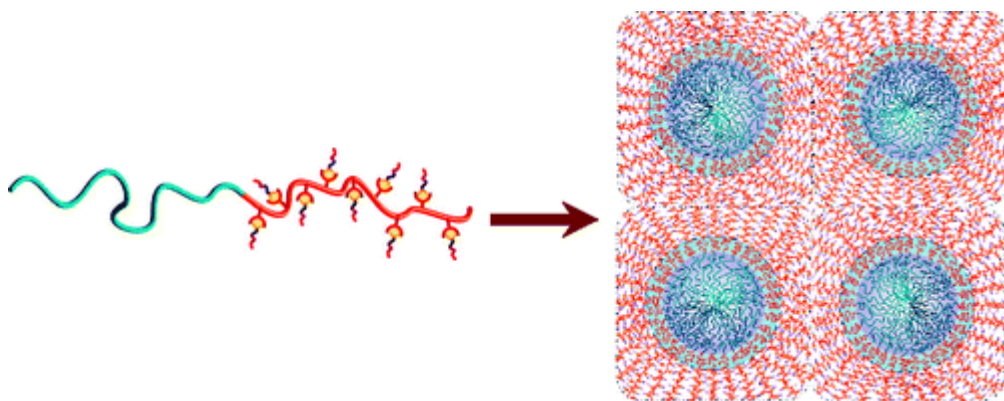
Fig. 2-20 Block copolymers constitute an important class of soft material capable of self-assembling into nanoscale microdomains with well-defined geometries. The cylindrical domains thus formed have been found to pack almost exclusively in hexagonal lattice.

(a)

(b)

(c)

(d)
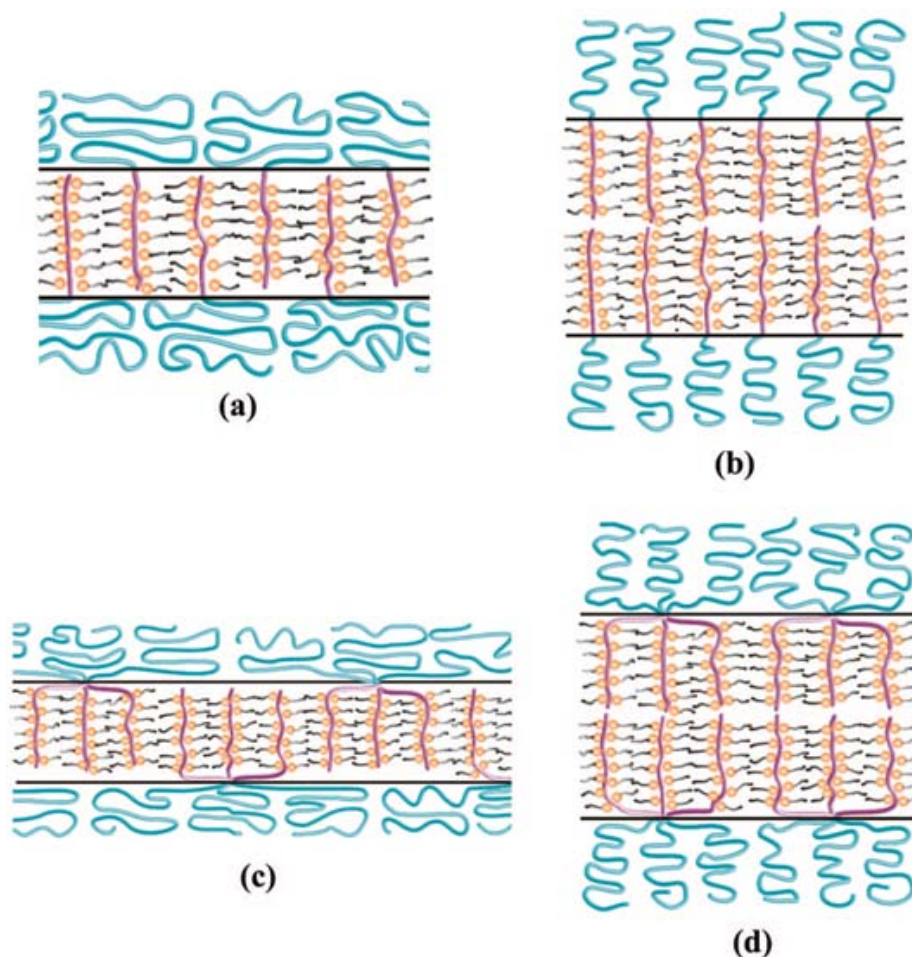
Figure 2-21. Schematic illustration of the possible arrangements of comb blocks in the comb-coil copolymers: (a) monolayer arrangement in linear architecture; (b) double-layer arrangement in linear architecture; (c) monolayer arrangement in heteroarm star architecture; (d) doublelayer arrangement in heteroarm star architecture.
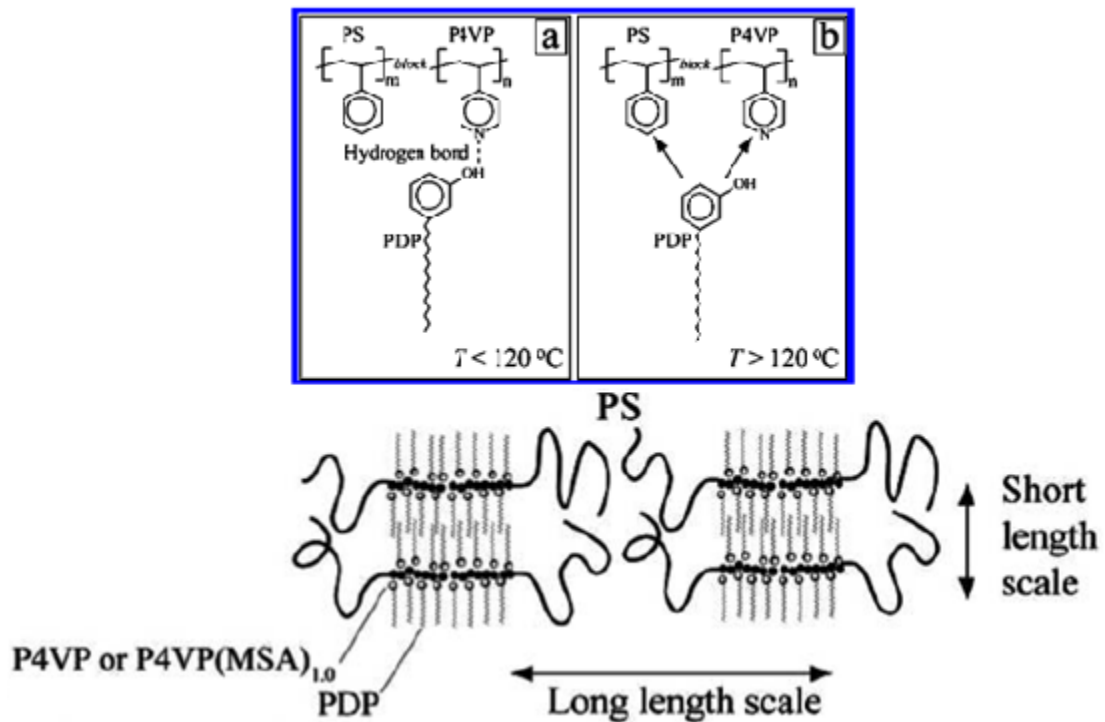
Figure 2-22 Schematics and morphologies of the interactions in PS-*block*-P4VP(PDP)$_{1.0}$
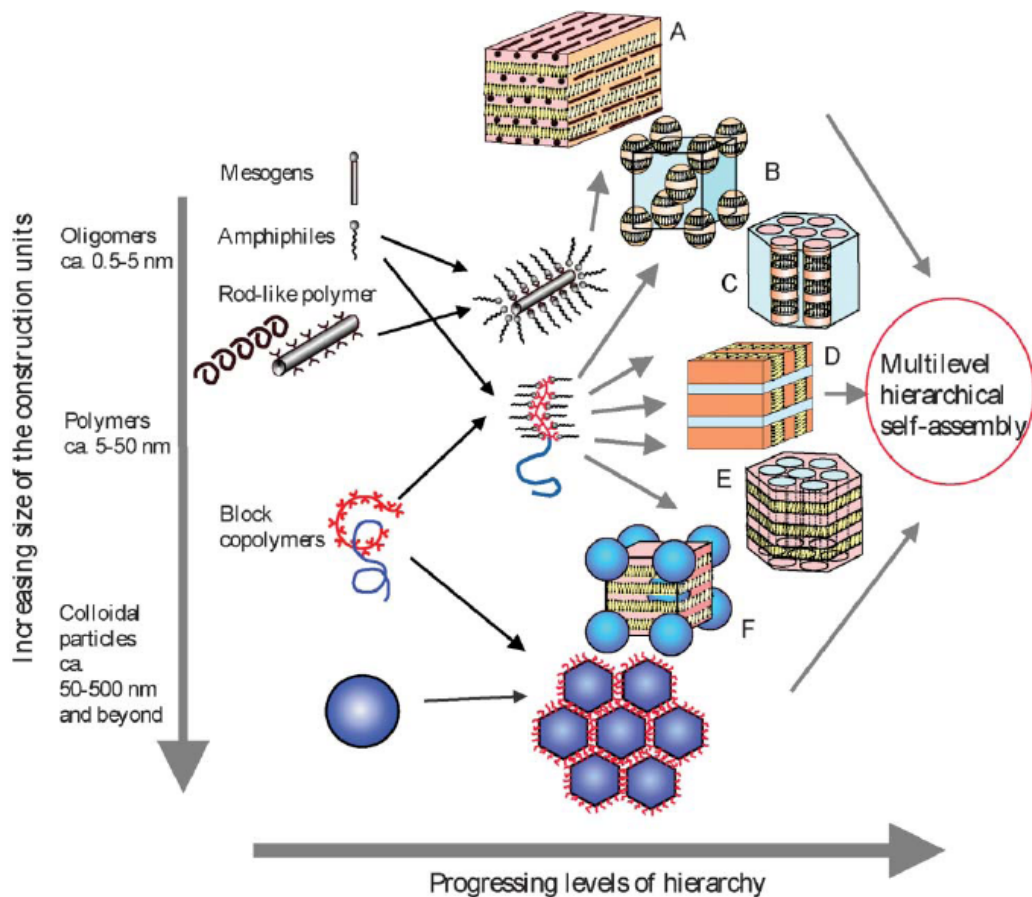
Figure 2-23 One of the potential scenarios to construct hierarchically self-assembled polymeric structures. Construction units of different sizes allow a natural selection of different self-assembled length scales

2-5 Motivation

In biological systems, complementary multiple-hydrogenbonding interactions are paramount and the basic concept of molecular recognition which occurs in adenine-thymine (A-T) and guanine-cytosine (G-C) base pairs in DNA. A wide variety of synthetic polymers were functionalized with the self-complementary nucleobases, such as adenine, thymine, and uracil; however, reports describing the incorporation of heteronucleobase unit in biocompatible materials are rare. In previous study,[155] we have studied the biocomplementary interaction of a DNA-like side-chain PVBT block complexed with alkylated nucleobases via hydrogen-bonded heterodimer recognition [thymine-adenine (T-A) base pairs]. The system formed well-ordered lamellar structures, with their *d*-spacings being controlled by the degree of crystallization of the alkyl side chians. Later, we reported the synthesis and assembly behavior of heteronucleobase-functionalized poly(ε-caprolaction).[156] Attachment of multiple hydrogen-bonding units to chain ends of PCL results in phase separation and substantial increase in the viscosity. Therefore, we also expect that introducing nucleobase units into the side-chain diblock copolymers may influence their phase behavior considerably. Thus, a series of biomimetic diblock copolymers, poly(ε-caprolaction)-*block*-poly 1-(4-vinylbenzyl uracil) were synthesized then complexed with AC16 by our group. The structure of PCL-*b*-PVBU/AC16 blends changes from lamellar to hexagonal and further to disorder as the increasing amount of AC16. The detail study on the phase behavior of PCL-*b*-PVBU/AC16 blend system will be published elsewhere. Recently, a new amorphous SPE composed of PUA_1 and $LiClO_4$ possessing both self-complementary interaction and ion conductive behavior was successfully synthesized. Upon adding $LiClO_4$ to the PUA_1 polymer, the increasing presence of the highly hydrogen-bonded amide I groups (highly interacted self-complementary sites) induces these PUA_1 SPEs to exhibit more ordered structure

as compared with a conventional poly(urethane amide)/LiClO$_4$ SPE and results in enhanced ionic conductivity. Taking above into account and also inspired by the concept of stoichiometric ionic complex[175] usually applied in polyelectrolytes, instead of bearing attached covalently acyl side chain to the backbone, molecular recognition via hydrogen bonding was introduced as side chain modification.

Herein, an alkylated nucleobase (U16) was incorporated into an alternative polymer (poly(amide urethan)) through complementary interaction in this study. The specific interactions and diversity of phase behaviors within these PUA$_1$/U16 blends were investigated and analyzed in detail through DSC, TGA, FT-IR, SAXS, WADX, AFM, and TEM measurements.
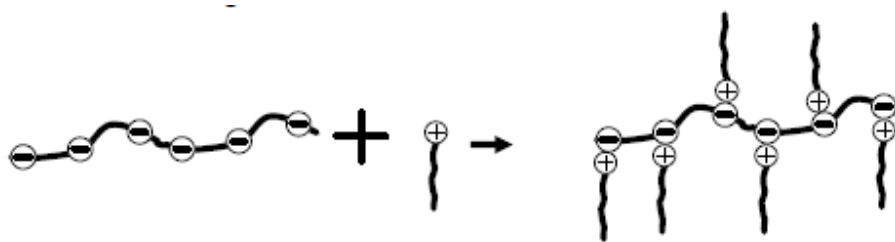
Figure 2-24.   Sketch of the formation of a stoichiometric polyelectrolyte/surfactant complex.
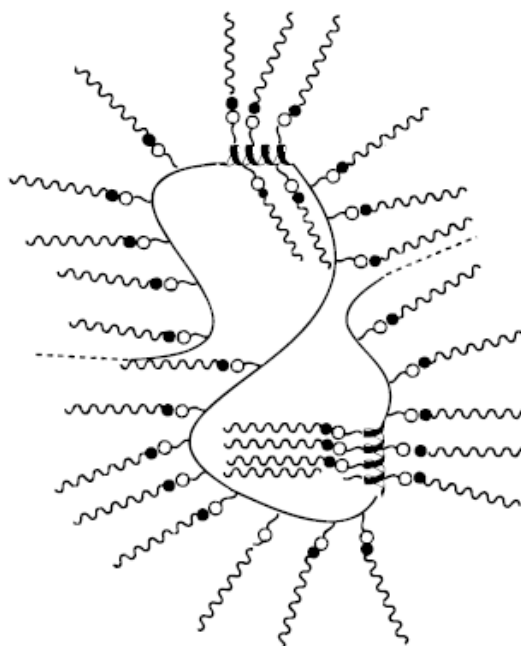
Figure 2-25. Schematic representation of the structure of the ionic complex.

Chapter 3

Experimental Section

3-1 Materials

3-1.1 Material Sources

(a) Succinic anhydride

Succinic anhydride were purchased from Acros Organics (Germany) and used as received without further purification.
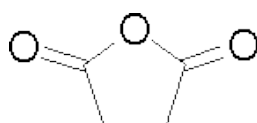
(b) 2,6-diaminopyridine

2,6-diaminopyridine were purchased from Acros Organics (Germany) and used as received without further purification.
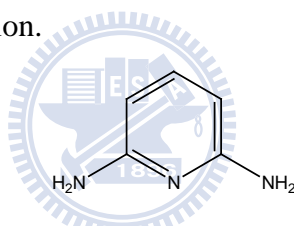
(c) Methylene di-p-phenyl diisocyanate (MDI)

Methylene di-p-phenyl diisocyanate (MDI) were purchased from Acros Organics (Germany) and used as received without further purification.
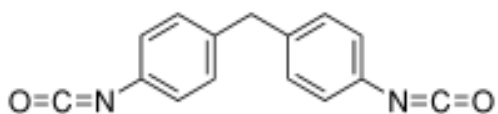
(d) Polyethylene glycol 1000 (PEG1000)

Polyethylene glycol 1000 (PEG1000) was purchased from SHOWA (Japan) and dried in a vacuum oven maintained at 60 °C for 2 h
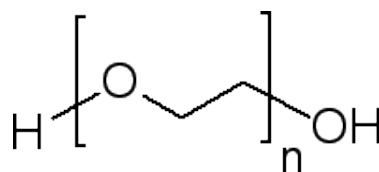
(e) Tin catalyst, T9 (stannous octoate)

Tin catalyst, T9 (stannous octoate), from Dabco and was used as received.

(f) 1-Bromohexadecane

1-Bromohexadecane was purchased from Sigma-Aldrich and used without further purifacation.

$$CH_3(CH_2)_{14}CH_2Br$$
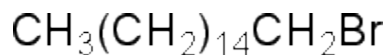
(g) Anhydrous potassium carbonate

Anhydrous potassium carbonate was purchased from SHOWA(Japan) and only used as received.
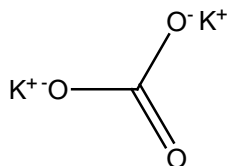
(h) Uracil

Uracil was bought from Alfa Aesar and used as received without further purifacation.
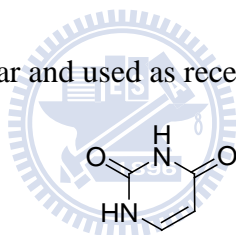
(i) Tetrahydrofuran (THF), methanol, dimethylformamide (DMF), and dimethyl sulfoxide (DMSO) were obtained from TEDIA (USA) and distillated over CaH_2 prior to use.
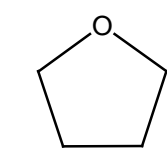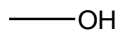
Tetrahydrofuran   methanol   N,N-dimethylformamide   dimethyl sulfoxide
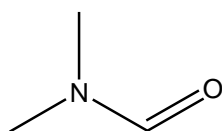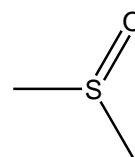
(j) Calcium Hydride

Calcium hydirde with 99% pure was purchase from ACROS. Mw=42.09 g/mol. CAS NO.: 7789-78-8.

3-1.2 Purification of Solvents

3-1.2.1 THF

Potassium hydride dispersion in mineral oil (30%) was put in a dry round bottomed flask under Argon atmosphere; hexane was added and stirred for 10 minutes to dissolve the mineral oil. After stated for a while, the liquid was sucked by syringe and thrown away. Repeat this process three times, the residual were dried by the vacuum pump to ensure that there's no mineral oil and hexane remained. THF was added via syringe and stirred for 12 hours under Argon atmosphere. After completely mixed, THF was distilled at 80 °C.

3-1.2.2 DMF

N,N-dimethylformamide, calcium hydride and a magnetic stirrer were placed in a dry round bottomed flask under Argon atmosphere; after stirred for 12 hours, N,N-dimethylformamide was distilled at 110 °C.

3-2 Synthesis of Diamidepyridine Diacid (Compound 1)

Succinic anhydride (35 g, 0.35 mol) and 2,6-diaminopyridine (15 g, 0.14 mol) were added to a 500-mL round-bottom flask containing 250 mL of dried THF equipped with a stirrer bar. After completely dissolving these reactants, the mixture was heated to 80 °C under an argon atmosphere for 24 h. Excess hot water was added to the residual following the evaporation of THF and then the precipitate was collected through filtration. The product, Compound 1, was obtained through recrystallization of the precipitate from THF and methanol (20:1). The reaction scheme of Compound 1 is illustrated in **Scheme 3-1**. The 1H NMR and 13C NMR spectra and elementary analysis data of Compounds 1 is illustrated in **Figure 3-1** and **Table 3-1**, respectively.

Scheme 3-1. Synthesis and chemical structure of Compound 1.
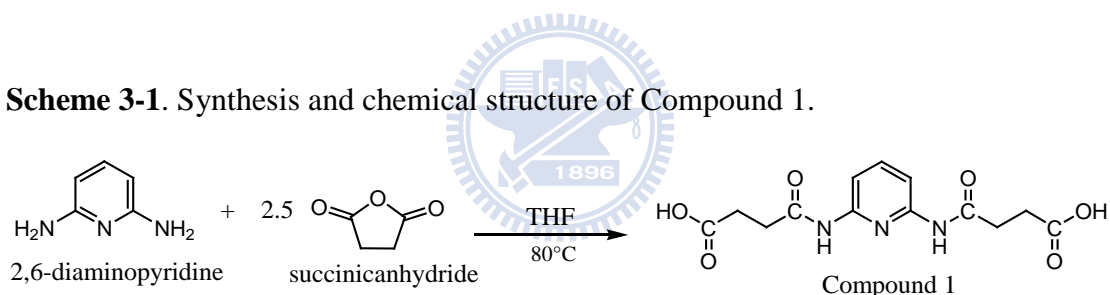
Table 3-1. The elementary analysis data of Compounds 1

		N %	C %	H %[a]
compound 1				
	theoretical	13.59	50.49	4.89
	experimental	12.74	48.52	5.34
	error	6.2	3.9	8.4[a]

[a]: The content of H atoms was slightly overestimated because of water sorption.

Figure 3-1. The (a) ^{1}H NMR and (b) ^{13}C NMR spectra of Compound 1

(a)

(b)

Chemical shift (ppm)

69
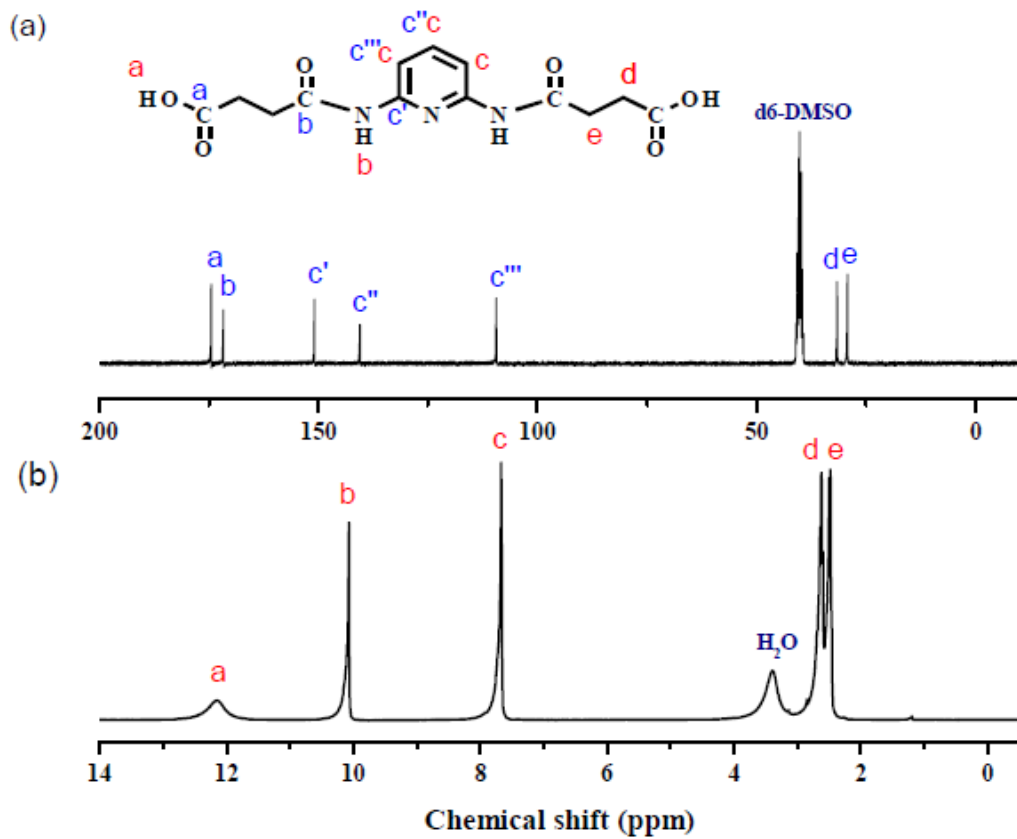
3-3 Syntheses of Poly(amide urethane), (PAU)

To synthesize the poly(urethane amide), first, dried PEG1000 was added via syringe to a solution of MDI in dried DMF under an argon atmosphere and sequentially one drop of T9 was added. Then, the mixture was maintained at 30 °C for 1.5 h until the IR stretching of the hydroxyl groups of PEG1000 disappeared to obtain the PEG1000 prepolymer. Compound 1 dissolved in dried DMF was added to the solution of PEG1000 prepolymer via syringe and then the resultant solution was heated to 80 °C for 12 h. The final product, PAU (brown powders), was purified by precipitation into methanol and then dried under vacuum at 60 °C for 48 h. The GPC data and intrinsic viscosity of these polymers were listed in **Table 3-2** and **3-3**, respectively. Also Notice that M_w is the most important factor influencing the viscosity of polymers (Nielsen L. W. *Polymer Rheology*, Marcel Dekker, New York, 1977, p 69.)[158]

Scheme 3-2. Syntheses and chemical structures of PAU.

PAU
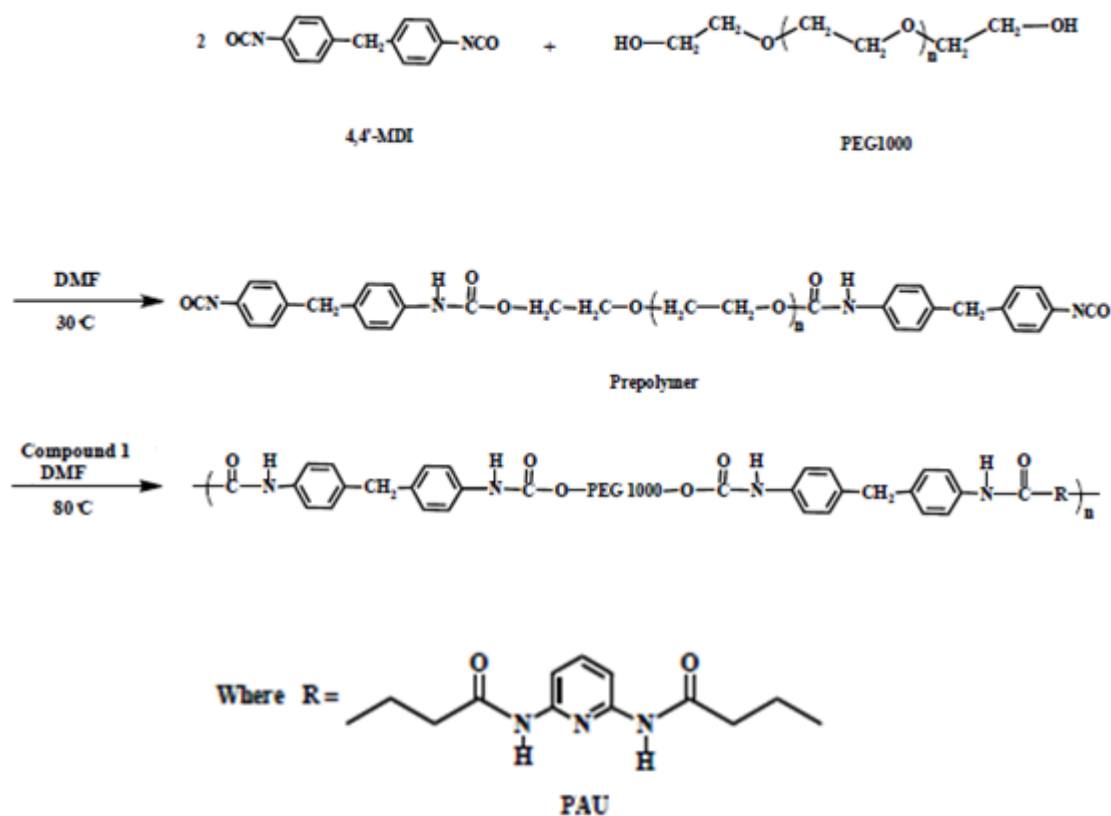
Table 3-2. The GPC data of PAU.

	Mw	*PDI*
PAU	34,610	1.82

Table 3-3. Intrinsic viscosity of PAU dissolved in DMSO (0.1 g/10 ml) obtained from Ostwald viscometer at 25 °C.

	Intrinsic viscosity η_s (*g/dL*)
PAU	0.2319

Figure 3-2 The ^{1}H NMR spectra of PAU.
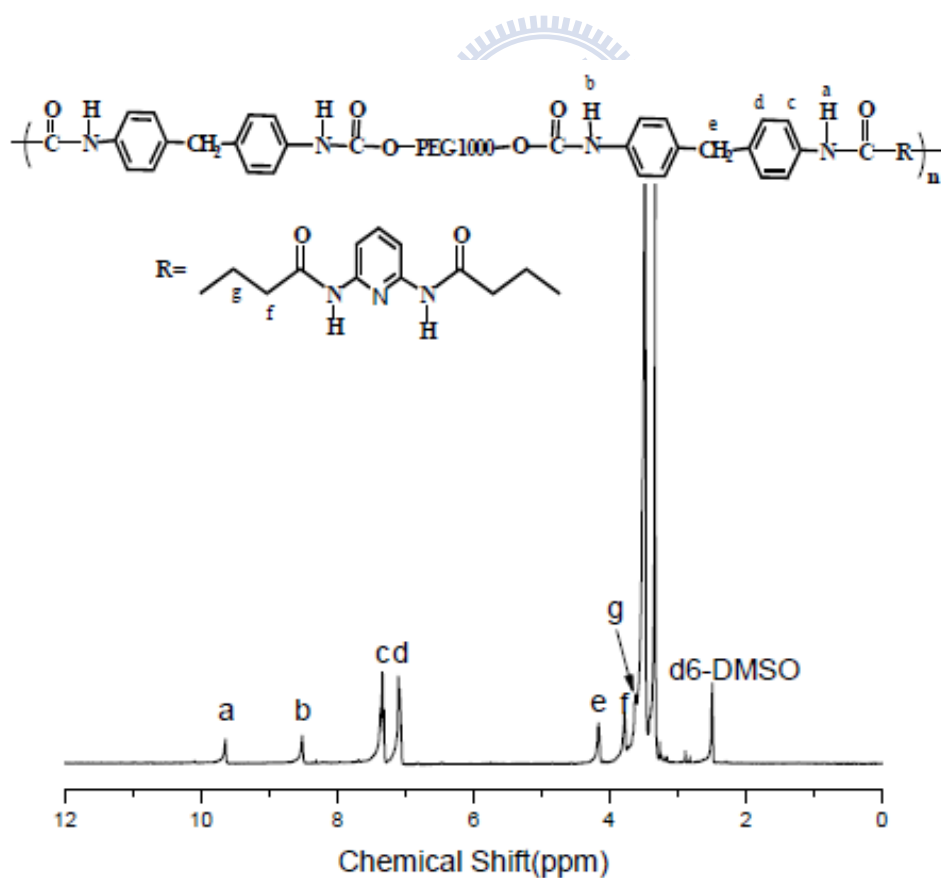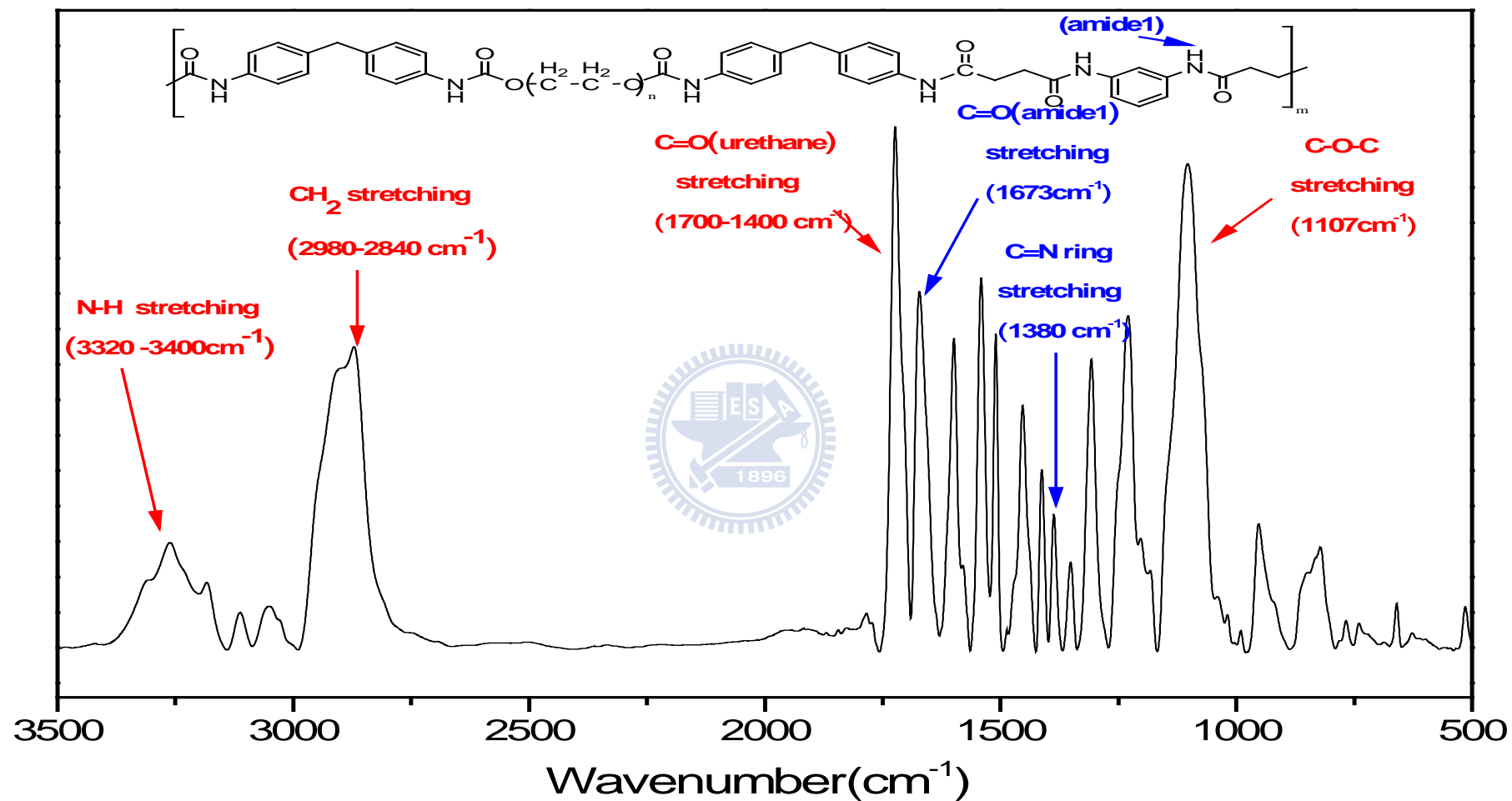
Figure 3-3. The Fourier Transform Infrared spectra of poly (amide urethane) .

3-4 Synthesis of 1-Hexadecyluracil (U-16)

1-Bromohexadecane (2.44 g, 8.00 mmol) and anhydrous potassium carbonate (1.08 g, 7.8 mmol) were added to a solution of uracil (0.83 g, 7.4 mmol) in DMF and then the resulting suspension was stirred at 60 °C for 48 h. The insoluble material obtained was filtrated out, washed with water, and recrystallized twice from toluene. Yield: 55%; m.p. 96 °C(J. Michas, C.M. Paleos, A. Skoulios and P. Weber , Structural study of recognizable adenine and thymine nucleobases functionalized with long aliphatic chains.[159] (Michas, J.; Paleos, C. M.; Skoulios, A.; Weber, P. *Mol. Cryst. Liq. Cryst.* **1995**, *239*, 245–255.)
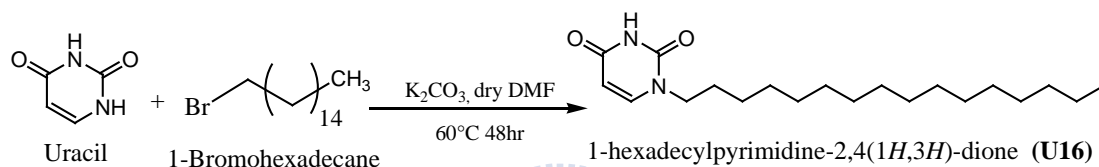
Scheme 3-3. Syntheses and chemical structures of U16.
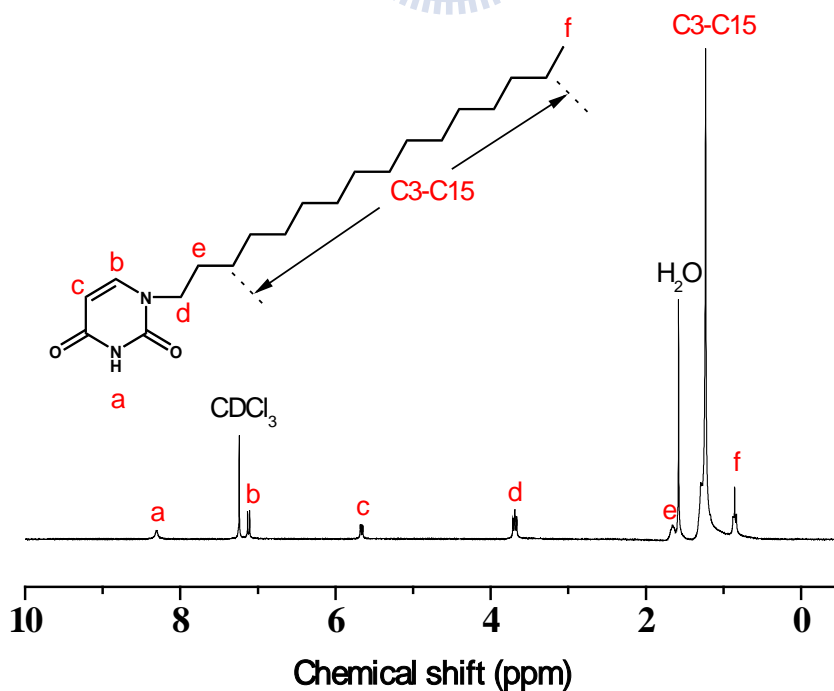
Figure 3-4 The ^{1}H NMR spectra of U16.

3-5 Preparation of Complexes

The solution blending of PAU/U16 complexes of various compositions was performed in a *N,N*-Dimethylformamide solution containing a total of 5 wt % polymer. The polymer blend solution was continuously stirred for 24 h at 40 °C, and then it was cast onto a Teflon dish. The solution was allowed to evaporate slowly at 100 °C for 1 day. The blend films were then dried at 120 °C for 48 hr under vacuum in order to the remove the residual solvent.

To eliminate possible effects of PAU crystallization and residual solvent on MDs, we annealed all bulk samples at 190 °C for 10 mins, which is above the glass transition temperature of PAU (T_g^{PAU}= 92 °C) and well above the equilibrium melting point (T_m^{0}) within PAU polymer, and then subjected samples to various thermal-annealing schemes under a nitrogen atmosphere.
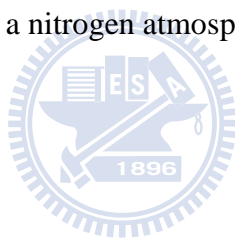
3-6 Characterizations

3-6.1 Thermogravimetric Analysis (TGA)

Thermal Gravimetric Analysis (TGA) is a simple analytical technique that measures the weight loss (or weight gain) of a material as a function of temperature. The weight loss over specific temperature range indicate the decomposition of the sample, thermal stability and absorbed moisture content, etc. After the sample treatment, the thermal properties of various concentration of PAU/ U16 samples were recorded. Thermal stability of the cured sample was investigated by a Du Pont TA Instrument 2050 TGA (TGA-Q50). The cured sample of 5-10 mg was placed in a Pt cell and heated at a heating rate of 10 °C /min from 30 to 800°C under a nitrogen gas flow (inert atmosphere) of 40 mL/min.

3-6.2 Differential Scanning Calorimetry (DSC)

Thermal analysis was performed with a differential scanning calorimeter from DuPont DSC-2010(DSC-Q20) controller operated under an atmosphere of dry N_2 with a scan rate of 20 °C/min and a temperature range of -90 ~ 200 °C. Temperature and energy calibrations were carried out with indium. The measurements were made with samples weighed ~5–10 mg sample on a DSC sample cell and sealed in an aluminum pan. Temperature and energy calibrations were carried out with indium. The measurements were made with a 5-10 mg sample in a DSC sample cell; in first scan, the sample was heated from room temperature to 200 °C, after the first heating run, the samples were then cooled to -90 °C and heat again to 200 °C to examine the temperature of glass transition (T_g) and the other transition temperatures. The T_g was obtained as the inflection point of the jump heat capacity with a scan rate of 20 °C/min and a temperature range of -90 °C to 200 °C.

3-6.3 Infrared Spectroscopy (FTIR)

Infrared spectroscopic measurements were recorded on a Nicolet Avatar 320 FTIR spectrophotometer, and 32 scans were collected with a spectral resolution of 1 cm^{-1}. Infrared spectra of polymer blend films were determined with the conventional KBr disk method. The sample was dissolved in dimethylformamide solution containing the blend was cast onto a KBr disk and dried under conditions similar to those used in the bulk preparation(Each DMSO solution was cast onto a KBr disk and then the solvent was evaporated at 60 °C for 48 h in a vacuum oven.). The film used in this study was sufficiently thin to obey the Beer–Lambert law. Infrared spectra recorded at elevated temperatures were obtained with a cell mounted inside the temperature-controlled compartment of the spectrometer.

3-6.4 Gel Permeation Chromatography (GPC)

The weight-average molecular weight (Mw), number-average molecular weight(Mn), molecular weight distributions and PDI (Mw/Mn) were determined through gel permeation chromatography (GPC) system using a Waters 510 HPLC, equipped with a 410 differential refractometer, a refractive index (RI) detector, and three Ultrastyragel columns (100, 500, and 1000 Å) which were connected in series in order to increase pore size, DMF was used as an eluent at a flow rate of 1.0 mL min-1 . The system and the molecular weight calibration curve was obtained by using polystyrene standards.

3-6.5 NMR Spectroscopy

Nuclear Magnetic Resonance Spectroscopy[1]H and ^{13}C NMR spectra were recorded on a Varian Inova 500 MHz spectrometer equipped with a 9.395 T Bruker

magnet and operated at 500 and 125 MHz, respectively; *d*-chloroform was the solvent. Samples ($\sim$5 mg for 1H NMR; $\sim$20 mg for 13C NMR) in deuterated solvent were analyzed at room temperature.

3-6.6 Transmission Electron Microscopy (TEM)

Transmission electron microscopy (TEM) is a microscopy technique that a beam of electrons is transmitted through ultrathin specimen, interacting with the specimen as it passes through. An image is formed from the interaction of the electrons transmitted through the specimen; the image is magnified and focused onto an imaging device, such as a fluorescent screen. The dark areas of the image correspond to areas on the specimen where fewer electrons were able to pass through; the lighter areas are where more electrons did pass through.

For Transmission Electron Microscopy studies, ultrathin sections of the sample were prepared using Ulatracut Methods. The PAU/U16 blends with the ratio 10:1 were cryo-microtomed at -120 °C for transmission electron microscopic (TEM) observations by Reicher Ultracut microtome equipped with a Reichert FCS cryochamber and a diamond knife; Pure PAU slices with ca. 700 Å thicknesses were cut by UCU microtome equipped with a diamond knife at room temperature. Then both of the samples were transferred onto the carbon-coated Cu TEM grid. Staining was accomplished by exposing the samples to the vapor of a 4 % aqueous RuO_4 solution for 30 min. The contrast between the hard segment and soft segments in Poly(amide urethane) increased in these samples because the hard segments of Poly(amide urethane) is selectively unstained.

TEM analysis was performed using a Hitachi H-7500 electron microscope operated at 100 kV.

3-6.7 Atomic force microscopy (AFM)

The Atomic Force Microscopy (AFM) is a very high-resolution type of scanning probe microscope, with demonstrated resolution of fractions of a nanometer, The AFM consists of a microscale cantilever with a sharp tip (probe) at its end that is used to scan the specimen surface. Atomic force microscopy images were acquired using a Digital Instruments---Veeco Dimension 5000 Scanning Probe Microscope (D5000) scanning probe microscope in National Nano Device Laboratory(NDL), Taiwan. Damage to both the tip and to the sample surface was minimized by employing AFM in the tapping mode. The Maximum Resolution of D5000 is about 1.5 nm in X-Y direction and angstrom(Å) scale in Z direction and the RMS of noise were tuned and controlled to the scale smaller than 0.5 Å. AFM micrographs were recorded at 37℃ in air using a Digital Instrument Multimode Nanoscope IV operating in the tapping regime mode using silicon cantilever tips (PPP-NCH-50, 204-497 kHz, 10-130 N/m). The model of the tips are Nanosensors SuperSharpSilicon-NCHR, the tip curvature radius < 2nm. The values of root mean-square (rms) roughness were calculated over scan areas of 1 µm×1 µm.

3-6.8 Small-Angle X-ray Scattering (SAXS)

Real-time small-angle X-ray scattering (SAXS) measurements were performed by using SWXS instruments of BL23A IASW (Small/Wide Angle X-ray Scattering) beamline at the National Synchrotron Radiation Research Center (NSRRC), Taiwan. The incident X-ray beam with a 0.5 mm diameter was focused vertically by a mirror and monochromated to the energy of 10 keV by a germanium (111) double-crystal monochromator. The wavelength of the X-ray beam was $\lambda=1.24$ Å. The beam stop was a round tantalum disk 4 mm in diameter. The scattering wavevector transfer

q=4πλ^{-1} sin θ is defined by λ and the scattering angle 2θ of X-rays (i.e. q= (4π/λ)× sin (θ), where 2θ is the scattering angle) and also calibrated in these patterns by using the two standard samples: silver behenate (SAXS). Samples for SAXS (thickness ～1 mm) were sealed between two thin Kapton windows (80 μm thickness each) and measured at an ambient temperature ~26 ℃

3-6.9 Wide-Angle X-ray Scattering (WAXS)

X-ray powder diffraction (XRD) is a rapid analytical technique used for phase identification of a crystalline material and can provide information on unit cell dimensions. The techniques are based on observing the scattered intensity of an X-ray beam hitting a sample as a function of incident and scattered angle. X-ray diffraction was used to investigate the crystallographic structure of PAUA/U16. All of them were allowed to dry under vacuum oven and then removes excess solvent to produce solid sample on holder. Wide angle X-ray diffraction (WAXD) measurements were carried out using a Bruker Nanostar U System, with incident X-ray radiation source which is Ni-filtered Cu Kα radiation at a wavelength(λ) = 0.1542 nm. The voltage and current were set at 30kV and 20Ma, respectively. The collimation system consisted of two cross-coupled Gobel Mirrors and four pinholes. A Histar area detector (Siemens) filled with pressurized xenon gas was used to record the SAXS and WAXD scattering patterns, with a sample to detector distance of 106.1 and 3 cm, respectively. All SAXS and WAXD measurements were performed at room temperature. Bragg's law(λ=2dsinθ) was used to compute the d-spacing corresponding to the complementary behavior. The scattering intensity profile was shown in the plot of the scattering intensity (I) versus function of the scattering vector, q= 4πsinθ/λ (θ is the scattering angle).

Chapter 4
Results and Discussion

Blends of various Poly(amideurethane) PAU/U16 compositions were prepared through solution casting. For being convenient, we define the PAU/U16 ratio as the ratio of the content of Poly(amideurethane) to the content of 1-Hexadecyluracil (U16) by weight. These non-covalently connected phase-separations by mixtures of PAU/U16 were analyzed by infrared spectroscopy, small angle X-ray Scattering, wide angle X-ray scattering, transmission electron microscopy and differential Scanning Calorimetry. The hydrogen bonding between DAP and Uracil is substantially stronger than that between DAP and DAP or DAP and urethane and results in interesting phase behaviors through multiple hydrogen bonds.

(a)

U16
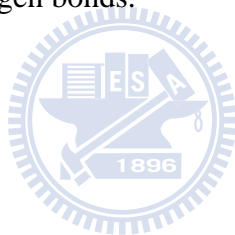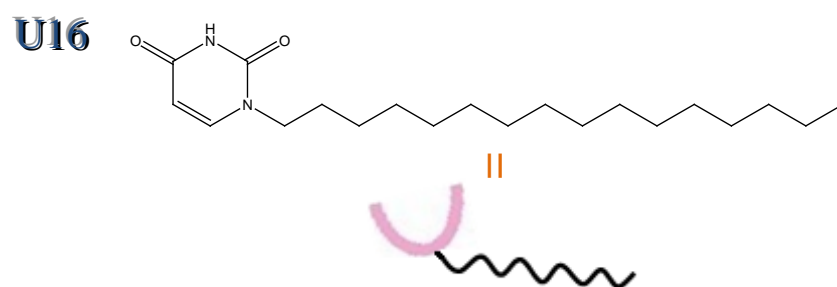
PAU
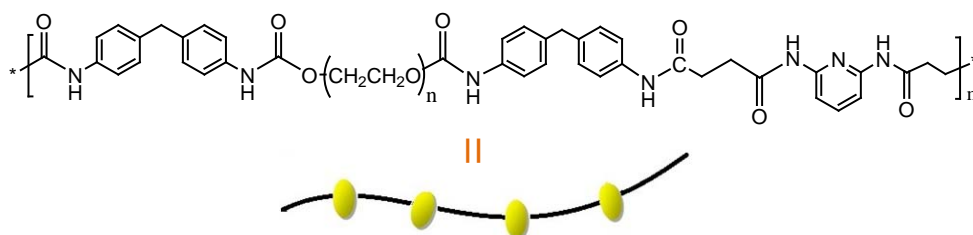
(b)
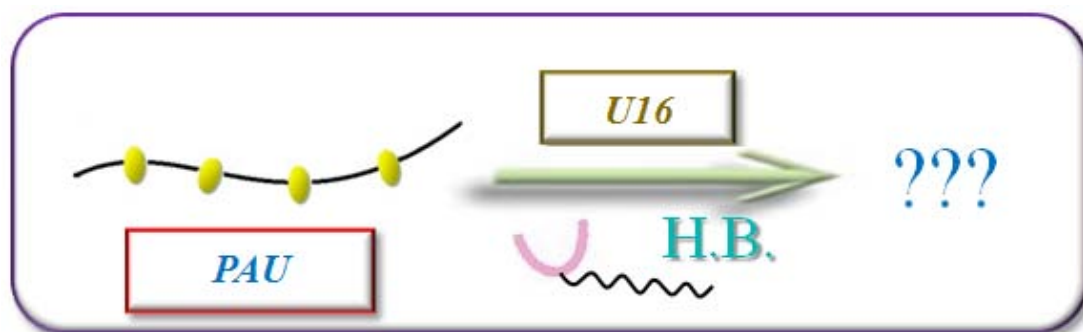
Scheme 4-1. Schematic representation of structures of PAU and U16 with the complex process.

4-1 The complementary interaction within the PAU/U16 blends

Molecular recognition is an interesting phenomenon that can result in various morphological changes. It would be more appropriate to consider the hydrogen bonding within PAU/U16 blends since PAU forms complexes with U16 through complementary interaction. The analysis of FTIR spectra of the blends enabled the hydrogen bond interaction to be identified.[160] On the basis of the harmonic oscillator model the reduction in force constant Δk (note that Hook's Law is $F(x) = -kx$) could be represented by following equation:

$$\Delta k = k_p - k_{np} = \frac{\mu (v_p^2 - v_{np}^2)}{4\pi^2}$$

where $\mu = m_1 m_2/(m_1 + m_2)$ corresponded to the reduced mass of the oscillator, v the oscillating frequency and f was the force constant. The subscripts np and p denoted non-plasticized and plasticized oscillators, respectively. The reduction of force constant brought about by some interaction was directly related to the frequency (or wave number) shift of stretching vibrations. Thus, the lower the wavenumber was, the stronger the hydrogen bond interaction was.

There were several hydrogen bonding motifs within the PAU/U16 blend as shown in **Scheme 4-2**. For PAU, the DAP group possessed self-complementary interaction with equilibrium constant (K_a) of 170 M^{-1} as previously reported.[77,80] The strength of the self-complementary interaction was relatively strong as compared with other hydrogen bonding interactions within PAU such as the urethane-urethane interaction and the urethane-DAP interaction because the numbers of the interacted sites played a critical role in determining the strength of the hydrogen bonds. [77,80] In addition, the uracil group of U16 also possessed self-complementary interaction and the equilibrium constant was calculated as $K_{UU} = 68\pm5$ M^{-1}.[161] For the multiple hydrogen bonded system, DAP is well-known that it posses DAD-ADA triple

hydrogen-bond arrays with uracil (or thymine). Of particular note, as U16 was incorporated into PAU, a strongest interaction, the uracil-DAP interaction, within the system would occur of which association constant (K_a) was calculated to be 800-1500 M^{-1} in the previous study[77] and representing a highly co-operative assembly. In principle, the higher the value of K_a (equilibrium constant) the stronger the complexation. Therefore, since the uracil-DAP interaction possessed highest K_a of all these K_as within the PAU/U16 blend, theoretically the formation of heterodimer recognition (uracil-DAP interaction) was the most preferred as U16 was incorporated into PAU.

Figure 4-1 illustrated the various temperatures FTIR spectra of C=O stretching region of PAU. The peaks centered at 1724, 1708, 1597, and 1609 cm^{-1} corresponded to the free urethane C=O, hydrogen bonded urethane C=O[176], C=C ring stretching within benzene[177] and pyridine[178] of PAU, respectively.[162] Upon heating, the intensities of peaks of the hydrogen bonded urethane C=O, amide I groups, and C=C ring stretching were gradually decreased, which resulted from the effect of temperature on the hydrogen bonding interaction. The FTIR spectra of C=O stretching of the PAU, U16, and various PAU/U16 blends were also shown in **Figure 4-2**. The U16 possessed imide and amide groups centered at 1731 and 1678 cm^{-1}, respectively, which were located almost in the same region of those PAU C=O groups and indicated the difficulty in observing the formation of hydrogen bonding interaction among each groups within this region. Therefore, the FTIR spectra within the NH stretching region of PAU obtained from various temperatures and different ratio of PAU/U16 blends were shown in **Figures 4-3** and **Figure 4-4**, respectively, were carried out. In **Figures 4-3**, there were four bands centered at 3315, 3259, 3229, and 3181 cm^{-1}, respectively. Upon heating, these bands were gradually shifted toward 3315 cm^{-1}, implying that the band at 3315 cm^{-1} was attributed to the free NH group

within PAU. In addition, the band centered at 3181 cm^{-1} was corresponded to the hydrogen bonded DAP NH group because of the highest K_a value between DAP groups and the bands at 3259 and 3229 cm^{-1} were attributed to the hydrogen bonded urethane-urethane and urethane-DAP groups, respectively, resulting from the relatively more interacted sites (two points) between the urethane-DAP interaction as compared with urethane-urethane interaction. The stronger the interaction, the lower the wavenumber.[163] In **Figures 4-4**, U16 possessed bands centered at 3161 and 3431 cm^{-1} corresponding to the hydrogen bonded and free uracil NH group, respectively. Furthermore, for the PAU/U16 (1/1) blend the band of the hydrogen bonded uracil NH group was shifted to 3181 cm^{-1} and therefore we can attribute the band at 3181 cm^{-1} to the hydrogen bonded uracil-DAP NH group. As U16 was incorporated into PAU, the urethane-DAP interaction was influenced, which resulted in a shift of the band at 3229 cm^{-1} because the incorporated uracil group of U16 would strongly associate with DAP group of PAU. The consequence was consistent with that from the comparison of the equilibrium constant (K_a) between each hydrogen bonding interaction.

= hydrogen bond

········· = attractive secondary interaction

= repulsive secondary interaction

DAP-DAP
$K_a = 170$ M^{-1}

DAP-Uracil
$K_a = 800\text{-}1500$ M^{-1}

Uracil-Uracil Self-dimerization
$K_a = 68$ M^{-1}

Urethane-DAP form 1

Urethane-DAP form 2
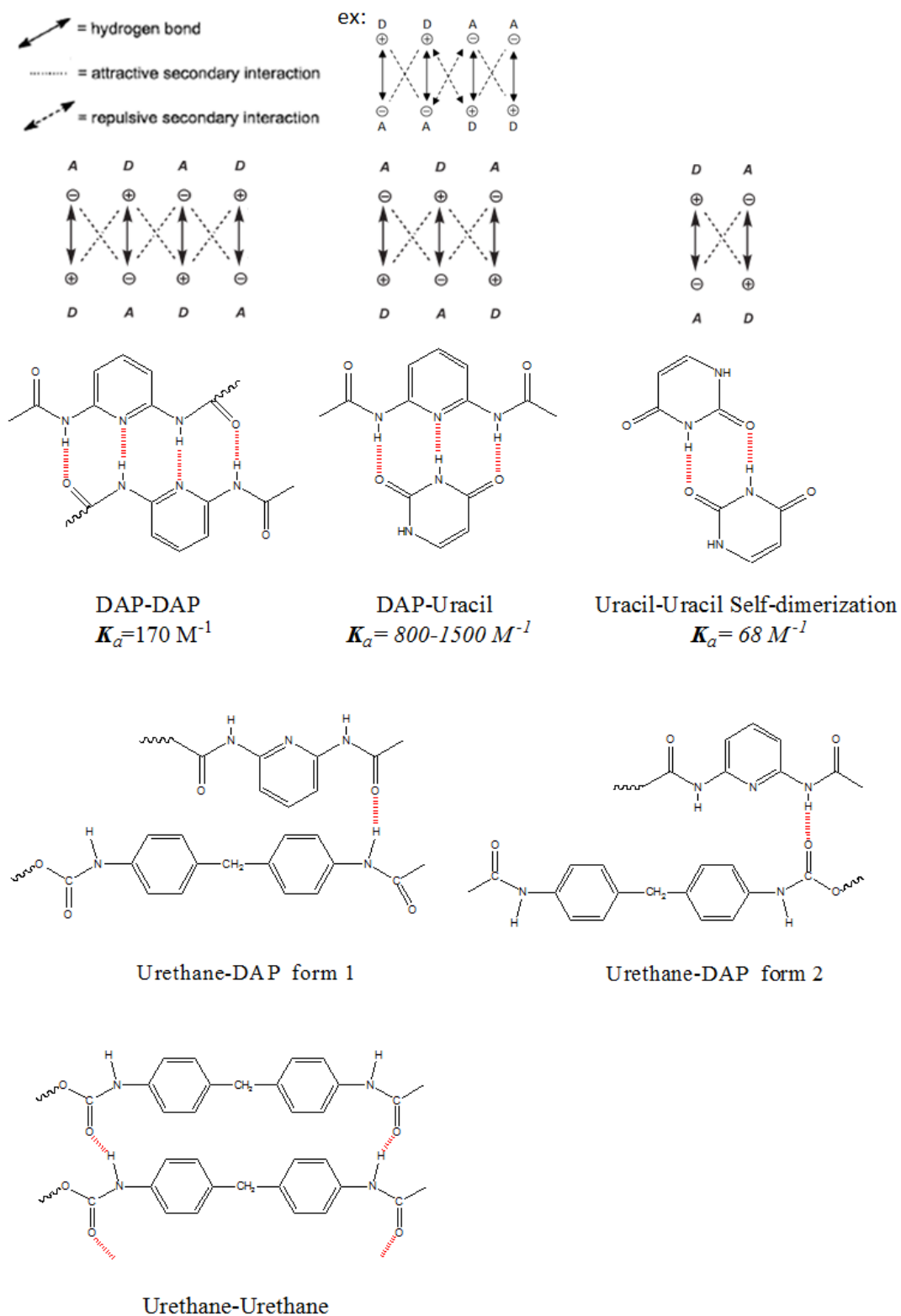
Urethane-Urethane

Scheme 4-2 Some different modes of hydrogen-bonding motifs within PAU/U16 complexes
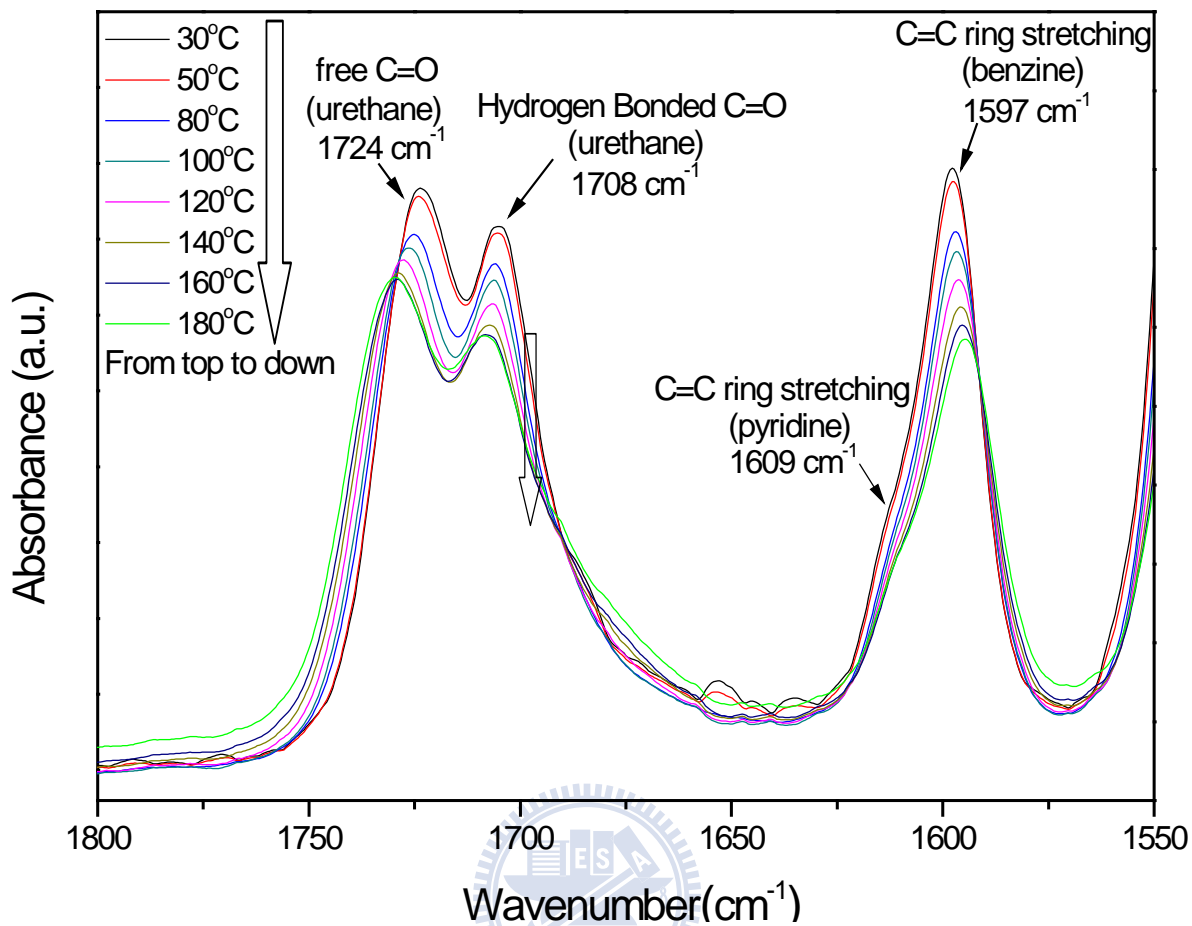
Figure 4-1. Variable temperature FT-IR spectra recorded in the 1550-1800 cm^{-1} region (C=O stretching region) of Poly (amide urethane) [PAU].
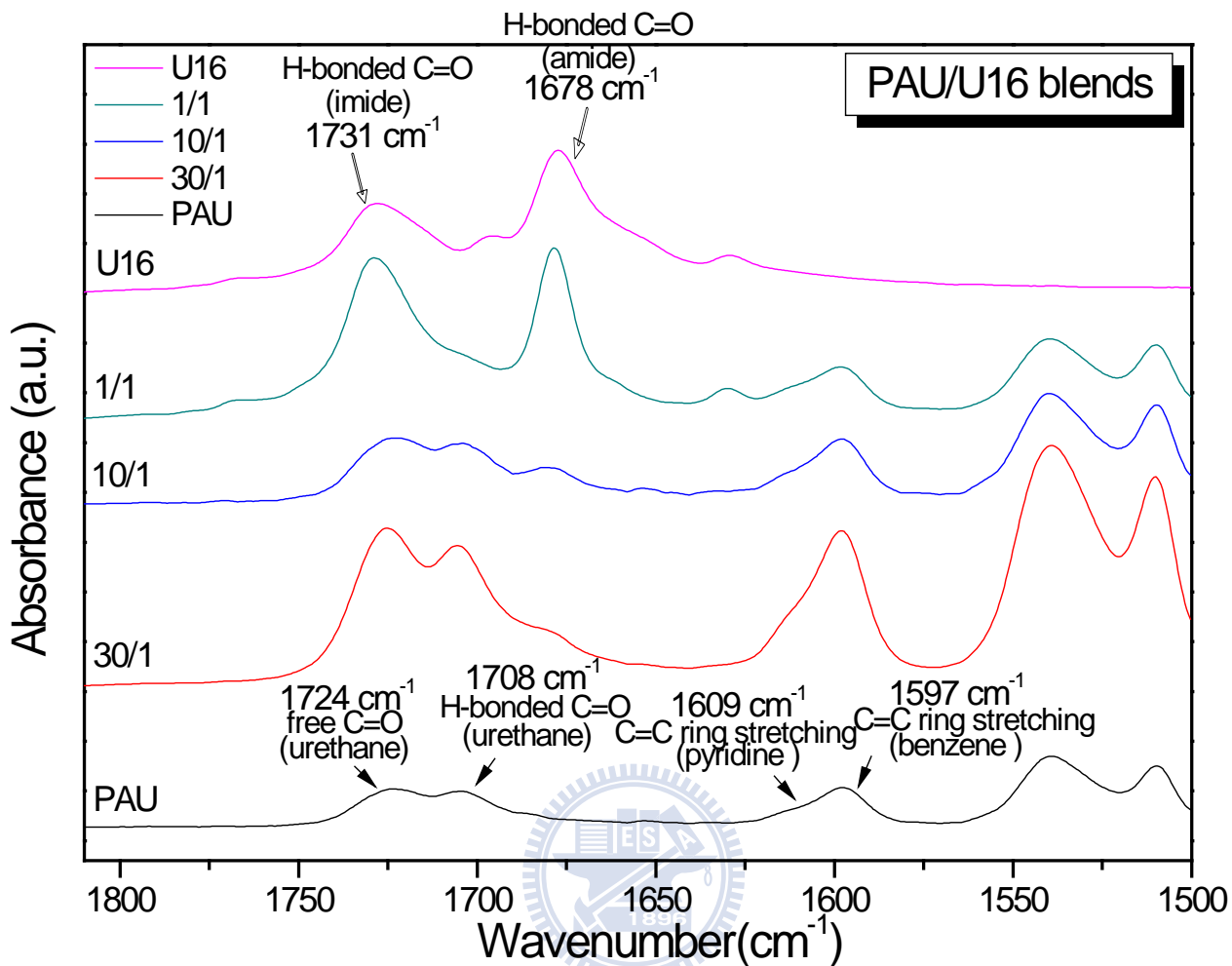
Figure 4-2. FTIR spectra of PAU/U16 blends incorporating various amount of U16 in the presence of bulk state and recorded at room temperature in the 1600-1800 cm^{-1} region.
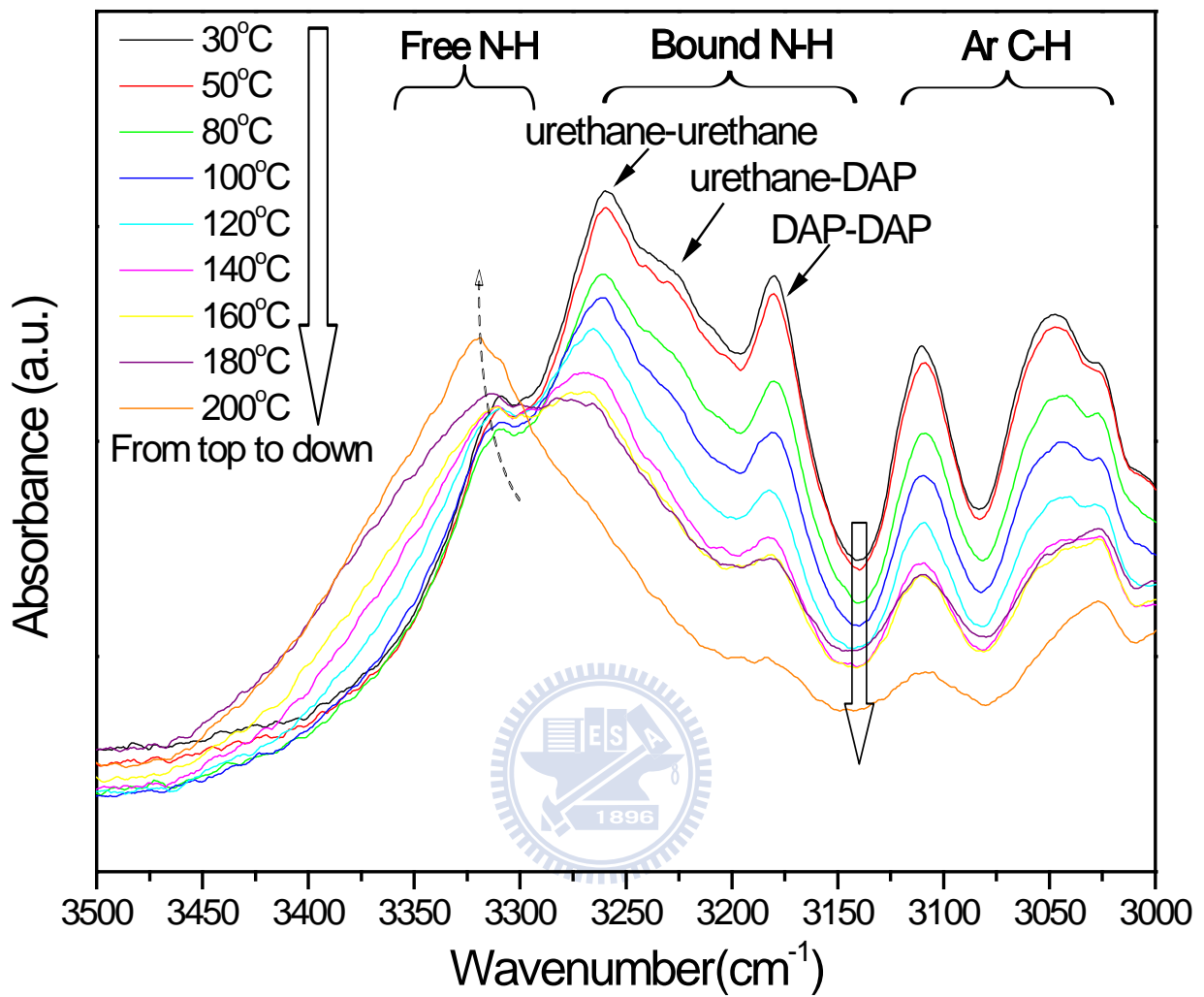
Figure 4-3. Variable temperature FT-IR spectra recorded in the 3000-3500 cm^{-1} region of Poly (amide urethane) [PAU].
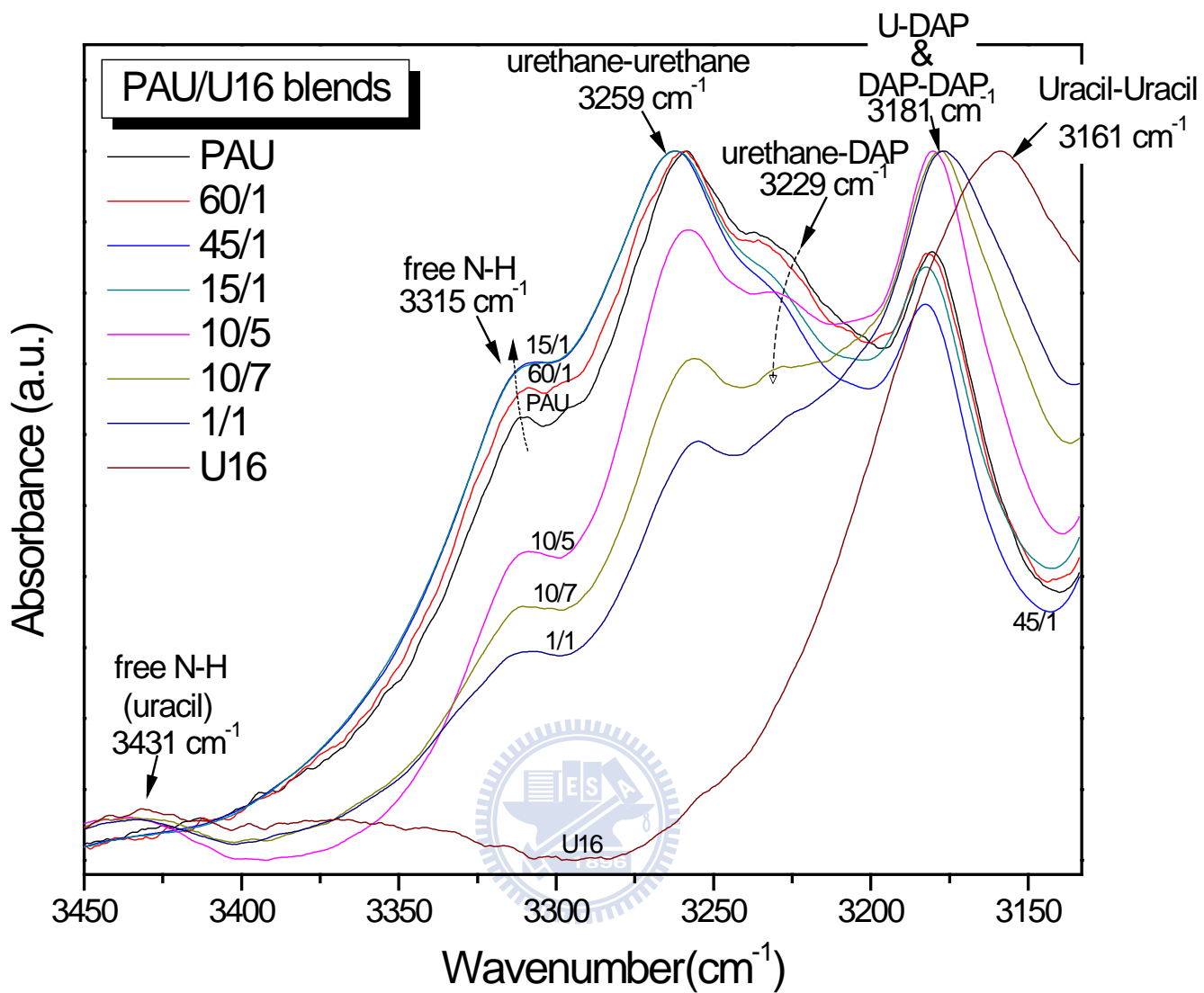
Figure 4-4. FTIR spectra of PAU/U16 blends incorporating various contents in the presence of bulk state and recorded at room temperature in the 3140-3400 cm^{-1} region.

4-2 Thermal Analyses

The measurements of weight loss of the PAU/U16 blends were performed on a Du Pont TA Instrument 2050 TGA (TGA-Q50) from 30 to 800°C under a nitrogen atmosphere. The gas flow rate is 50mL/min. The heating rate employed was 10°C/min. Differential scanning calorimetry (DSC) thermograms were recorded with a Thermal Analysis DSC-Q20 differential scanning calorimeter. Samples weighed (ca. 4–10 mg) and sealed in an aluminum pan were cooled to -90°C and then scanned from -90 to 210 °C at a scan heating rate of 20 °C /min under a nitrogen gas flow of 40 mL. The glass transition temperature was taken as the midpoint of the heat capacity transition between the upper and lower points of the deviation from the extrapolated glass and liquid lines.

Thermal Gravitivity Analysis (TGA) curves of PUA/U16 blends of different compositions were shown in **Figure 4-5**. The thermal decomposition temperature (T_{d5}) of PAU is significantly higher than U16 since the hydrogen bonding within PU material and higher molecular weight of PAU. It is obviously that the thermal degradation of various PAU/U16 complexes can simply attribute to two procedures, the first one is the decomposition of U16 and the other is the degradation of PAU. The char yield of PAU/U16 complexes are all located at ca. 5%, which shows that most compositions of PAU/U16 blends are organic.

In general, differential scanning calorimetry (DSC) is one of the convenient methods to determine the miscibility in copolymer or polymer blends. **Figures 4-6(a)** displays the DSC thermogram traces of various PAU/U16 [poly(amideurethane)/1-Hexadecyluracil] complexes. As can be seen, U16 possess two melting points (T_m) at 80°C and 91°C, respectively. The polyurethane control sample consists of polyethylene glycol (PEG) (Mn=1000) soft segments and

90

MDI+DAP (Diamidepyridine Diacid) hard segments. After quenching from molten state, pure PAU exhibit two glass transitions; the first glass transition temperature (T_g) bring about by the soft segment was observed at ca. -45°C and the second glass transition (T_g) contribute by partially mixable of hard and soft segments was at about 92°C [illustrated in **Figure 4-6(b)**], respectively, corresponding to the amorphous domains in the two complex systems. These results are totally in agreement with previous studies and shows the nature of microphase separation of PU materials. As the slight incorporation of U16, for the 60/1 complex, the value of T_g was shift from -45°C to -26°C comparing with pure PAU, implying that the highly complementary hydrogen bonding was occurring within the PAU/U16 complex. The value of T_g was increased by the presence of the side-chain alkyl groups of U16, which may bring about from the constitution of more ordered phase as the molecular recognition process taking place. The strong physical cross-linkage within the hard segments of PAU also lead to a confinement of the molecular motion of neighbor soft segments, therefore, the mobility of soft segments decreases and results in smaller free volume and higher T_g. Thus, an incorporation of U16 led to a non-uniform glass transition upon heating.[164-169] Increasing the U16 content to a ratio of PAU/U16=10/3 led to the side-chain alkyl groups of U16 forming more regular crystalline phase, arranged perpendicularly to the amorphous sheets. The crystallization of the alkyl tails occurred in sheets that separated the amorphous regions,[164-169] as we can deduce from the value of melting point (T_m) of 94°C. Furthermore, the value of T_m increased and shifted significantly from 91°C to 96°C for 10/5 PAU/U16 complex as compared with pure U16 (see **Figure 4-7**). The change in the melting temperature indicated that the incorporated U16 was crystallized in confined domains within the lamella structure of PAU and all of them were crystallized within the confined domain without exclusion even there was excess of U16 as in our previous report.[170] Also, we noted that DSC

analysis revealed co-crystallization on a scale of ca. 20-40nm (as sensitivity) for PAU/U16 blends.[171,172] This intriguing behavior led us to investigate the microstructures of these complexes in more detail through WXRD, SAXS, TEM, and AFM characterization.
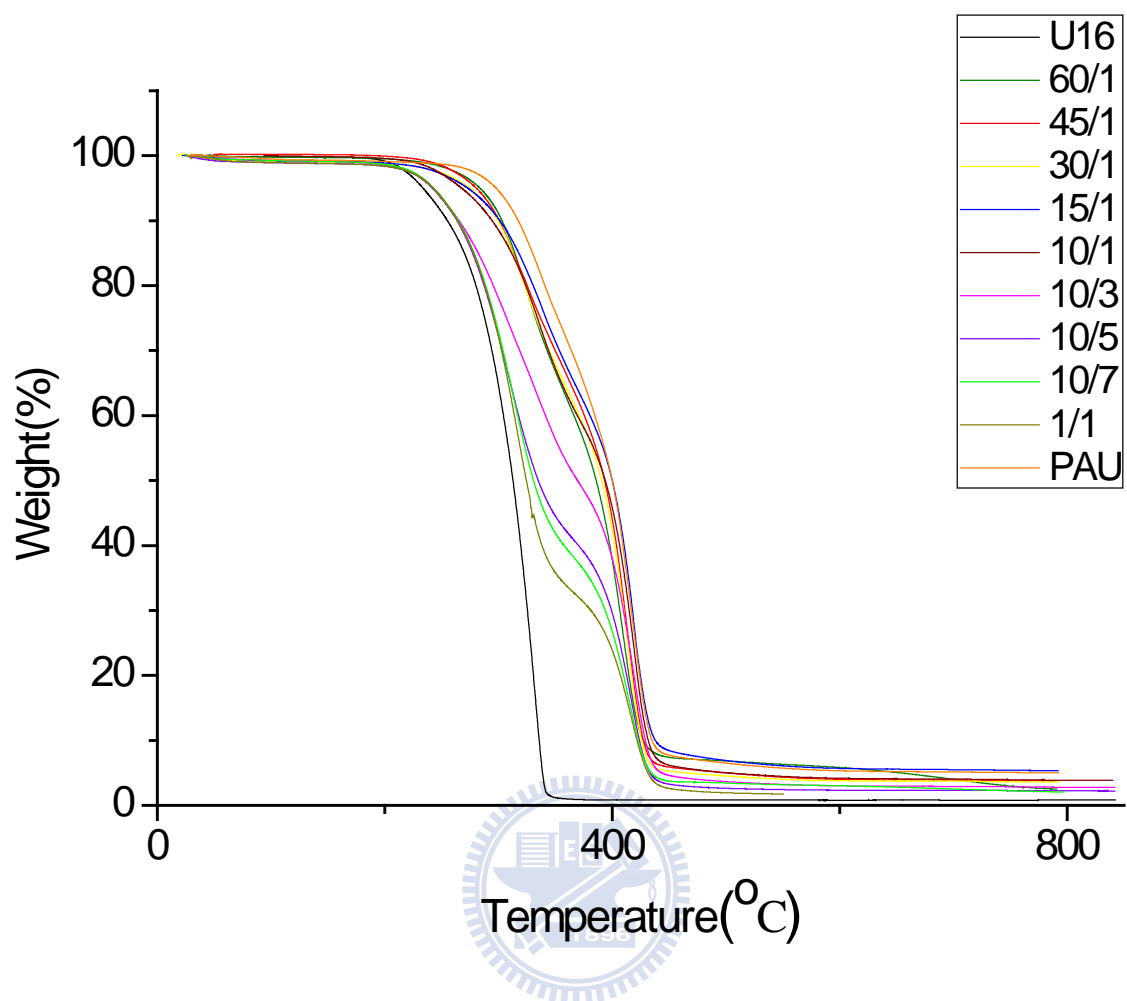
Figure 4-5. Thermal Gravitivity Analysis (TGA) curves of PUA/U16 blends of different compositions.
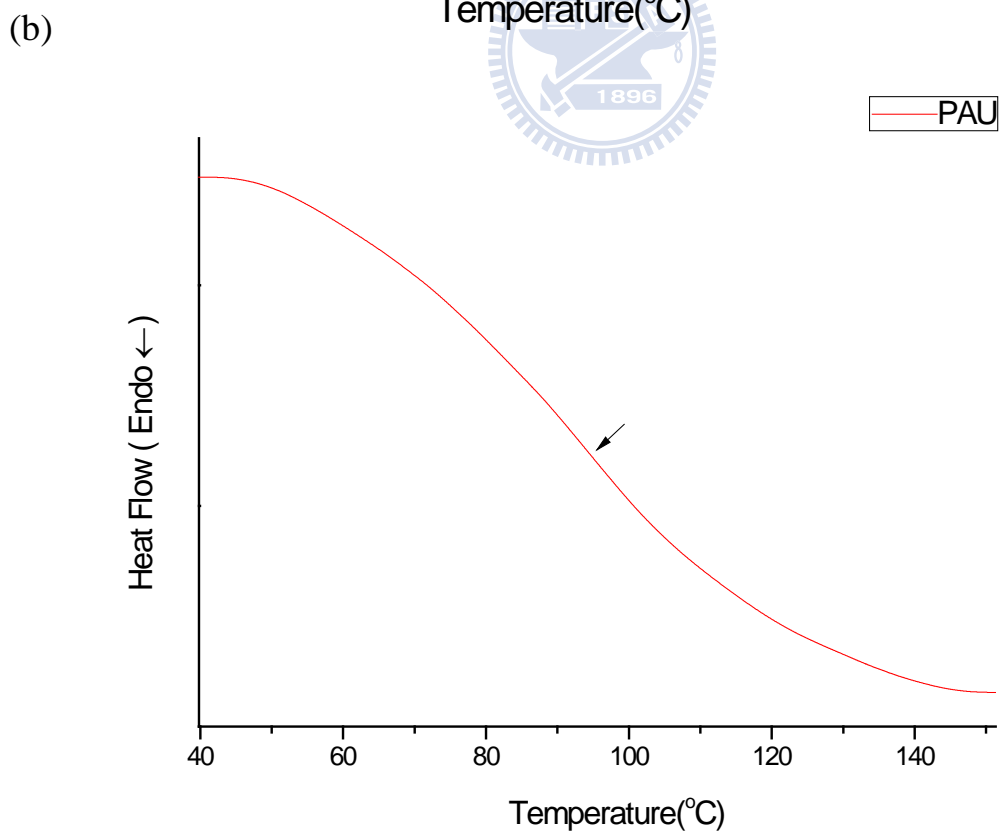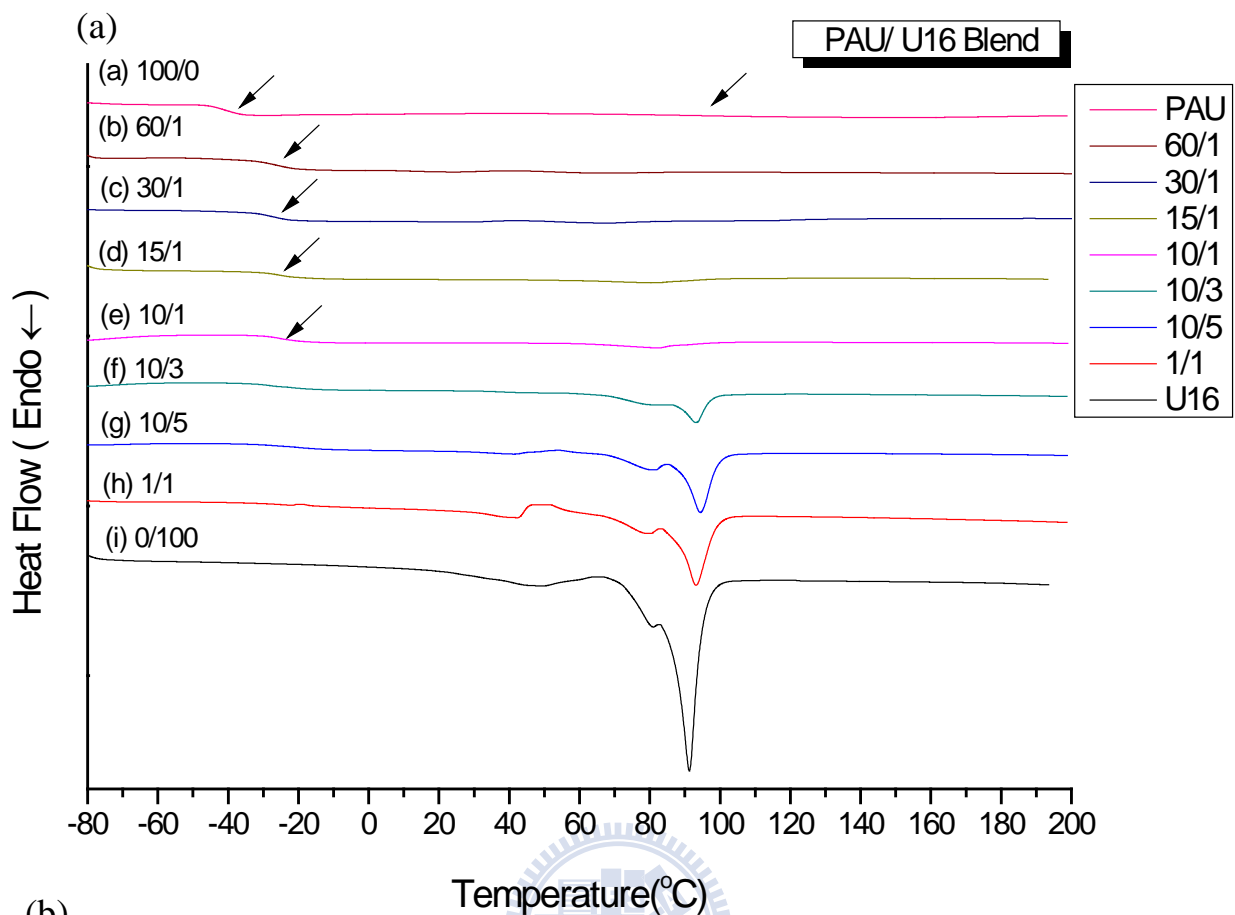
Figure 4-6. DSC thermograms of (a) PUA/U16 blends of different compositions. (b) PAU ranges from 40°C to 150°C shows the second T_g.
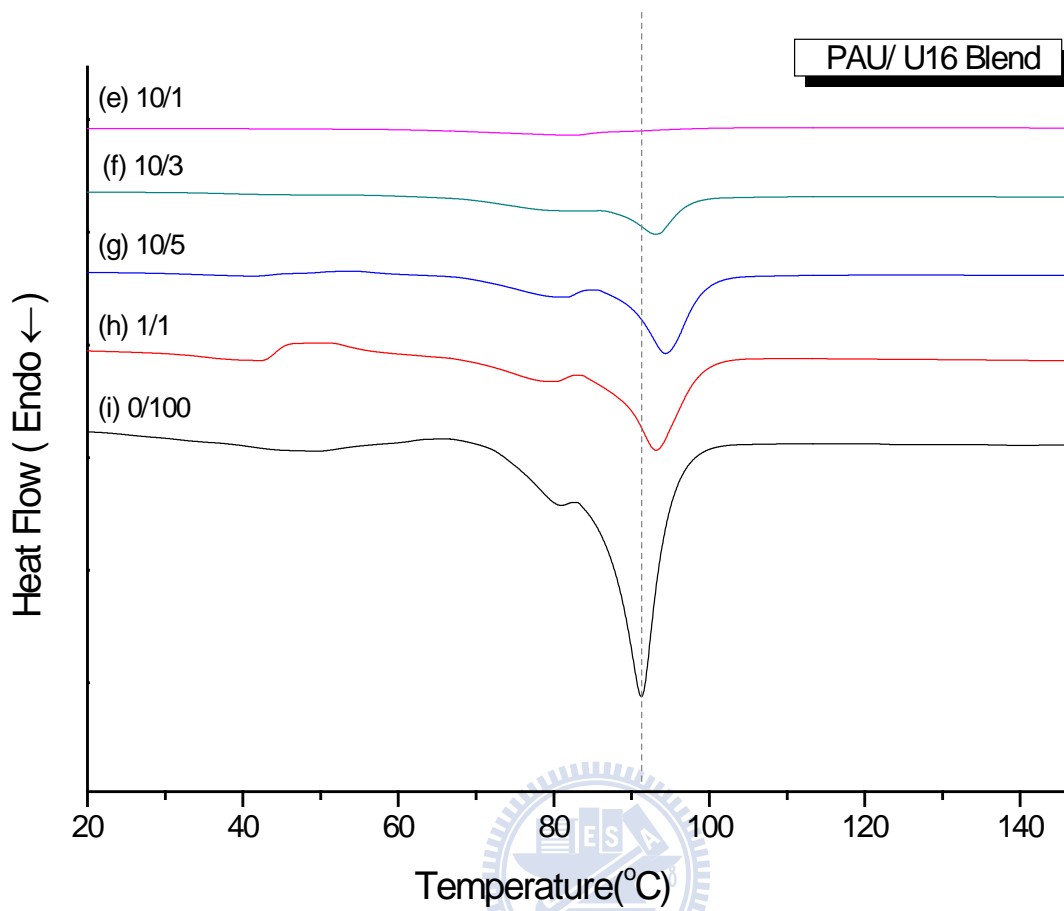
Figure 4-7. DSC curves indicate the change in melting points (T_m) of PUA/U16 blends in the presence of various amounts of U16.

4-3 Small angle X-ray scattering and Wide angle X-ray scattering

Figures 4-9 and **4-10** illustrated the SAXS and WXRD profiles of the PAU, U16, and various PAU/U16 blends, respectively. As shown in the **Figures 4-9** and **Figure 4-10**, U16 possessed two series of highly long ranged ordered reflection q/q* ratios of 1:2:3, where q* is the 1st value of peak series, as an indication of two series of lamella structures. The 1st series contains peaks at q_1=1.6, q_2=3.2, and q_3= 4.8 nm^{-1} where the 2nd series possess peak values at q_1'=2.6, q_2'=5.2, and q_3'= 7.8 nm^{-1}, respectively. According to the simulation from the software, ChemDraw, the lamella structures with size of 2.4.nm and 3.9 nm could be attributed to packing of the U16 with uniformly stretched and interpenetrated alkyl chains, respectively as shown in **Scheme 4-3**. Thus, the experimental results are totally coincide with theoretical calculated *d*-spacing of PAU/U16 blends (d= $\frac{2\pi}{q_1}$ = 3.9 nm, d' = $\frac{2\pi}{q_1'}$ =2.4nm). In addition, the PAU also exhibited a lamella structure with relatively larger size and lower degree of order as our previous report,[162] the SAXS pattern of this lamella structure is also shown in **Figure 4-8**. For the PAU/U16 blends with lower U16 content such as PAU/U16 (60/1) and PAU/U16 (45/1) blends, the SAXS profile of PAU was not influenced through the incorporation of U16, coinciding with the occurrence of one series of highly long ranged ordered reflection of U16, which indicated that the incorporated U16 did not influence the lamella structure of PAU while it only possessed the lamella structure with stretched alkyl chain. As the U16 content was increased, the SAXS profile of PAU still remained unchanged and however several peaks corresponding to the change in the packing of U16 were occurred as shown in **Figure 4-9** and **Figure 4-10**. Although the U16 content was increased, the lamella structure within PAU was still not influenced, and these peaks at q = 1.73 and 1.91 nm^{-1} were attributed to the semi-interpenetrated structure of U16

as shown in **Scheme 4-3**. For the PAU/U16 (1/1) blend, the long ranged order reflection of U16 was fully transformed from one to the other without the change in the lamella structure of PAU even the content of the incorporated U16 was over that of its complementary DAP group of PAU. In addition, the melting temperature of the incorporated U16 was gradually pronounced and slightly higher than that of the neat U16 as shown in the DSC data (**Figure 4-7**) of the PAU, U16, and various PAU/U16 blends. The change in the melting temperature indicated that the incorporated U16 was crystallized in confined domains within the lamella structure of PAU and all of them were crystallized within the confined domain without exclusion even there was excess of U16.[170] Based on the above, the PAU/U16 blends possessed nano-scale lamella structure (from U16 phase) within lamella structure (from PAU phase) and the nano-scale lamella structure corresponding to the packing of U16 was gradually transformed from the stretched structure to semi-interpenetrated one, and further to interpenetrated structures only. All the microphase transitions of structures was illustrated in **Scheme 4-3**. Although the heterodimer recognition coincided with several other hydrogen bonding motifs within the PAU/U16 blends, the plug and play behavior and the microstructure change were similar to those of the homo poly[1-(4vinylbenzyl thymine)]/9-hexadecyladenine (PVBT/AC16) blend proposed in our previous report, which indicated the strongly complementary behavior of the heterodimer recognition.
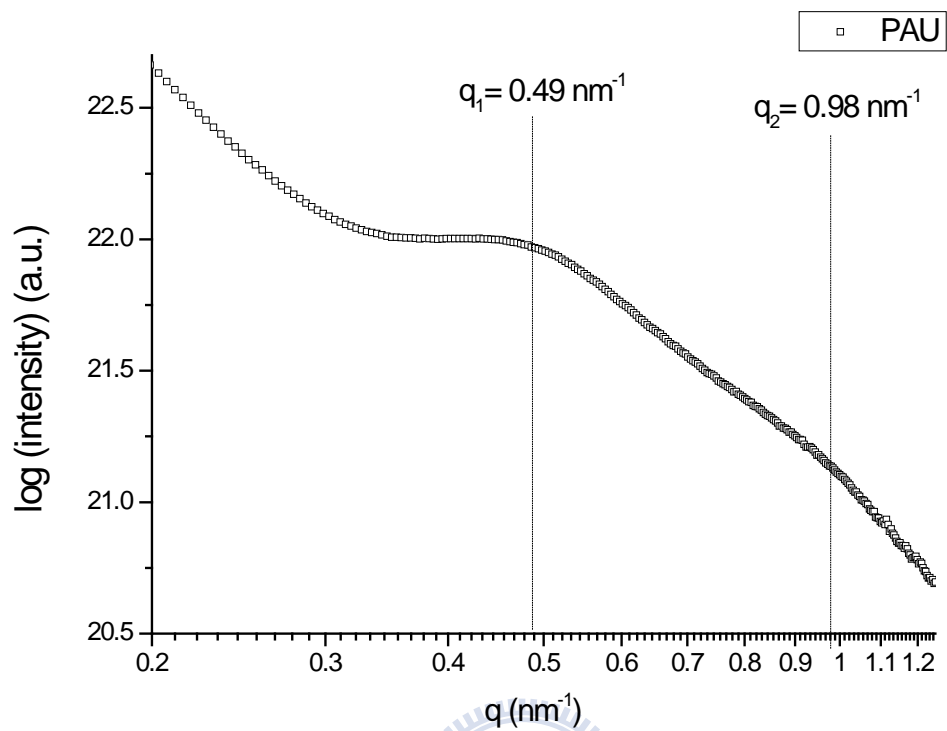
Figure 4-8. The SAXS patterns indicate that both PAU and other PAU/U16 blends possess lamella structures.
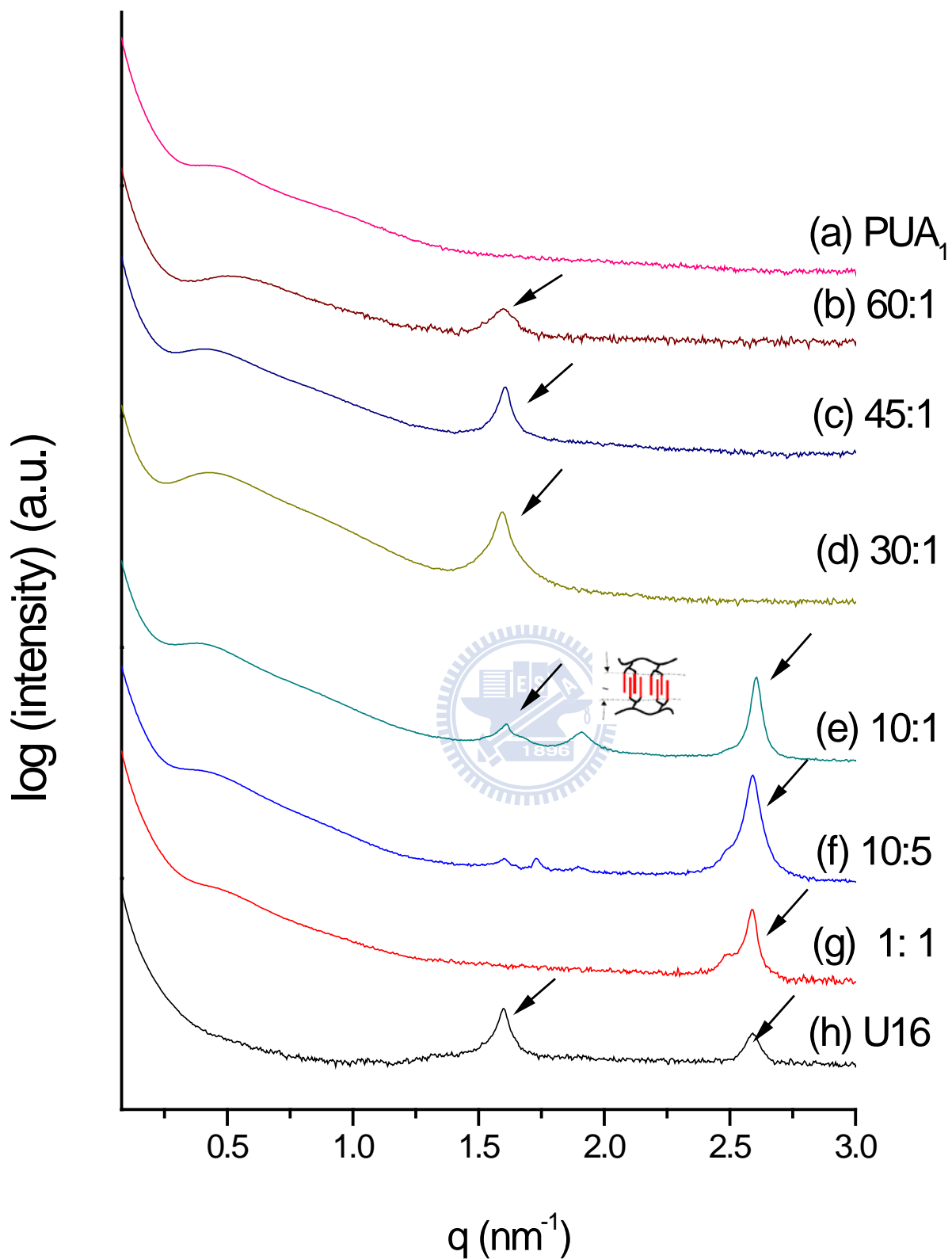
Figure 4-9. Representative synchrotron small angle X-ray scattering (SAXS) data as a function of the scattering vector (q) for a series of poly(amide urethane)/ 1-Hexadecyluracil (PAU/U16) blends having different PAU to U16 weight ratios.

99
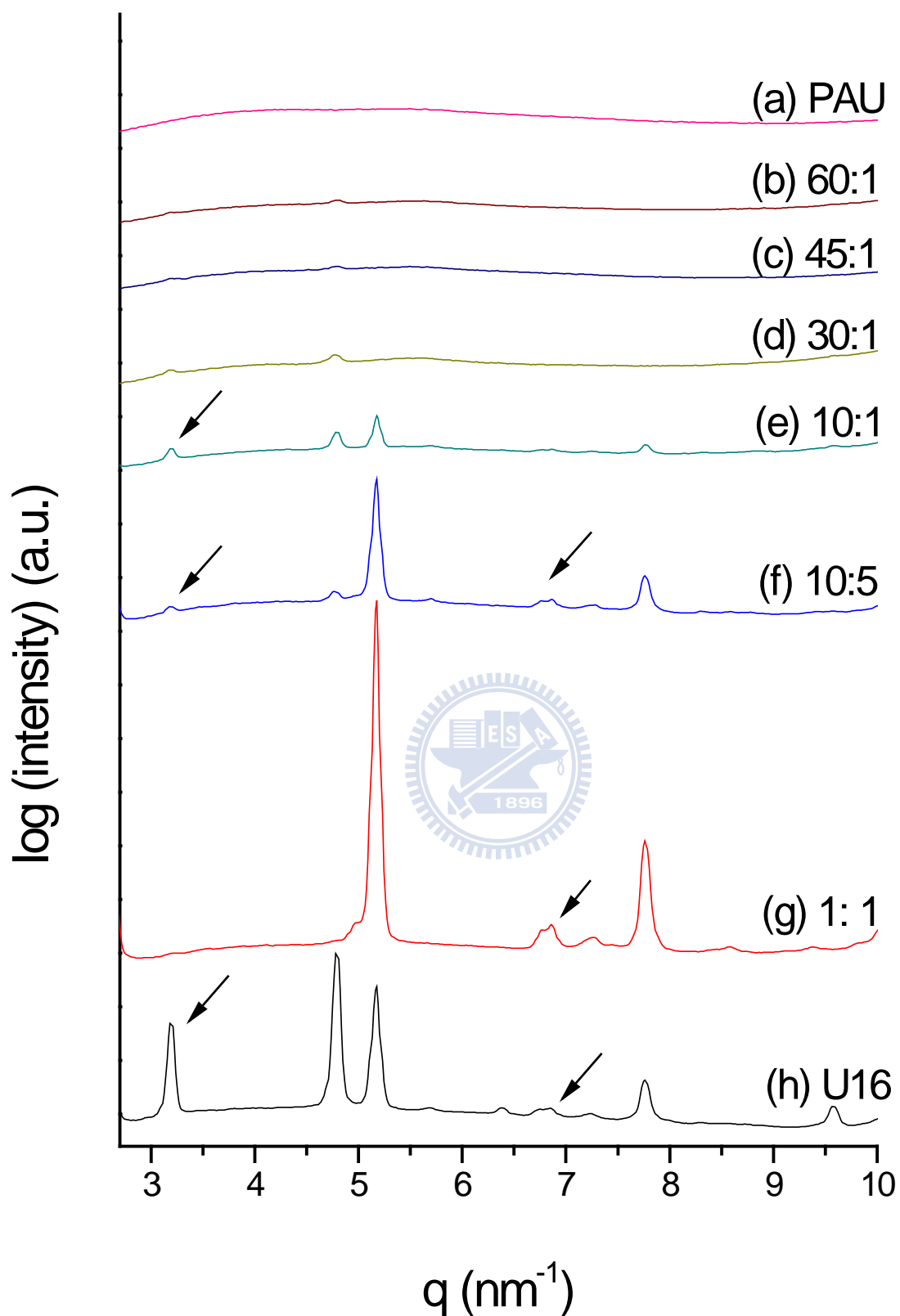
Figure 4-10. Representative wide angle X-ray diffraction (WAXD) patterns for PAU/U16 complexes with different weight ratios. The magnitude of the scattering vactor is given by $q=(4\pi/\lambda) \sin\theta$, where 2θ is the scattering angle and $\lambda=1.54$Å. Arrows are a guide for eyes.
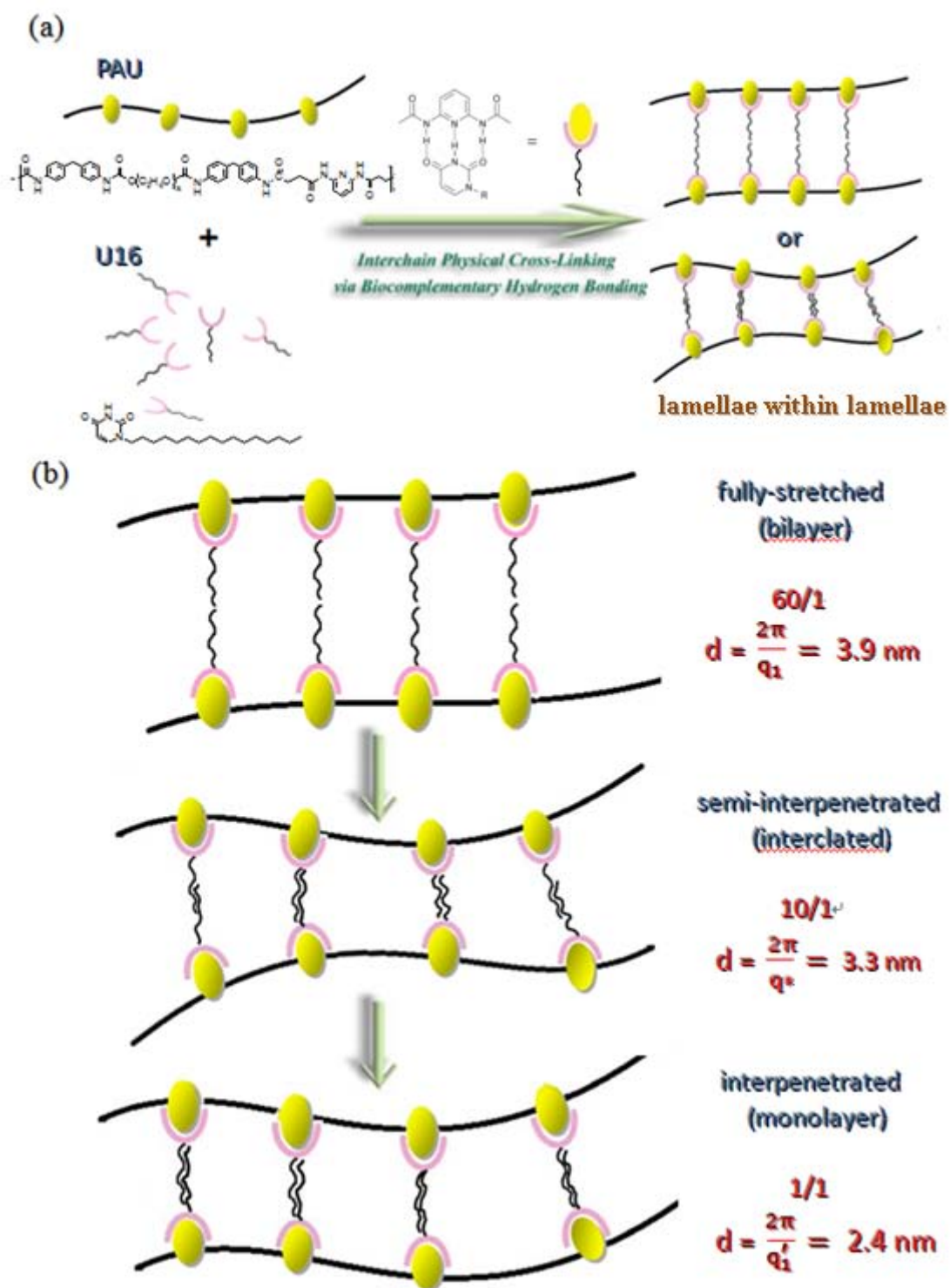
Scheme 4-3. Graphical representations of (a) the physical cross-linked structure formed.from PAU/U16 complexes in the bulk state and (b) the transition of the lamellar structures of various PAU/U16 complexes in bulk state.

4-4 TEM Observation of the Morphology

To visually investigate the molecular recognition morphology of the sample, transmission electron microscopy was used since transmission electron microscopy is one of the most powerful tools to reveal and study on the microstructure and morphology within materials. Also, the most important and the first thing to comprehend the morphology within materials is to prepare the ultrathin film of samples. The thickness of film varies as the requirement of samples being studied. The smaller the domain size, the thinner of the sample films is in need. In this section, the sample undergoing researched in this section(PAU/U16 blends) possess with rarely small domain size (<10nm), which is also the reason only a few articles studied PU by TEM, thus it is better to prepare ultrathin films in order to investigate the detail morphology within the system under studied. In general, there are two routes to prepare the films. The first one is solution-cast method, and the other is ultrathin microtome method (ultracut method) The former method may change the original morphology of PU since the solvent applied and interface during the procedures of solution-casting. Therefore, we utilized the second method in order to present the original bulk morphology and properties of surface. Besides, the limited thickness of ultracut microtome method is 40nm.

Because the glass transition temperature (T_g) of all PAU/U16 complexes are below room temperature, the samples were prepared by using an ulatramicrotome Reichert equipped with a diamond knife and obtained 60nm thick ultrathin sections. Samples were cut at -100℃. Cutting the material in the glassy state (below $T_{g,SS}$) enables one to avoid a major part of the deformation of cutting. Also, the sections were stained on copper grids with RuO_4 vapors to enhance contrast between hard and soft phases by exposing the samples with a 2%-RuO_4 solution during 90 min before TEM observations. **Figure 4-11** and **Figure 4-12** shows the TEM image of the sample

cryo-microtomed at -120 °C which indicates a phase-saparated structure within long-range order lamellar structure. The presence of a two-phase nature has been strongly suggested from the DSC and SAXS results listed above. Also, **Figures 4-11** and **Figure 4-12** illustrated the TEM micrographs of PAU and PAU/U16 (10/1), respectively. As shown in **Figure 4-11**, PAU possessed a microphase separated structure with long-range order lamellar structure, which was consistent with the SAXS profiles. When U16 was incorporated to PAU **(Figure 4-12)**, the microphase separated structure was mediated without the change in the long-range order lamella structure of PAU matrix. That is to say, the surface structure did not change appreciably and still remained lamellae. The size of the dark regions was varied from ca. 10 to 20 nm because of the coexistence of these tail-to-tail, semi-interpenetrated, and interpenetrated structures of U16 within the lamella structure of PAU as indicated in the SAXS and WXRD profiles.

On the other hand, the microphase separation of PAU/U16 blends has reached nano-scale aggregation since the hard segment domains dispersed in soft segment matrixes uniformly. These TEM images support the trends observed and commented on SAXS analysis. Also, the *d-spacing* is in good agreement with data obtained during the SAXS analysis. It is worth to be noted that rare articles studied the morphologies within PU system by TEM observations since the partial miscible of hard segments and soft segments. However, we successfully present the microstructure of PAU/U16 here by both TEM and AFM.

Figure 4-11. Transmission electron micrograph of the cryo-microtomed film of the pure PAU stained with RuO_4. The dark region (matrix) corresponds to the phase of hard segments—PAU; the white region corresponds to the excluded PEG soft segment. The scale bar represents 100 nm.
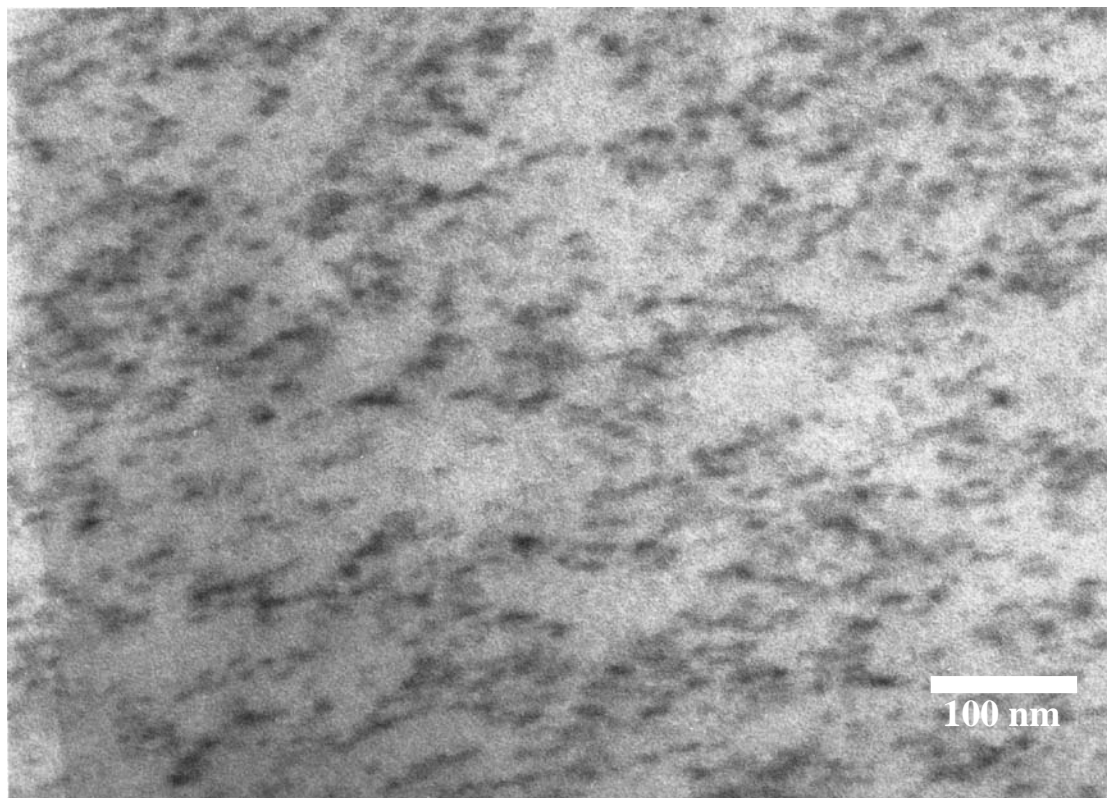
Figure 4-12. Transmission electron micrograph of the cryo-microtomed film of the PAU/U16 (10/1) blend stained with RuO_4. The dark region (matrix) corresponds to the phase of hard segments—PAU; the white region corresponds to the excluded PEG soft segment. The scale bar represents 100 nm.

4-5 Atomic Force Microscopy Analysis

The morphology of spin-coated PAU/U16 was also observed by AFM. Tapping-mode AFM was used on thin films to obtain height and phase imaging data simultaneously on a Veeco Dimension 5000 Scanning Probe Microscope. Microscopy revealed a complex multiscale morphology and allowed observing microscale phase separation. As shown in the phase images of (**Figure 4-13** and **4-14**), a strong contrast between domains with higher and lower hardness was obtained. The darker areas are indicative of softer material and lighter areas represent harder material.[173,174] Similar to those of thermoplastic polyurethane materials in some previous study, the phase-separated morphology in pure PAU and PAU/U16 complexes can be observed. The lighter spots and region were dispersed simultaneously in darker areas, suggesting there are various hard segments in the samples. It might be caused by the rigidity difference between different parts of hard segments, which are composed of diaminopyridine (DAP) and Methylene di-p-phenyl diisocyanate (MDI) and Uracil of U16. In addition, AFM images indicate that microscale domain is dispersed within mesoscale domain, both micro- and mesoscale domain with hard and soft regions inside. Also, a contrast in phase can be due to the result of differences in mechanical properties of the components near the surface of the scanned material. Soft segments are anticipated to give dark contrast in the phase imaging, while hard segments appear as bright areas, provided that phase angle differences due to adhesion contrast do not have significant effects.

Considering other experiments results (SAXS and TEM) and AFM data, we can depict the molecules should be arranged into layer plane. From **Figure 4-13(a)** and **(b)**, various hard segments dispersed within whole matrix can be seen. This is similar to those in many of the previous study on polyurethane surface morphology. Upon

adding U16 into PAU matrix, the surface structure did not change appreciably. As U16 was incorporated into PAU [for the PAU/U16=60/1 blend] (**Figure 4-13(c)**), these light (hard) spots and regions were separated and less pronounced because the hard phase would be mediated though the incorporation as illustrated in the results of FTIR spectra(i.e. the distance between chain and chain was not so close as pure PAU). In addition, **Figure 4-13(d)** also displayed the microscale domains dispersed within mesoscale domains as shown in TEM micrographs. Specifically, as the excess content of U16 continuously increase to a ratio of PAU/U16=10/1, there is a discernable, albeit not dramatically, increase in the amount of light-colored region seen in the images(**Figure 4-13(e) and (f)**) since the excess amount of U16 may crystallize or arrange stacked together. The images support the trends observed and commented on during the SAXS analysis.

Several mothods presented here, SAXS, AFM, and even TEM, lead to mutually supportive conclusion regarding the microphase separation characteristics. It should again be recalled that the SAXS results presented here is more close to real microstructure bulk state within polymer blends, and the slightly larger mesoscale phase separation of PAU/U16 observed by AFM is a result of aggregate induced by physical crosslink.

(Surface Height)   (Phase image)
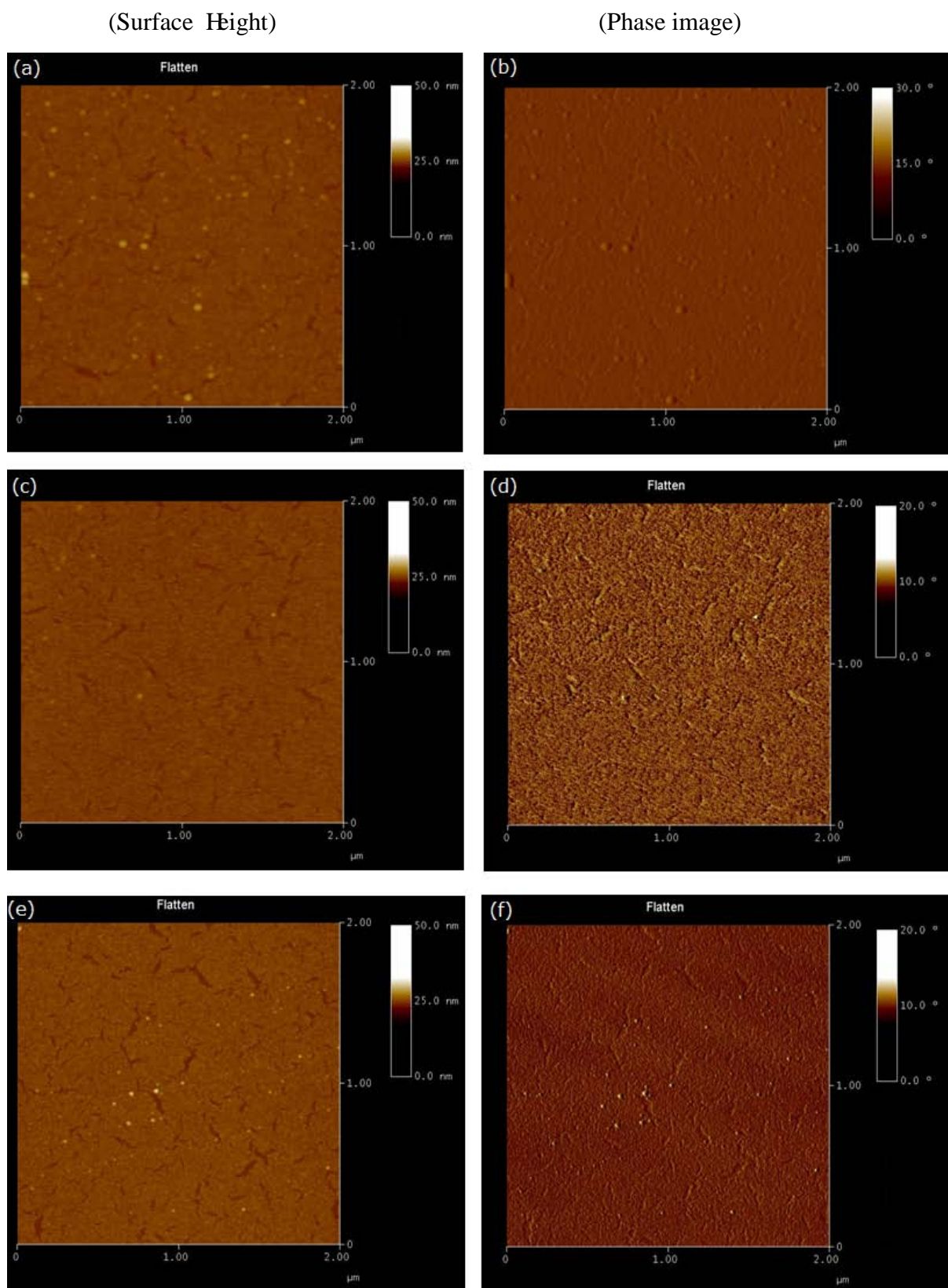
Figure 4-13. AFM 2D height and phase images of different ratio of blends:
(a)(b) PUA1 and (c)(d) 60:1 (e)(f) 10:1 with scale of $2\times 2 \ \mu m^2$.
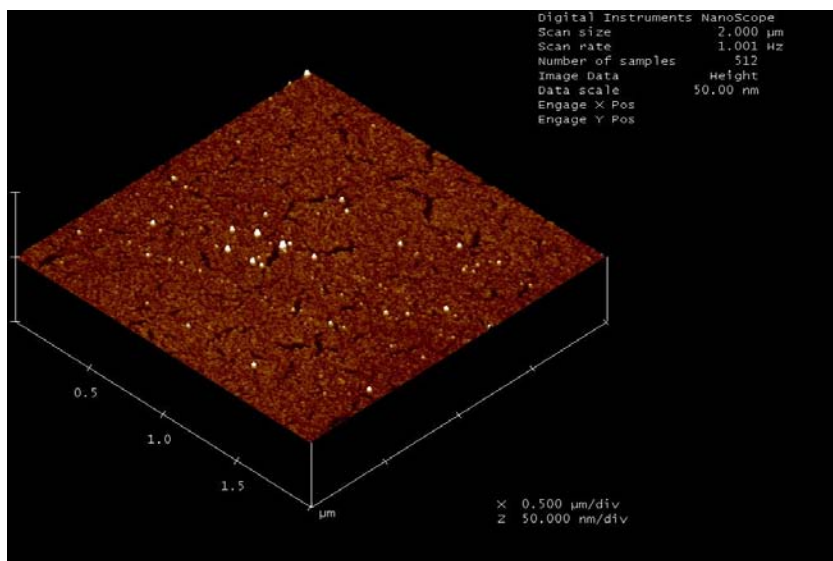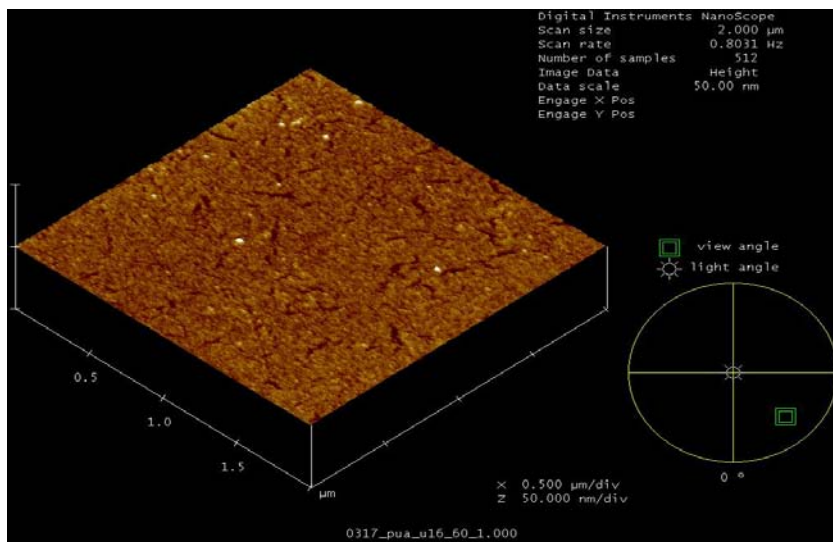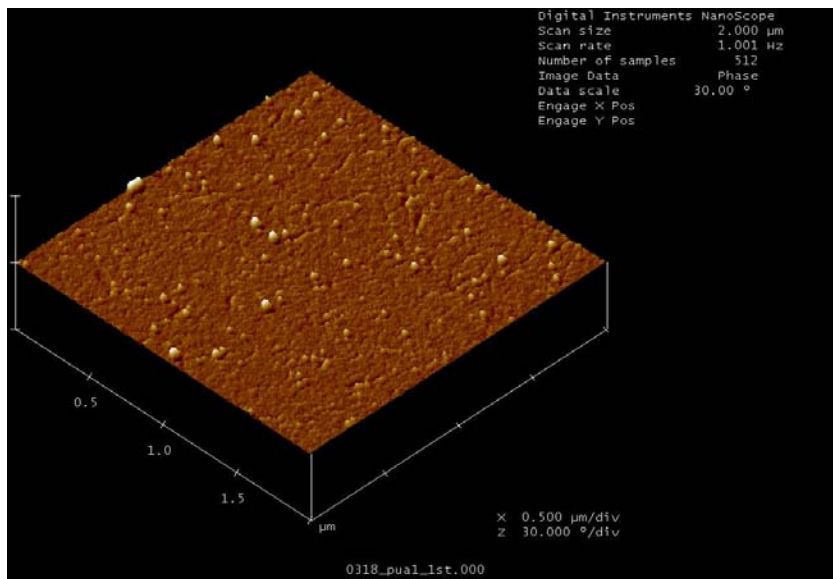
Figure 4-14. AFM 3D was used in the investigation of the morphology of different ratio of blends (a) PUA1 and (b) 60:1 (c) 10:1 with scale of $2 \times 2\ \mu m^2$.

Chapter 5
Conclusion

In this study, specific interaction, morphologies and phase behaviors, mediated by hydrogen bonding interactions of PAU/U16 blends, have been studied. An novel alternative copolymer, poly (amide urethane), have been successfully synthesized through the incorporating of complementary unit (DAP) into a prepolymer consist of 4-4' MDI and PEG1000 on main chain. FTIR, DSC, WAXD, SAXS, AFM, and TEM techniques have been employed to investigate in detail the hydrogen-bonding interaction mechanism, miscibility, phase behavior and hierarchical structures of the novel PAU/U16 blends composed of U16 and poly(amide urethane) bearing DAP as complementary sites on main chain. Complementary between the guest molecules and polymer functionalities proved to be a key factor and efficient tool for directing the segregation preference of the molecules to the different structure transition. In a complementary study, the amphiphilic alkylated nucleobase, hexadecyluracil (U16) was incorporated into poly(amide urethane) synthesized ourselves with self-complementary group and several hydrogen bonding motifs for the study on the heterodimer recognition behavior within the alternative polymer. The effect of the heterodimer recognition on the microphase separation was investigated, revealing that the heterodimer recognition led the poly(amide urethane) to possessing the "plug and play" behavior even the heterodimer recognition coincided with several other hydrogen bonding motifs. TEM images and SAXS analyses indicate that different compositions of PAU/U16 blends results in different microphase separation structures through the mediation of hydrogen bonding interactions. The period and morphlogies of PAU/U16 complexes can be rationally tuned by the amount of U16. Upon the adding of U16, the lamellar structure within long-range lamellar changes from bilayer to bilayer with interclated and further to monolayer. The concept allows for rich varieties of morphologies and phase transitions form recognition unit-functionalized copolymer scaffolds by modifying the recognition units or the amount of amphiphiles.

Acknowledgment
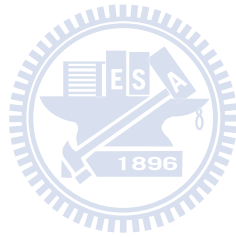
Chapter 6

Reference

1 Wang CB, Cooper SL. Morphology and properties of segmented polyether polyurethaneureas. *Macromolecules* **1983**;*16*:775–86.

2 Sperling LH. Introduction to physical polymer science. New York: Wiley; **2001**.

3 Howard GT. Biodegradation of polyurethane: a review. Int Biodeter Biodegr **2002**;*49*:245–52.

4 Szycher, Handbook of Polyurethane , pp.1-4

5 Deterich, D. Prog Org Coat **1981**, 9, 281.

6 Yen, M. S.; Kuo, S. C. *J Appl Polym Sci* **1998**, *67*, 1301.

7 Wen, T. C.; Wu, M. S.; Yang, C. H. *Macromolecules* **1999**, *32*, 2712.

8 Kim, B. K.; Seo, J. W.; Jeong, H. M. *Eur Polym J* **2003**, *39*, 85.

9 Gunatillake PA, Martin DJ, Meijs GF, McCarthy SJ, Adhikari R. Designing biostable polyurethane elastomers for biomedical applications. *Aust J Chem* **2003**; *56*(6):545–57.

10 Gogolewski S. Leading contribution. Selected topics in biomedical polyurethanes. A review. *Colloid Polym Sci* **1989**;*267*:757–85.

11 G. Behrendt, B. W. Naber *Journal of the University of Chemical Technology and Metallurgy, 44, 1,* **2009***, 3-23*

12 Chattopadhyay DK, Raju KVSN. Structural engineering of polyurethane coatings for high performance applications. *Prog Polym Sci* **2007**; *32*:352–418.

13 E. Tocha, H. Janik, M. De̜bowski, and G. J. Vancso *JOURNAL OF MACROMOLECULAR SCIENCE* Part B—Physics Vol. B**41**, Nos. 4–6, pp. 1291–1304, **2002**

14 L. G. Wade, Jr. Organic Chemistry , A Simon and Schuster Company Englewood Cliffs,New Jersy(**1995**)

15 J. H. Saunders and K. C. Frisch. Polyurethane; Chemistry and Technology, Parts Ⅰ and Ⅱ, Interscience, New York (**1962**)

16 P. Wright and A. P. C. Cumming, Solid Polyurethane Elastomers, Maclaren and Sons, London (**1969**).

17 C. Hepburn, Polyurethane elastomers, Applied Science Publishers LTD (**1982**).

18 Wang, G.C.; Fang, B.; Zhang, Z.P. Study of the Domain-Structure and Mechanical-Properties of the Ethylene-Oxide Endcapped Poly(Propylene Oxide) Polyol 4,40-Diphenylmethane Diisocyanate Ethylenediol Polyurethane System. *Polymer* **1994**,*35* (15), 3178–3183.

19 Hong, J.L.; Lillya, P.; Chien, J.C.W. Degree of Phase-Separation in Polyether: Polyurethane Copolymers with Different Chemical Structures of Hard Segments. *Polymer* **1992**, *33* (20), 4347–4351.

20 Balas, A.; Pałka, G.; Foks, J.; Janik, H. Properties of Cast Urethane Elastomers Prepared from Poly(1-Caprolactone)s. J. Appl. Polym. Sci. **1984**, *29*, 2261–2270.

21 Cooper, S.T.; Tobolsky, A.V. Properties of Linear Elastomeric Polyurethanes. J. Appl. Polym. Sci. **1966**, *10*, 1837–1844.

22 Serrano, M.; MacKnight, W.J.; Thomas, E.L.; Ottino, J.M. Transport–Morphology Relationships in Segmented Polybutadiene Polyurethanes: 1. Experimental Results. *Polymer* **1987**, *28*, 1667–1673.

23 Fridman, I.D.; Thomas, E.L. Morphology of Crystalline Polyurethane Hard Segment Domains and Spherulites. *Polymer* **1980**, *21*, 388–392.

24 Leung, L.M.; Koberstein, J.T. Small-Angle Scattering Analysis of Hard-Microdomain Structure and Microphase Mixing in Polyurethane Elastomers. *J.Polym. Sci.: Polym. Phys.* Ed. **1985**, *23*, 1883–1913.

25 Chu, B.; Gao, T.; Li, Y.J.; Wang, J.; Desper, C.R.; Byrne, C.A. Microphase Separation Kinetics in Segmented Polyurethanes—Effects of Soft Segment

Length and Structure. *Macromolecules* **1992**, *25* (21), 5724–5729.

26   Koberstein, J.T.; Stein, R.S. Small-Angle X-Ray Scattering Studies of Microdomain Structure in Segmented Polyurethane Elastomers. *J. Polym. Sci.: Polym. Phys.* Ed. **1983**, *21*, 1439–1472.

27   Estes, G.M.; Seymour, R.W.; Cooper, S.L. Infrared Studies of Segmented Polyurethane Elastomers. II. Infrared Dichroism. *Macromolecules* **1971**, *4* (4), 452–457.

28   Bonart, R. X-Ray Investigations Concerning the Physical Structure of Cross-Linking in Segmented Urethane Elastomers. *J. Macromol. Sci.—Phys.* **1968**, *B2* (1), 115–138.

29   Bonart, R.; Morbitzer, L.; Hentze, G. X-Ray Investigations Concerning the Physical Structure of Cross-Linking in Urethane Elastomers. II. Butanediol as Chain Extender. *J. Macromol. Sci.—Phys.* **1969**, *B3* (2), 337–356.

30   Bonart, R. Thermoplastic Elastomers. *Polymer* **1979**, *20*, 1389–1403.

31   Li, C.; Goodman, S.L.; Albrecht, R.M.; Cooper, S.L. Morphology of Segmented Polybutadiene–Polyurethane Elastomers. *Macromolecules* **1988**, *21*, 2367–2375.

32   Petrovic ZS, Ferguson J. Polyurethane elastomers. *Prog Polym Sci* **1991**;*16*:695–836.

33   Estes GM, Seymour RW, Cooper SL. Infrared studies of segmented polyurethane elastomers. II. Infrared dichroism. *Macromolecules* **1971**;*4*:452–7.

34   Qi HJ, Boyce MC. Stress–strain behavior of thermoplastic polyurethanes. *Mech Mater* **2005**;*37*:817–39.

35   Masiulanis, B.; Zielinski, R. *J Appl Polym Sci* **1985**, *30*, 2731.

36   Lin, M.-F.; Shu, Y.-C.; Tsen, W.-C.; Chuang, F.-S. *Polym Int* **1999**, *48*, 433.

37   Petrovic, S.; Zavargo, Z.; Flynn, J. H.; Mackinght, W. J. *J Appl Polym Sci* **1994**, *51*, 1087.

114

38   Lin, M.-F.; Tsen, W.-C.; Shu, Y.-C.; Chuang, F.-S. *J Appl Polym Sci* **2001**, *79*, 881.

39   Chuang, F.-S.; Tsen, W.-C.; Shu, Y.-C. *Polym Degrad Stab* **2004**, *84*, 66.

40   Koberstein, J.T.; Galambos, A.F.; Leung, L.M. Compression-Molded Polyurethane Block Copolymers. 1. Microdomain Morphology and Thermomechanical Properties. *Macromolecules* **1992**, *25* (23), 6195–6204.

41   Li, C.; Cooper, S.L. Direct Observation of the Micromorphology of Polyether Polyurethanes Using High-Voltage Electron Microscopy. *Polymer* **1990**, *31*, 3–7.

42   Chen-Tsai, C.H.Y.; Thomas, E.L.; MacKnight, W.J.; Schneider, N.S. Structure and Morphology of Segmented Polyurethanes: 3. Electron Microscopy and Small Angle X-Ray Scattering Studies of Amorphous Random Segmented Polyurethanes. *Polymer* **1986**, *27*, 659–666.

43   Chang, A.L.; Briber, R.M.; Thomas, E.L.; Zdrahala, R.J.; Critchfield, F.E. Morphological Study of the Structure Developed During the Polymerisation of a Series of Segmented Polyurethanes. *Polymer* **1982**, *23*, 1060–1068.

44   Chau, K.W.; Geil, P.H. Domain Morphology in Polyurethanes. *Polymer* **1985**, *26*, 490–500.

45   Chen, C.H.Y.; Briber, R.M.; Thomas, E.L.; Xu, M.; MacKnight, W.J. Structure and Morphology of Segmented Polyurethanes: 2. Influence of Reactant Incompatibility. *Polymer* **1983**, *24*, 1333–1340.

46   Foks, J.; Janik, H.; Russo, R.; Winiecki, S. Morphology and Thermal-Properties of Polyurethanes Prepared Under Different Conditions. Eur. *Polym. J.* **1989**, *25* (1), 31–37.

47   McLean, R.S.; Sauer, B.B. Tapping-Mode AFM Studies Using Phase Detection for Resolution of Nanophases in Segmented Polyurethanes and Other Block Copolymers. *Macromolecules* **1997**, *30 (26)*, 8314–8317.

48 Karbach, A.; Drechsler, D. Atomic Force Microscopy—A Powerful Tool for Industrial Applications. *Surf. Interface Anal*. **1999**, *27 (5–6)*, 401–409.

49 Foks, J.; Michler, G.; Nauman, I. Determination of Lamellae in Segmented Polyurethanes by Electron Microscopy. *Polymer* **1987**, *28,* 2195–2199.

50 Janik, H.; Foks, J. Microscopic Investigations of Segmented Polyurethanes. In Advances in Urethane Science and Technology; Frisch, K.C., Klempner, D., Eds.; Technomic Pub. Co.: Lancaster, **1992**; Vol. *11*, 137–172.

51 Fridman, I.D.; Thomas, E.L.; Lee, L.J.; Macosko, C.W. Morphological Characterisation of Reaction Injection Moulded (RIM) Polyester-Based Polyurethanes. *Polymer* **1980**, *21*, 393–402.

52 Janik, H.; Foks, J. The Solidification of Bulk and Solution Cast Segmented Polyurethanes. Prog. Colloid *Polym. Sci*. **1992**, *90*, 241–246.

53 Colton, R.J.; Engel, A.; Frommer, J.E.; Gaub, H.E.; Gewirth, A.A.; Guckenberger,R.; Rabe, J.; Heckl, W.M.; Parkinson, B., (Eds.) Procedures in Scanning Probe Microscopy; Wiley: New York, **1998**.

54 Ratner, B.D.; Tsukruk, V.V. Scanning Probe Microscopy of Polymers, Symposium Series 694; ACS: Washington, **1996**.

55 Magonov, S.N.; Whangbo, M.-H., (Eds.) Surface Analysis with STM and AFM; VCH: *Weinheim*, **1996**.

56 Pearce, R.; Vancso, G.J. Imaging of Melting and Crystallization of Poly(Ethylene Oxide) in Real-Time by Hot-Stage Atomic Force Microscopy. *Macromolecules* **1997**, *30 (19)*, 5843–5848.

57 Scho¨nherr, H.; Snetivy, D.; Vancso, G.J. A Nanoscopic View at the Spherulitic Morphology of Isotactic Polypropylene by Atomic Force Microscopy. *Polym. Bull*. **1993**, *30 (5)*, 567–574.

58 Trifonova-van Haeringen, D.; Varga, J.; Ehrenstein, G.W.; Vancso, G.J. Features
116

of the Hedric Morphology of Beta-Isotactic Polypropylene Studied by Atomic Force Microscopy. *J. Polym. Sci.,* Part B: Polym. Phys. **2000**, *38 (5)*, 672–681.

59　Vancso, G.J.; Nisman, R.; Snetivy, D.; Scho̤nherr, H.; Smith, P.; Ng, C.; Yang, H.F. Morphological-Studies of Ordered, Solid Polymers by Scanning Force Microscopy. *Colloid Surf.* A **1994**, *87 (3)*, 263–275.

60　Harold Schonhorn, *Macromolecules*, **1968**, *1*,145,

61　T. K. Kwei, H. Schonhorn, and H. L. Frisch, *J. Appl . Phys.*, **1967**, *38*, 2512,

62　Souheng Wu., Polymer Interface and Adhesion,M. Dekker, New York, p323.

63　Seymour, R. W.; Cooper, S. L. *Macromolecules* 1973, 6, 48.

64　Jacques, C. H. M. "Polymer Alloys"; Klempner, D. K.; Frisch, K. C., Eds.; Plenum Press: New York, **1977**; p 287.

65　Hesketh, T. R.; Van Bogart, J. W. C.; Cooper, S. L. *Polym. Eng. Sci.* 1980, 20(1), 190. 66. Van Bogart, J. W. C.; Bluemke, D. A.; Cooper, S. L. *Polymer* **1981**, *22*, 1428

67　Alexander F. Goncharov, M. Riad Manaa, Joseph M. Zaug, Richard H. Gee, Laurence E. Fried, and Wren B. Montgomery (2005). "Polymerization of Formic Acid under High Pressure". *Phys. Rev. Lett.* **94** (*6*): 065505..

68　George A. Jeffrey. *An Introduction to Hydrogen Bonding (Topics in Physical Chemistry)*. Oxford University Press, USA (March 13, **1997**). ISBN 0-19-509549-9

69　Jignesh P. Sheth, Ashish Aneja et al. *Polymer* 2004, 45, 5979–5984

70　Blackwell, J., and Gardner, K. H., *Polymer*, **1979**, *20*, 13.

71　Blackwell, J., and Nagarajan, M. R., *Polymer*, **1981**, *22*, 202.

72　Brunsveld, L.; Folmer, B. J. B.; Meijer, E. W.; Sijbesma, R. P. *Chem. Rev.* **2001**, *101*, 4071–4097.

73　Sessler, J. L.; Lawrence, C. M.; Jayawickramarajah, *J. Chem. Soc. Rev*. **2007**, *36*,

314–325.

74   Binder, W. H.; Zirbs, R. *Adv. Polym. Sci.* **2007**, *207*, 1–78.

75   South, C. R.; Burd, C.; Weck, M. *Acc. Chem. Res.* **2007**, *40*, 63–74.

76   Hoogenboom, R.; Fourniera D.; Schubert, U. S. *Chem. Commun.*, 2008, 155–162.

77   Wilson, A. J. *Soft Matter* **2007**, *3*, 409–425.

78   Gu Y.; Kar T.; Scheiner S., *J. Am. Chem. Soc.* **1999**, *121*, 9411–9422.

79   Wilson, A. J. *Soft Matter* **2007**, *3*, 409–425.

80   Sijbesma, R. P.; Beijer, F. H.; Brunsveld, L.; Folmer, B. J. B.; Ky Hirschberg, J. H. K.; Lange, R. F. M.; Lowe, J. K. L.; Meijer, E. W. *Science* **1997**, *278*, 1601–1604.

81   Askew, B.; Ballester, P.; Buhr, C.; Jeong, K. S.; Jones, S.; Parris, K.; Williams K. and Rebek, J. Jr. *J. Am. Chem. Soc.*, **1989**, *111*, 1082.

82   Zimmerman, S. C.; Wu, W .and Zeng, Z. *J. Am. Chem. Soc.*, **1991**, *113*, 196.

83   V. A. Bloomfield, D. M. Crothers and I. Tinoco, Jr., Nucleic Acids: Structures, Properties, and Functions, University Science Books, Sausalito, CA, **2000**.

84   K. Hoogsteen, *Acta Crystallogr.*, **1963**, *16*, 907 and references therein.

85   See for example: W. Saenger, *Principles of Nucleic Acid Structures*, Springer, New York, **1984**.

86   See for example: Soyfer, V.N.; Potaman, V.N. *Triple-Helical Nucleic Acids*, Springer, New York, **1995**.

87   Davis, J. T. *Angew. Chem. Int. Ed.*, **2004**, *43*, 668. 35

88   Sartorius, J. and Schneider, H.-J. *Chem. Eur. J.* **1996**, *2*, 1446 and references cited therein.

89   Gottarelli, G.; Masiero, S.; Mezzina, E.; Spada, G. P.; Mariani, P. and Recanatini, M. *Helv. Chim. Acta*. **1998**, *81*, 2078.

90   For a recent example, see: T. Giorgi, F. Grepioni, I. Manet, P. Mariani, S. Masiero, E. Mezzina, S. Pieraccini, L. Saturni, G.P. Spada, G. Gottarelli, *Chem. Eur. J.*

2002, *8*, 2143-2152 and reference cited therein.

91 Lehn J.-M., *Angew. Chem.,Int. Ed. Engl.*, **1988**, *27*, 89.

92 Lehn, J.-M. *Angew. Chem. Int. Ed. Engl.* **1990**, *29*, 1304.

93 Philp, D.; Stoddart, J. F. *Angew. Chem., Int. Ed. Engl.*, **1996**, 35, 1155–1196.

94 Ciferri, A. Supramolecular Polymers, 2nd edn, Taylor and Francis, Boca Raton, Florida, **2005**.

95 Brunsveld, L.; Folmer, B. J. B.; Meijer E. W.; Sijbesma, R. P. *Chem. Rev.*, **2001**, 101, 4071–4097.

96 De Greef, T. F. A.; Smulders, M. M. J.; Wolffs, M.; Schenning, A. P. H. J.; Sijbesma, R. P.; Meijer, E. W. *Chem. Rev.*, **2009**, *109*, 5687–5754.

97 South, C. R.; Burd, C.; Weck, M. *Acc. Chem. Res.* **2007,** *40*, 63–74.

98 Lehn, J.-M. *Supramolecular Chemistry*; Wiley-VCH, **1995**.

99 Pedersen, C. J. *J. Am. Chem. Soc.* **1967**, *89*, 7017–7036.

100 Cram, D. J.; Cram, J. M. *Science* **1974**, *183*, 803–809.

101 Dietrich, B.; Lehn, J. M.; Sauvage, J. P. *Tetrahedron Lett.* **1969**, 2889–2892.

102 Loeb, S. J.; Tiburcio, J.; Vella, S. J. *Org. Lett.* **2005**, *7*, 4923–4926.

103 Atwood, J. L.; Davies, J. E. D.; MacNicol, D. D.; Vögtle, F. *Comprehensive Supramolecular Chemistry*; Pergamon: Oxford, **1996**.

104 Goshe, A. J.; Steele, I. M.; Ceccarelli, C.; Rheingold, A. L.; Bosnich, B. *Proc. Natl. Acad. Sci.* **2002**, *99*, 4823–4829.

105 Prins, L. J.; Reinhoudt, D. N.; Timmerman, P. *Angew. Chem. Int. Ed.* **2001**, *40*, 2382–2426.

106 Brunsveld, L.; Folmer, B.J.B.; Meijer, E.W.; Sijbesma, R.P. *Chem. Rev.* **2001**, 101, 4071-4097.

107 Ciferri, A. Macromol *Rapid Commun* **2002**, 23, 511-529.

108 Supramolecular Polymers Credi, A., Ed.; Marcel Dekker: New York, **2000.**

109 Zimmerman, S.C.; Zeng, F.W.; Reichert, D.E.C.; Kolotuchin, S.V. *Science* **1996**, 271, 1095-1098.

110 Castellano, R.K.; Nuckolls, C.; Eichhorn, S.H.; Wood, M.R.; Lovinger, A.J.; Rebek, Jr., J. *Angew. Chem. Int. Ed* **1999**, 38, 2603-2606.

111 Yamaguchi, N.; Gibson, H.W. *Angew. Chem. Int. Ed.* **1999**, 38, 143-147.

112 Zhang, P.; Moore, J.S. *J. Polym. Sci. Part A Polym. Chem.* **2000**, 38, 207-219.

113 Zubarev, E.R.; Pralle, M.U.; Sone, E.D.; Stupp, S.I. *J. Am. Chem. Soc.* **2001**, 123, 4105-4106.

114 Archer, E.A.; Krische, M.J. *J. Am. Chem. Soc.* **2002**, 124, 5074-5083.

115 Sijbesma, R.P.; Beijer, F.H.; Brunsveld, L.; Folmer, B.J.B.; Hirschberg, J.H.K.K.; Lange, R.F.M.; Lowe, J.K.L.; Meijer, E.W. *Science* **1997**, 278, 1601-1604.

116 Hirschberg, J.H.K.K.; Beijer, F.H.; van Aert, H.A.; Magusin, P.C.M.M.; Sijbesma, R.P.; Meijer, E.W. *Macromolecules* **1999**, 32, 2696-2705.

117 Lohmeijer, B.G.G.; Schubert, U.S. *J. Polym. Sci. Part A Polym. Chem.* **2003**,41, 1143-1427.

118 R. R. Sinden, DNA Structure and Function, Academic Press, Inc., New York, **1994**.

119 J. D. Watson and F. H. Crick, *Nature*, **1953**, *171*, 737.

120 (a) E. Snip, S. Shinkai and D. N. Reinhoudt, *Tetrahedron. Lett*., **2001**, *42*, 2153; (b) R. J. Thibault, T. H. Galow, E. J. Turnberg, M. Gray, P. J. Hotchkiss and V. M. Rotello, *J. Am. Chem. Soc.*, **2002**, *124*, 15249; (c) S. Sivakova and S. J. Rowan, *Chem. Commun.*, **2003**, 2428; (d) J. Chen and N. C. Seeman, *Nature,* **1991**, *350*, 631; (e) J. J. Storhoff and C. A. Mirkin, *Chem. Rev.*, **1999**, *99*, 1849; (f) F. Nakamura, K. Ijiro and M. Shimomura, *Thin Solid Films*, **1998**, 327–329, 603; (g) T. Shimizu, R. Iwaura, M. Masuda, T. Hanada and K. Yase, *J. Am. Chem. Soc.*, **2001**, *123*, 5947.

[121] For reviews see: (a) L. J. Prins, D. N. Reinhoudt and P. Timmerman, *Angew. Chem. Int. Ed.*, 2001, *40*, 2382; (b) D. C. Sherrington and K. A. Taskinen, *Chem. Soc. Rev*., **2001**, *30*, 83; (c) M. M. Conn and J. Rebek, Jr., *Chem. Rev*., **1997**, *97,* 1647; (d) M. J. Krische and J.-M. Lehn, *Struct. Bond*., **2000**, *96*, 3; (e) T. Kato, *Struct. Bond*., **2000**, *96*, 95; (f) R. E. Melendez, A. J. Carr, B. R. Linton and A. D. Hamilton, Struct. Bond., 2000, 96, 31; (g) S. C. Zimmerman and P. S. Corbin, *Struct. Bond.*, **2000**, *96*, 63; (h) G. M. Whitesides, J. P. Mathias and C. T. Seto, *Science*, **1991**, *254*, 1312; (i) J.-M. Lehn, *Polym. Int.*, **2002**, *51*, 825; (j) R. P. Sijbesma and E. W. Meijer, *Chem. Commun.*, **2003**, *1*, 5.

[122] For a recent review see: (a) S. Sivakova and S. J. Rowan, *Chem. Soc. Rev*., **2005**, *34*, 9; (b) M. Kim and G. W. Gokel, *J. Chem. Soc., Chem. Commun.*, **1987**, 1686; (c) A. D. Hamilton and D. V. Engen, *J. Am. Chem. Soc.*, **1987**, *109*, 5035; (d) V. Malinovski, L. Tumir, I. Piantanida, M. Zinic and H.-J. Schneider, *Eur. J. Org. Chem.,* **2002**, 3785; (e) M. M. Conn, G. Deslongchamps, J. de Mendoza and J. Rebek, Jr., *J. Am. Chem. Soc.*, **1993**, *115*, 3548; (f) S. C. Zimmerman and W. Wu, *J. Am. Chem. Soc.*, **1989,** *111*, 8054; (g) M. Takase and M. Inouye, *J. Org. Chem.*, **2003**, *68*, 1134; (h) J. C. Adrian and C. S. Wilcox, *J. Am. Chem. Soc.*, **1989**, *111*, 8055; (i) J. S. Nowick, T. Cao and G. Noronha, *J. Am. Chem. Soc.*, **1994**, *116*, 3285; (j) J. F. Constant, J. Fahy and J. Lhomme, *Tetrahedron Lett.,* **1987**, *28*, 1777; (k) J. T. Davis, S. Tirumala, J. R. Jenssen, E. Radler and D. Fabris, *J. Org. Chem.*, **1995**, *60*, 4167; (l) M. G. M. Purwanto and K. Weisz, *J. Org. Chem.*, **2004**, *69*, 195; (m) C.-C. Zeng, Y.-L. Tang, Q.-Y. Zheng, L.-J. Huang, B. Xin and Z.-T. Huang, *Tetrahedron Lett.*, **2001**, *42*, 6179; (n) A. Marsh, N. W. Alcock, W. Errington and R. Sagar, *Tetrahedron*, **2003**, *59*, 5595; (o) H. T. Baytekin and E. U. Akkaya, *Org. Lett.*, **2000**, *2*, 1725; (p) R. K. Castellano, V. Gramlich and F. Diederich, *Chem. Eur. J.*, **2002**, *8*, 118; (q) V. Gubala, J. E. Betancourt and J. M.

Rivera, *Org. Lett*., **2004**, *6*, 4735.

123 This article will not cover the rich metalation chemistry of the individual nucleobases. For a review on this subject see: B. Lippert, Coord. *Chem. Rev.*, **2000**, *200*, 487.

124 (a) Rieth, S.; Baddeley, C.; Badjic, J. D. *Soft Matter* **2007**, 3, 137. (b) Sivacova, S. ;Rowan, S. J. *Chem. Soc. Rev.* **2005**, 34, 9. (c) Yamauchi, K.; Lizotte, J. R.; Long, T. E. *Macromolecules* **2002**, 35, 8745. (d) Snip, E.; Shinkai, S.; Reinhoudt, D.N. *Tetrahedron Lett.* **2001**, 42, 2153

125 (a) Sijbesma, R. P.; Beijer, F. H.; Brunsveld, L.; Folmer, B. J.; Hirschberg, J. H. K. K.; Lange, R. F. M.; Lowe, J. K. L.; Meijer, E. W. *Science* **1997**, 278, 1601. (b) Beijer, F. H.; Sijbesma. R. P.; Kooijman, H.; Spek, A. J.; Meijer, E. W. *J. Am. Chem. Soc.* **1988**, 120, 6761. (c) Folmer, B. J. B.; Sijibesma, R. P.; Kooijman, H.; Spek, A. L.; Meijer, E. W. *J. Am. Chem. Soc.* **1999**, 122, 9001.d) Hrchschberg, J. H. K. K.; Beijer, F. H.; van Aert, H. A.; Magusin, P. C. M. M.; Sijbesma, R. P.;Meijer, E. W. *Macromolecules* **1999**, 32, 2696

126 (a) Brunsveld, L.; Folmer, B.J.B.; Meijer, E.W.; Sijbesma, R.P. *Chem. Rev*. **2001**, *101*, 4071; (b) Ciferri, A. *Macromol. Rapid Commun.* **2002**, *23*, 511. (c) Ciferri, A. "Supramolecular Polymers" Marcel Dekker: New York, 2000.

127 (a) Liang, Z.; Cabarcos, O.M.; Allara, D.L.; Wang, Q. *Adv. Mater.* **2004**, *16*, 823-827. (b) Kosonen, H.; Ruokolainen, J. Knaapila, M.; Torkkeli, M.; Jokela, K.; Serimaa, R.; Brinke, G –t.; Bras, W.; Monkman, A.P.; Ikkala, O. *Macromolecules* **2000**, *33*, 8671-8675. (c) Calzolari, A.; Di Felice, R.; Molinari, E. Garbesi, A. *Physica E* **2002**, *13*, 1236-1239. (d) Tew, G.N.; Pralle, M.U.; Stupp, S.I. *Angew. Chem. Int. Ed.* **2000**, *39*, 517-521. (e) Chen, X.L.; Jenekhe, S.A. *Macromolecules* **2000**, *33*, 4610-4612. (f) Beck, J. B.; Rowan, S.J. *J. Am. Chem. Soc.* **2003**, *125*, 13922-13923.

128 (a) Kato, T. *Supramolecular Science,* **1996**, *3*, 53-59. (b) Kato, T.; Fréchet, J.M.J. *Macromol. Symp*. **1995**, *98*, 311-326. (b) (c) Lee, C.M.; Griffin, A.C. *Macromol. Symp*. **1997**, *117*, 281-290. (d) Kato, T.; Fréchet, J.M.J. *J. Am. Chem. Soc*. **1989**, *111*, 8533-8534. (e) Kato, T. "Hydrogen-Bonded Systems", in: *Handbook of Liquid Crystals*, Demus, D.; Goodby, J.W; Gray, G.W.; Spiess, H.-W.; Vill, V.; Eds., Wiley-VCH, Weinheim 1998, Vol. 2B, p. 969. (f) Kato, T. *Struct. Bonding* **2000**, *96*, 95-146.

129 (a) Lehn, J.-M. *Makromol. Chem., Macromol. Symp*. **1993***, 69,* 1-17. (b) Paleos, C. M.; Tsiorvas, D. *Angew. Chem. Int. Ed. Engl.* **1994**, *34*, 1696-1711.　(b) Zimmerman, N.; Moore, J. S.; Zimmerman, S.C. *Chem. Ind. (London)* **1998**, 604. (c) Muthukumar, M.; Ober, C.K.; Thomas, E.L. *Science* **1997**, *277*, 1225-1232. (d) "*Structure & Bonding*". Vol 96, Fujita, M. Ed., Springer, Berlin 2000. (e) Lehn, J.-M. "*Supramolecular Chemistry*", VCH, Weinheim 1995. (f) Treybig, A.; Dorscheid, C.; Weissflog, W.; Kresse, H. 1995 *Mol. Cryst. Liq. Cryst.*, **260***, 369-376.* (g) Torgova, S.I.; Strigazzi, A. 1995 *Mol. Cryst. Liq. Cryst.*, **336***,* 229 (h) Percec, V.; Heck, J.; Johansson, G.; Tomazos, D.; Kawasumi, M.; Chu, P.; Ungar, G. *Mol. Cryst. Liq. Cryst. Sci. Technol., Sect A*. **1994**, *419*, 384-387. (i) Percec, V. *Macro. Symp.* **1997***,117*, 267-273.

130 (a) Park, L. Y.; Hamilton, D. G.; McGehee, E. A.; McMenimen, K. A. *J.　Am. Chem. Soc*. **2003**, *125*, 10586-10590. (b) McMenimen K. A.; Hamilton D.G. *J. Am. Chem. Soc.* **2001,** *123*, 6453-6454. (c) Castellano, R.K.; Clark, R.; Craig, S.L.; Nuckolls, C.; Rebek, J.J. *Proc. Natl. Acad. Sci. USA* **2000,** *97*, 1241812421.

131 Lehn, J. M.; Mascal, M.; DeCian, A.; Fischer, J.; *Chem. Soc., Chem. Commun.* **1990**, 479-481.

132 Hilger, C.; Stadler, R. *Polymer* **1991**, *32*, 3244-3249.

133 He, C.; Donald, A.M.; Griffin, A.C.; Waigh, T.; Windle, A.H. *J. Polmy. Sci: Part*

B: Poly. Phys. **1998**, *36*, 1617-1624.

134   Brienne, M.J.; Gabard, J.; Lehn, J.M.; Stibor, I. *J. Chem. Soc. Chem. Commun.* **1989**, 1868-1870.

135   (a) Lehn, J.-M. *Poly. Int.* **2002**, *51*, 825-839. (b) Kato, T.; Mizoshita, N.; Kanie, K. *Macromol. Rapid Commun*. **2001**, *22*, 797-814. (c) Paleos, C.M; Tsiourvas, D. *Liq. Cryst*. **2001**, *28*, 1127-1161. (d) Ciferri, A. *Liq. Cryst*. **1999**, *26*, 489-494.

136   (a) Gulik-Krzywicki, T.; Fouquey, C.; Lehn, J.-M. *Proc. Natl. Acad. Sci. USA*, **1993**, *90*, 163-167. (b) Bladon, P.; Griffin, A.C. *Macromolecules* **1993**, *26*, 6604-6610. (c) Kotera, M.; Lehn, J.-M.; Vigneron, J.-P; *J. Chem. Soc. Chem. Commun.* **1994**, *2*,197-199. (d) Kotera, M.; Lehn, J.-M.; Vigneron, J.-P. *Tetrahedron* **1995**, *51*, 1953-1972. (e) Pourcain, C. St.; Griffin, A.C. *Macromolecules* **1995**, *28*, 4116.

137   Shibaev, V.P.; Bobrovsky, A.Y.; Boiko, N.I. *J. of Photochemistry and Photobiology A: Chemistry* **2003**, *155*, 3-19.

138   (a) O'Neill, M.; Kelly, S.M. *Adv. Mater.* **2003**, *15*, 1135-1146. (b) Shiyanovskaya, I.; Singer, K.D. *Phys. Rev. B.* **2003**, *67*, 35204-1:35204-7.

139   Kato, T.; Mizoshita, N. *Curr. Opin. Solid State Mater. Sci.* **2002**, *6*, 579-587.

140   Shimizu, T.; Iwaura, R.; Masuda, M.; Hanada, T. and Yase, K. *J. Am. Chem. Soc.*, **2001**, *123*, 5947.

141   S. Sivakova, S. J. Rowan, *Chem. Commun.* **2003**, 2428 – 2429.

142   For examples of the use of DNA sequences in supramolecular polymerization processes, see: a) J. Xu, E. A. Fogleman, S. L. Craig, *Macromolecules* **2004**, *37*, 1863 – 1870; b) F. R. Kersey, G. Lee, P. Marszalek, S. L. Craig, *J. Am. Chem. Soc.* **2004**, *126*, 3038 –3039; c) E. A. Fogleman, W. C. Yount, J. Xu, S. L. Craig, *Angew. Chem.* **2002**, *114*, 4198 – 4200; *Angew. Chem.* Int. Ed. **2002**, *41*, 4026 –4028; d) S. M. Waybright, C. P. Singleton, K. Wachter, C. J. Murphy, U.

H. F. Bunz, *J. Am. Chem. Soc*. **2001**, *123*, 1828 –1833.

143 For examples, see: a) W. Saenger, Principles of Nucleic Acid Structures, Springer, New York, 1984; b) S. Sivakova, S. J. Rowan, *Chem. Soc. Rev.* **2005**, *34*, 9 –21.

144 K. Yamauchi, J. R. Lizotte, T.E. Long, *Macromolecules* **2002**, *35*, 8745 – 8750.

145 S. J. Rowan, P. Suwanmala, S. Sivakova, *J. Polym. Sci*. Part A: Polym. Chem. **2003**, *41*, 3589 – 3596.

146 W. H. Binder, M. J. Kunz, C. Kluger, Thibault, R. J.; Hotchkiss, P. J.; Gray, M. and Rotello, V. M. *J. Am. Chem. Soc.*, **2003**, *125*, 11249.

147 S. Valkama, H. Kosonen, J. Ruokolainen, T. Haatainen, M. Torkkeli, R. Serimaa, G. Ten Brinke and O. Ikkala, *Nat. Mater.*, **2004**, *3*, 872–876.

148 Thibault, R. J.; Galow, T. H.; Turnberg, E. J.; Gray, M.; Hotchkiss, P. J. and Rotello, V. M. *J. Am. Chem. Soc.*, **2002**, *124*, 15249.

149 Hamley, I. W. *The Physics of Block Copolymers*; Oxford University Press: New York, **1998**

150 Platé, N. A.; Shibaev, V. P. *Comb-Shaped Polymer and Liquid Crystals*; Plenum Press: New York, **1987**.

151 (a) Ikkala. O.; ten Brinke, G. *Science* **2002**, *295*, 2407. (b) Chen, H. L.; Lu, J. S.; Yu, C. H.; Yeh, C. L.; Jeng, U. S.; Chen W. C. *Macromolecules* **2007**, 40, 3271. (c) Chiang, W. S.; Lin, C. H.; Nandan, B.; Yeh, C. L.; Rahman, M. H.; Chen, W. C.; Chen, H. L. *Macromolecules*, **2008**, 41, 8138.

152 (a) Ruokolainen, J.; Mäkinen, R.; Torkkeli, M. Mäkelä, T.; Serimaa, R.; ten Brinke, G.; Ikkala, O. *Science* **1998**, *280*, 557. (b) Ruokolainen, J.; ten Brinke, G.; Ikkala, O. *Adv. Mater.* **1999**, 11, 777 (c) S. Valkama, H. Kosonen, J. Ruokolainen, T. Haatainen, M. Torkkeli, R. Serimaa, G. Ten Brinke and O. Ikkala, Nat. Mater., 2004, 3, 872–876. (d) O. Ikkala and G. ten Brinke, *Chem. Commun.*, **2004**, 19, 2131–2137. (e) S. Valkama, T. Ruotsalainen, A. Nykalnen,

A. Laiho, H. Kosonen, G. ten Brinke, O. Ikkala and J. Ruokolainen, *Macromolecules*, **2006**, *39*, 9327–9336.

153 Valkama, S.; Ruotsalainen, T.; Kosonen, H.; Ruokokainen, J.; Torkkeli, M.; Serimma, R.; ten Brinke, G.; Ikkala, O. *Macromolecules* **2003**, 36, 3986.

154 Binder, W. H.; Kunz, M. J. and Ingolic, E. *J. Polym. Sci:* Part A: *Polym. Chem.*, **2004**, *42*, 162.

155 Cheng, C. C.; Huang, C. F.; Yen, Y. C.; Chang F. C. *J. Polym. Sci., Part A: Polym. Chem.* **2008**, 46, 6416.

156 Lin, I. H.; Cheng, C. C.; Yen, Y. C.; Vhang, F. C. *Macromolecules* **2010**, 43,1245.

157 (a) Canilho, N., Kasëmi, E., Mezzenga, R. and Schlﾘter, A. D. *J. Am. Chem. Soc.* **2006**, 128, 13998 (b) Ponomarenko, E. A.; Tirrell, D. A.; MacKnight, W. J. *Macromolecules* **1996**, *29*, 8751.

158 Nielsen L. W. *Polymer Rheology*, Marcel Dekker，New York，1977, p 69.

159 Michas, J.; Paleos, C. M.; Skoulios, A.; Weber, P. *Mol. Cryst. Liq. Cryst.* **1995**, *239*, 245–255.

160 K. Aoi, A. Takasu, M. Okada, *Macromol. Chem. Phys.,* **1998**, *199*, 2805.

161 N. Iza, M. Gil, J. L. Montero and J. Morcillo, *Journal of Molecular Structure* Volume **143**, March 1986, Pages 353-356

162 Yen, Y. C.; Cheng, C. C.; Kuo, S. W.; Chang, F. C. *Macromolecules* **2010**, *43*, 2634-2637.

163 Yang, J. H. et al**,** *Chinese Chemical Letters,* **2006***,* Vol. 17, No. 1, pp 133-136, 2006

164 Edmund, F.; Jordan, E. F., Jr.; Feldeisen D. W.; Wrigley, A. N. *J Polym Sci* Part A-1: Polym Chem **1971**, *9*, 1835–1851.

165 Ballauff, M. *Makromol Chem Rapid Commun* **1986**, *7*, 407–414.

[166] Ballauff, M.; Schmidt, G. F. *Makromol Chem Rapid Commun* **1987**, *8*, 93–97.

[167] Ponomarenko, E. A.; Tirrell, D. A.; MacKnight, W. J. *Macromolecules* **1998**, *31*, 1584–1589.

[168] Zhou, S.; Zhao, Y.; Cai, Y.; Zhou, Y.; Wang, D.; Han, C. C.; Xu, D. *Polymer* **2004**, *45*, 6261– 6268.

[169] Inomata, K.; Sakamaki, Y.; Nose, T.; Sasaki, S. Polym J 1996, 28, 986–991.

[170] Cheng, C. C.; Huang, C. F.; Yen, Y. C.; Chang, F. C. *J. Polym. Sci*., Part A: Polym. Chem. **2008**, *46*, 6416–6424.

[171] Utracki, L. A. Polymer Alloys and Blends: Thermodynamics and Rheology; Hanser: Mü nich, **1989**.

[172] Guo, M. Trends *Polym Sci* **1996**, *4*, 238–244.

[173] M. O'Sickey, B. Lawrey, G. Wilkes, *J. Appl. Polym. Sci.* **84**, 229 (2002).

[174]   J. Garrett, C. Siedlecki, *J. Runt, Macromolecules* **34**, 7066 (2001).

[175] (a) Nadia Canilho et al. *J. AM. CHEM. SOC*. **2006**, 128, 13998-13999 (b) Ponomarenko et al. *Macromolecules, Vol. 29, No. 27, 1996*

[176] V. V. Zharkov, A. G. Strikovsky, T. E. Verteletskaya, *Polymer*, **1993**, 34, 938.

[177] Takahashi, H. ; Mamola, K. ; Plyler, E. K. *J. Mol. Spectrosc.* **1966**, 21, 217.

[178] Steven, C. Ringwald. Jeanne, E. Pemberton. Environ. *Sci. Technol.* **2000**, 34, 259.

Introduction to Author

Name:Jia-You Tsai (蔡佳佑)

Personal Information:

Birth date: 1984/12/06	Birth Place: Yunlin County
Sex：male	Blood type：B
Height：174cm	Weight：67kg
Present Address: Room 101,SB Ⅱ, No.1001, Daxue Rd., East Dist., Hsinchu City 300, Taiwan (R.O.C.)	
Permanent Address: 4F., No.14-1, Lane. 48, Kangle St., Neihu Dist., Taipei City 114, Taiwan (R.O.C.)	
Mobile-phone: 0975219619 TEL：(03)571-2121 # 56558 E-mail: sephiroth.ac97g@g2.nctu.edu.tw	

【Education】

Post Graduate: **National Chiao Tung University Department of Applied Chemistry**

2008/9～2010/6

University: **National Taiwan University Depart of Chemical Engineering Double Major in Atmospheric Science**

2003/9～2008/6

High School: **Taipei Municipal Chien Kuo Senior High School**

2000/9～2003/6

【Research Field & Thesis Topic】

1.Syntheses, Characterizations, Properties of Benzoxazine-based Thermally Curable Polymers and its Application in Low Surface Energy Material

2.The Study on the Supramolecular Recognition within Polymer System

【Research & Thesis Abstract Undergoing】

1. Synthesis of various kind of Benzoxazine monomer containing special functional group and the measurement of its mechanical and thermal Properties.

2. Benzoxazine as an application in Nanoimprint、Wettability Pattern and Low Surface Energy Material.

【Director Professor/Laboratory】

Professor Fung-Chih Chang (Chair Professor & Dean, College of Science, NCTU. Coordinator, Polymer Program, NSC) / Polymer Research Center